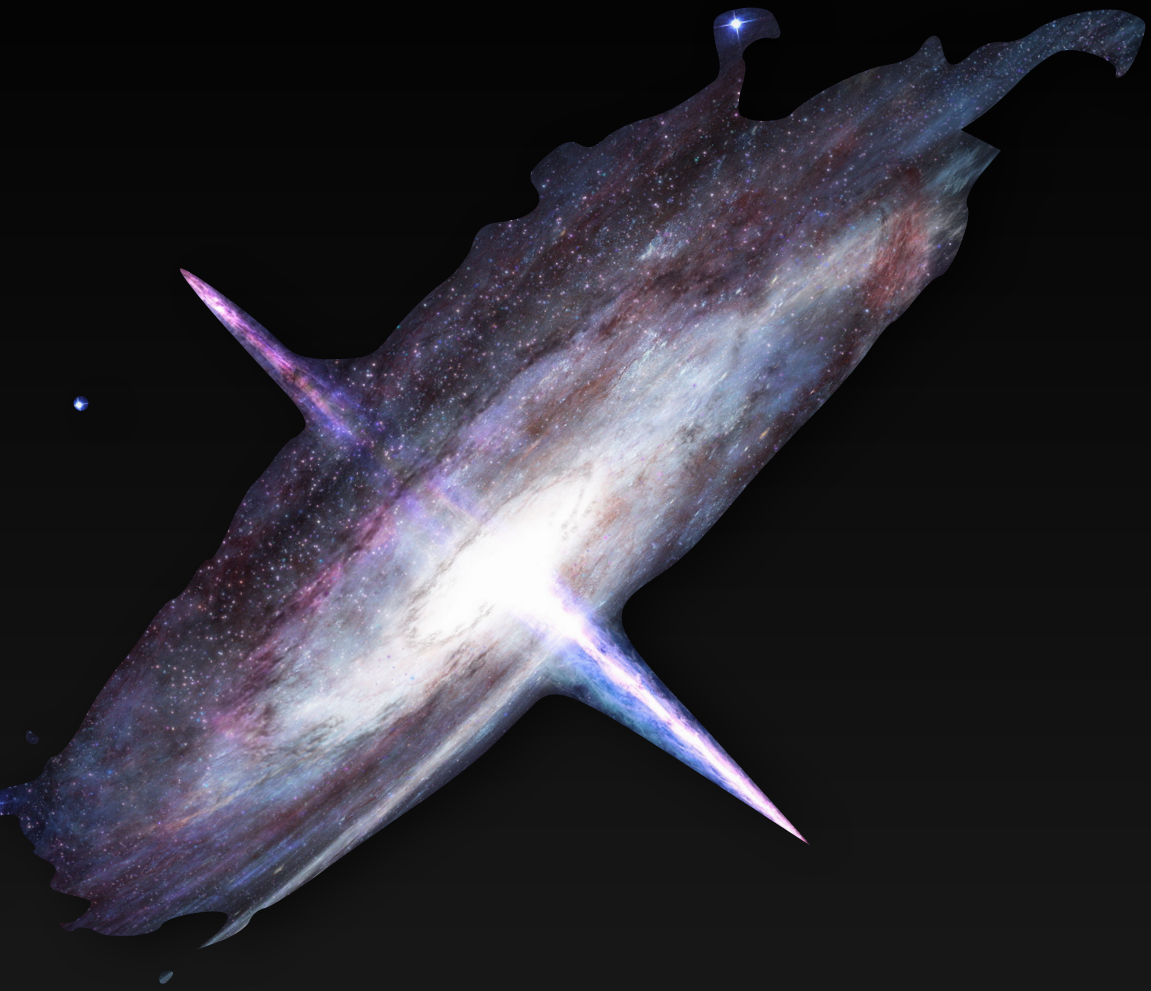


Probing the intergalactic magnetic field through gamma-ray observations with the *Fermi* LAT and H.E.S.S.

Manuel Meyer for the H.E.S.S. and Fermi LAT collaborations

mey@sdu.dk

Cosmic Magnetism in Voids and Filaments Conference, Bologna, January 25, 2023

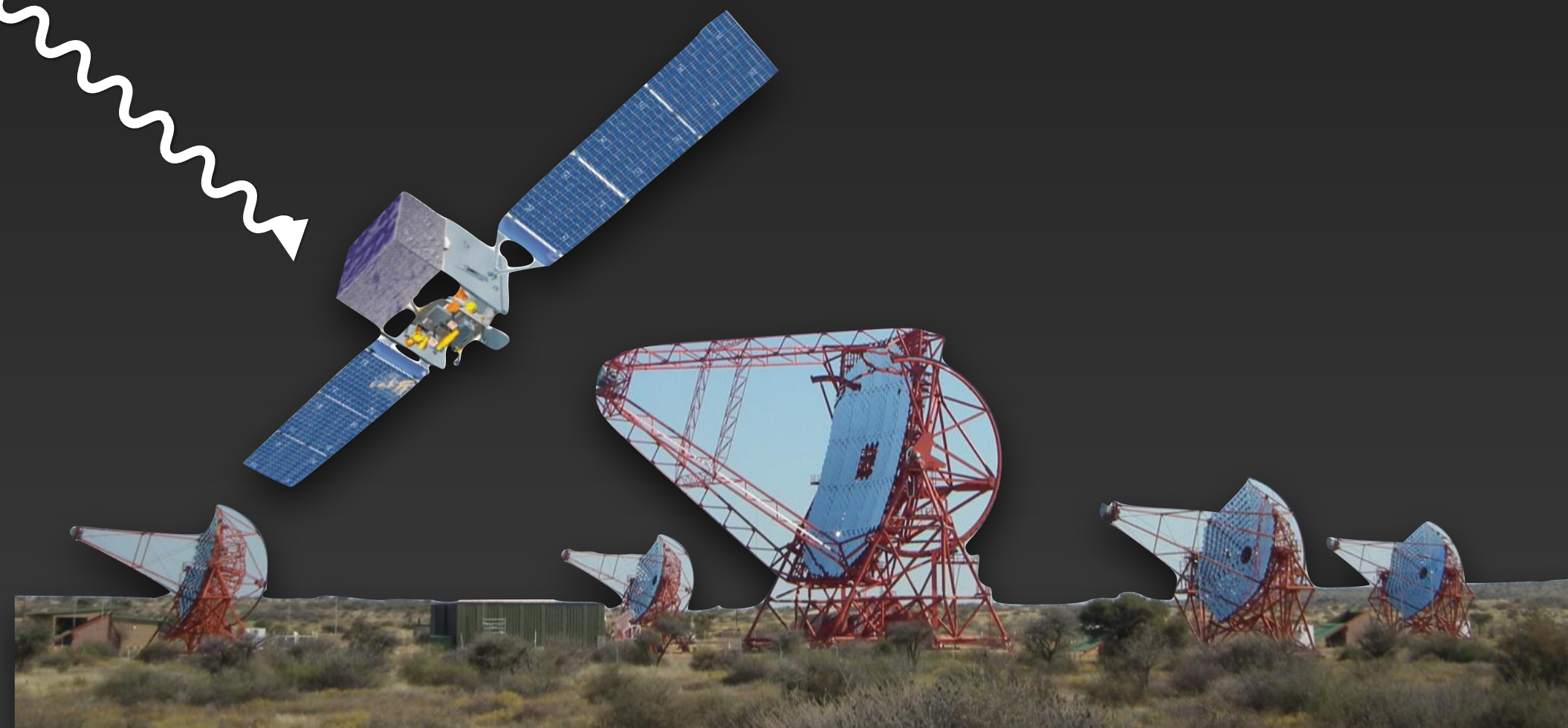
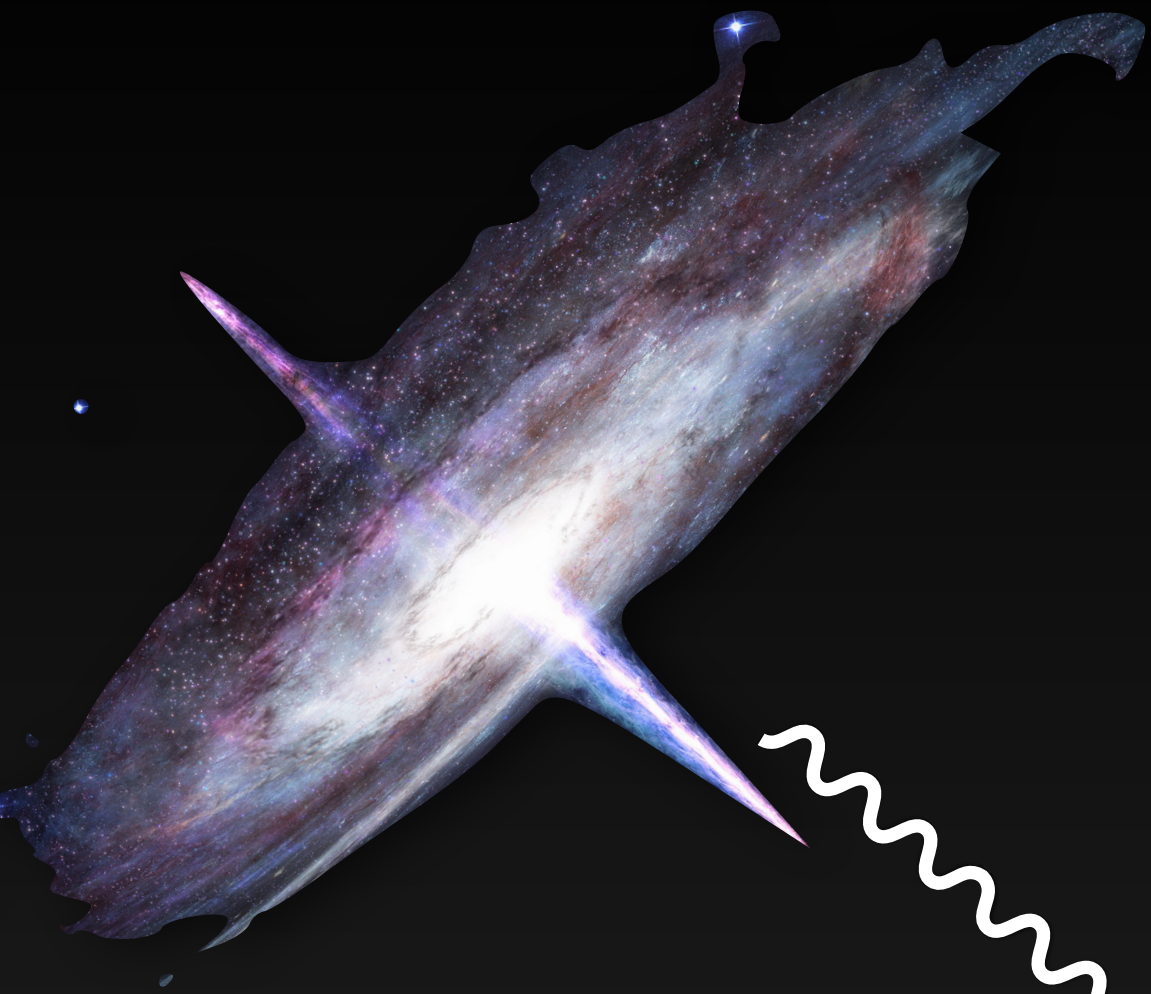


Indirect detection of the IGMF

Using gamma-ray observations of blazars

Indirect detection of the IGMF

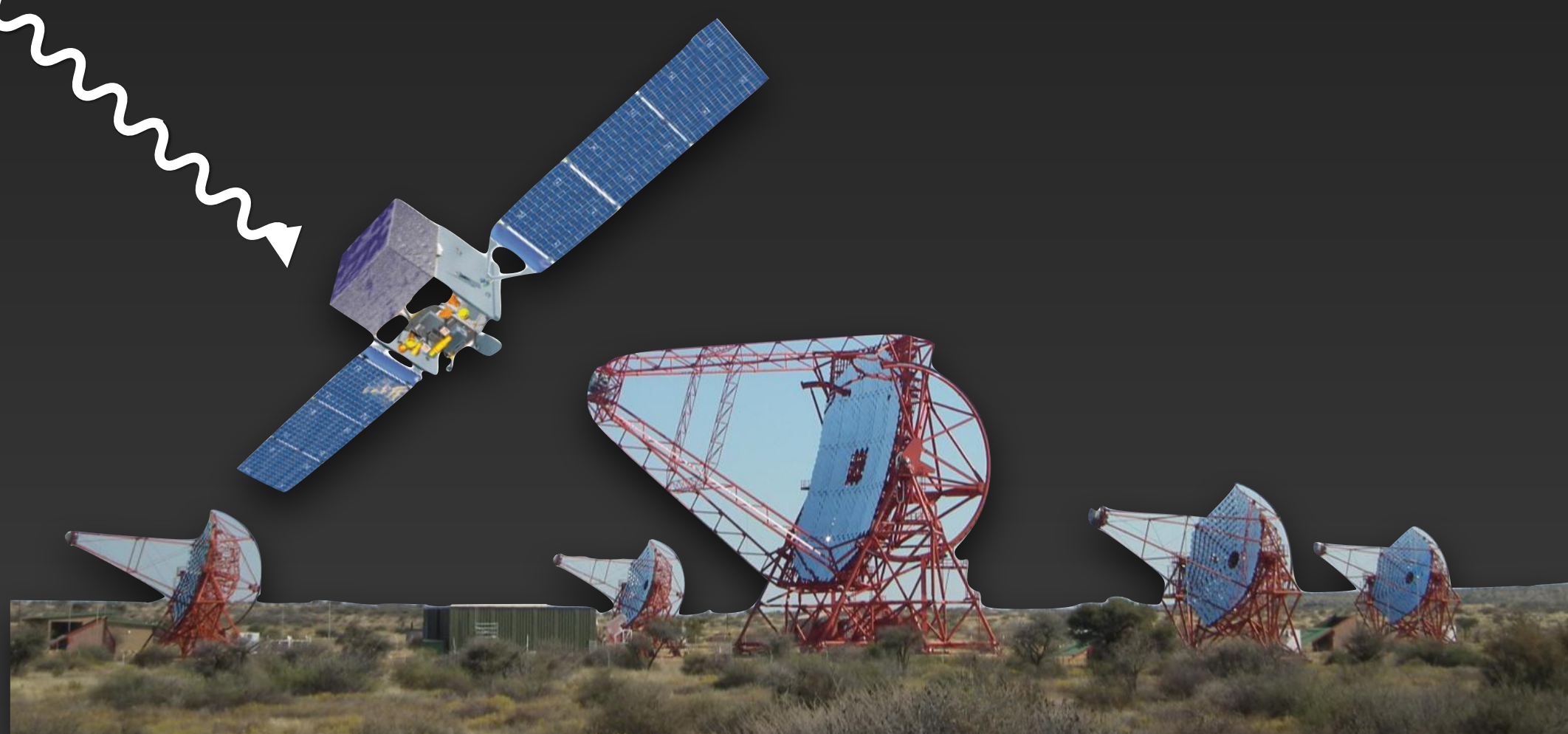
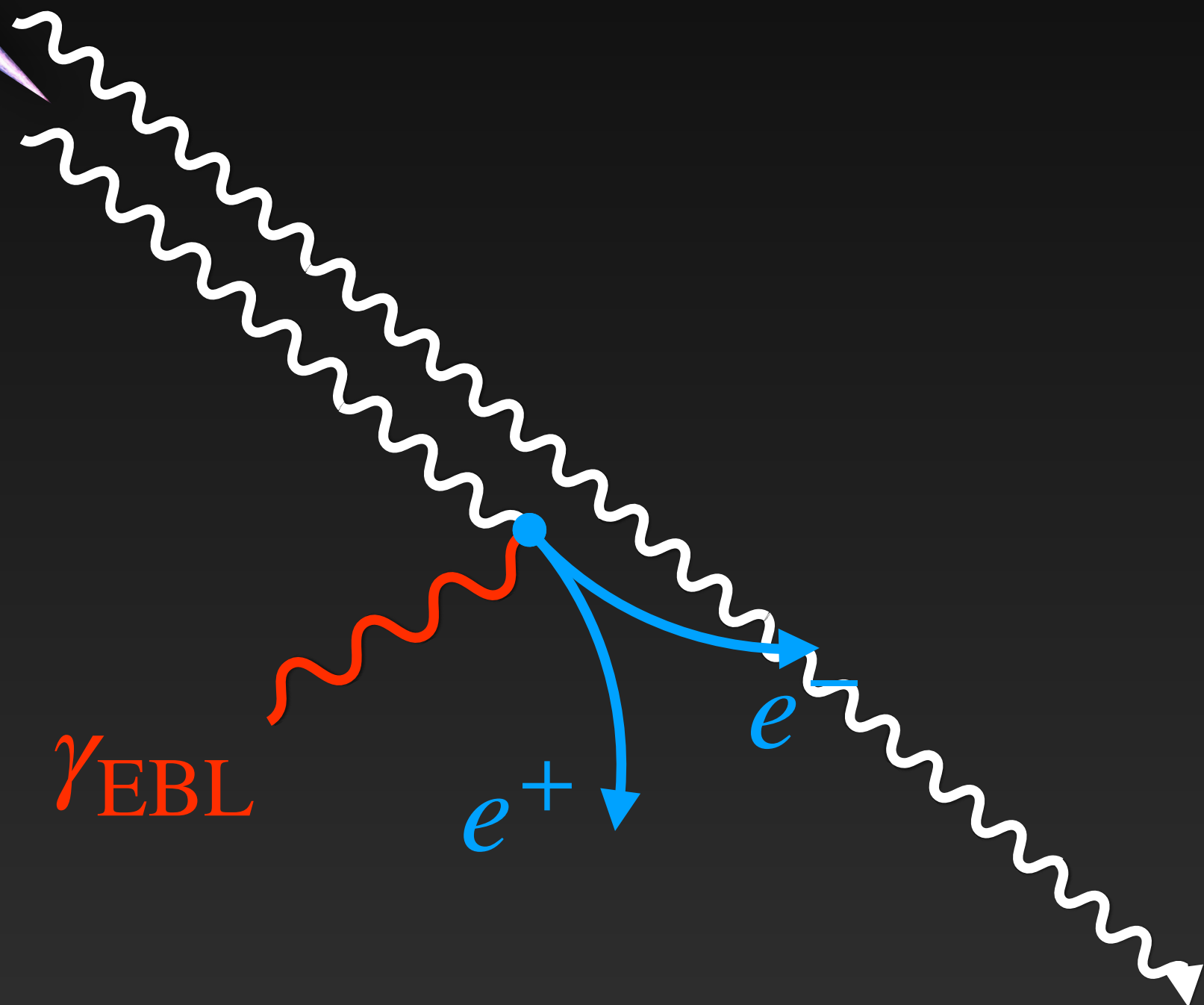
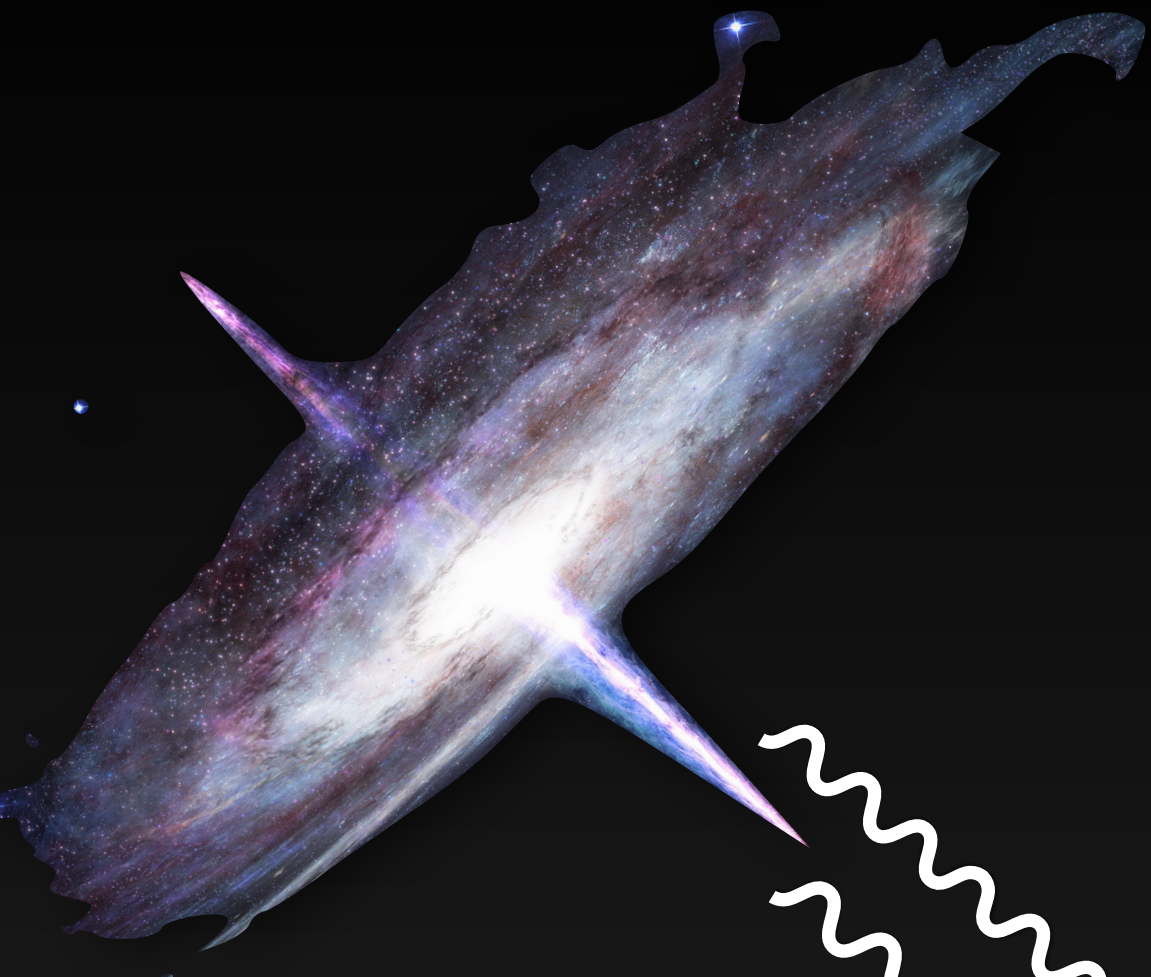
Using gamma-ray observations of blazars



See also talk by R. Alves Batista and A. Neronov

Indirect detection of the IGMF

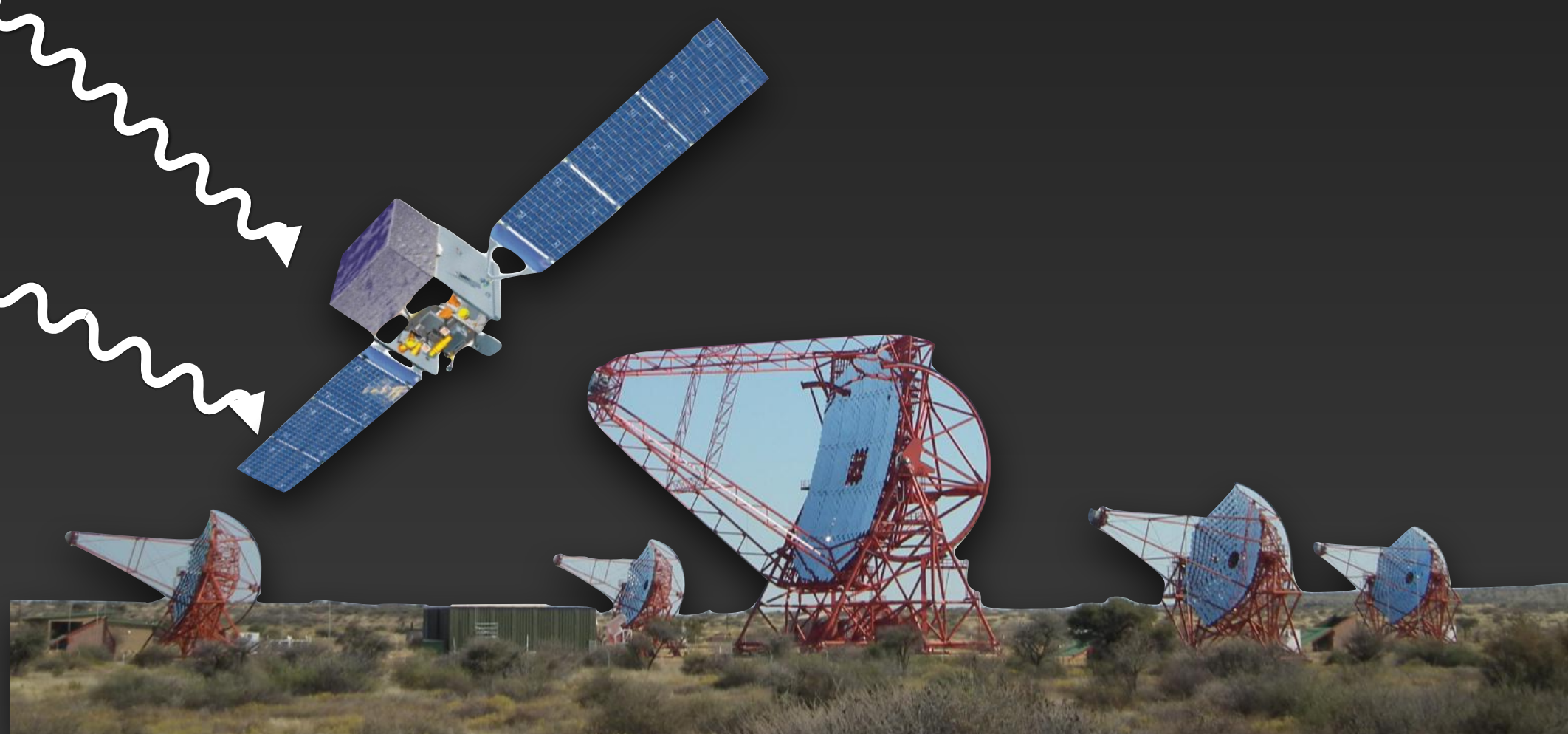
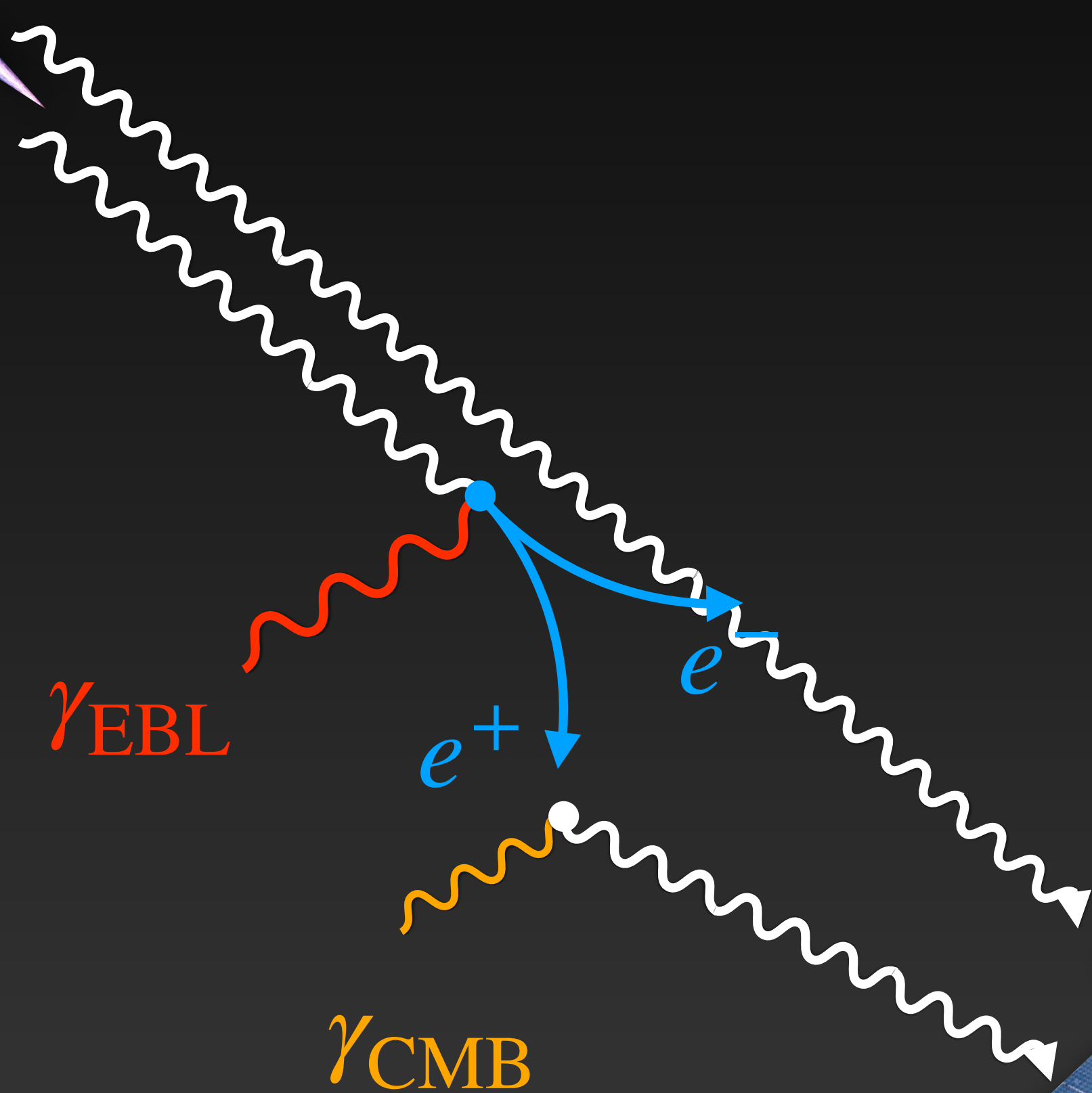
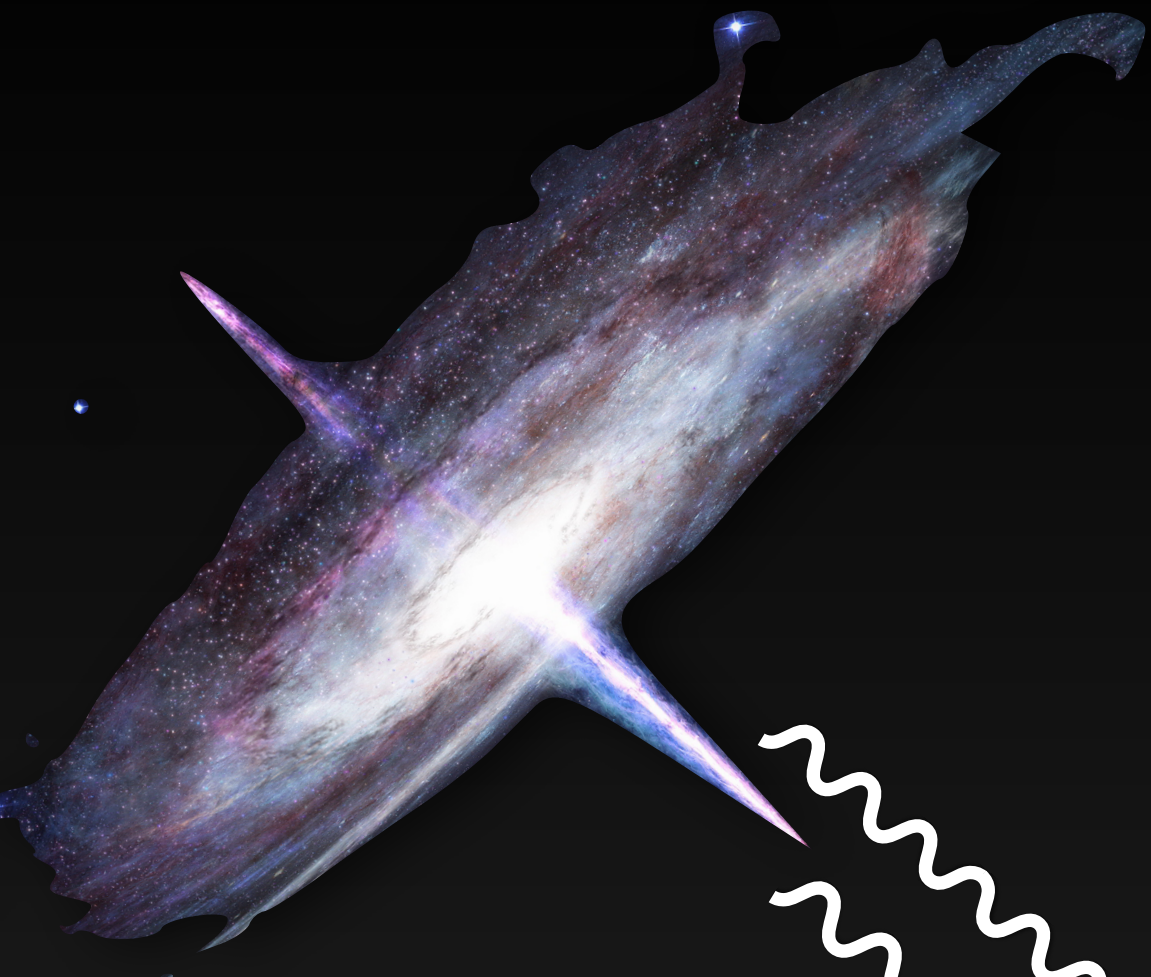
Using gamma-ray observations of blazars



See also talk by R. Alves Batista and A. Neronov

Indirect detection of the IGMF

Using gamma-ray observations of blazars

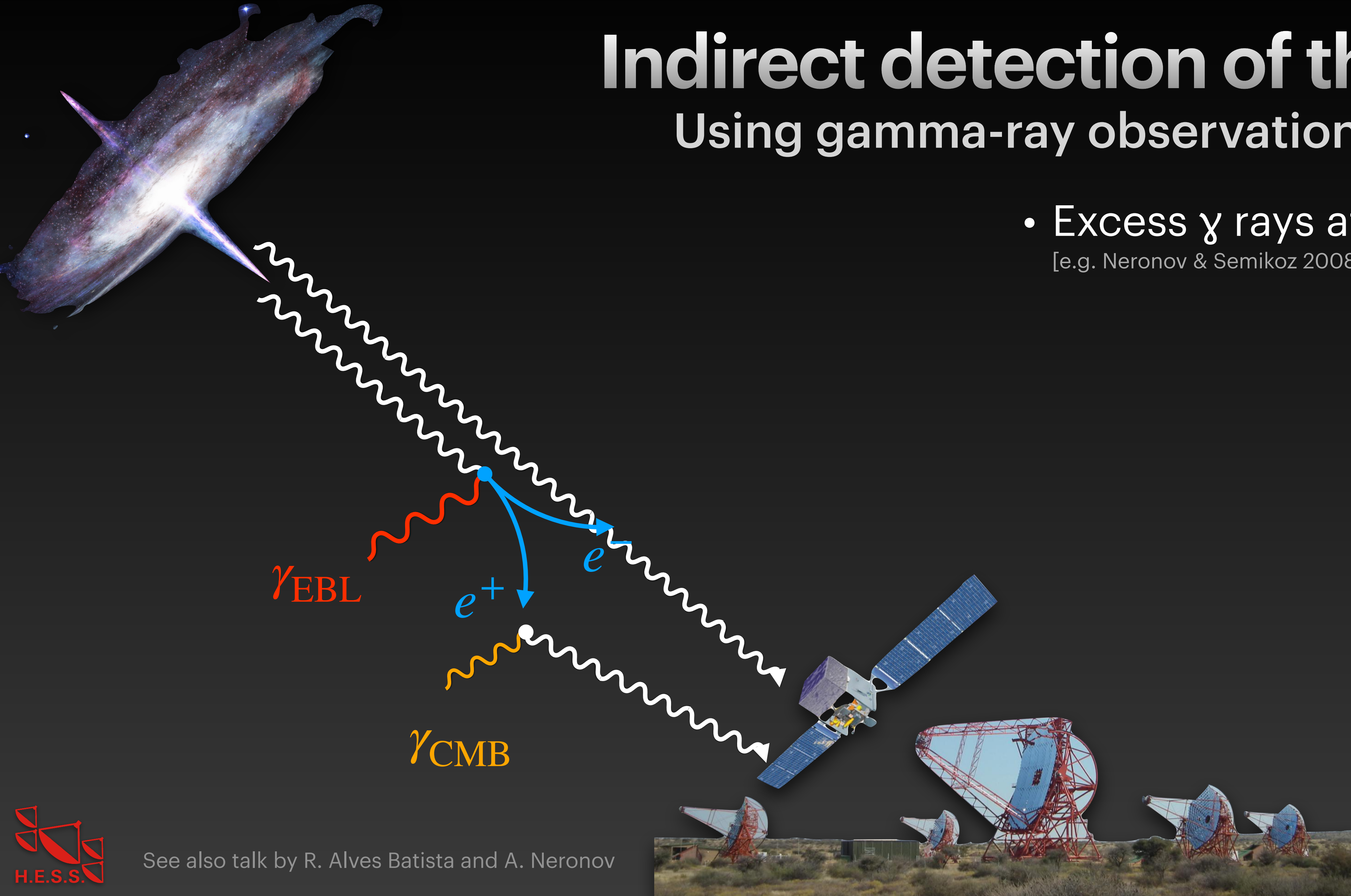


See also talk by R. Alves Batista and A. Neronov

Indirect detection of the IGMF

Using gamma-ray observations of blazars

- Excess γ rays at lower energies
[e.g. Neronov & Semikoz 2008]

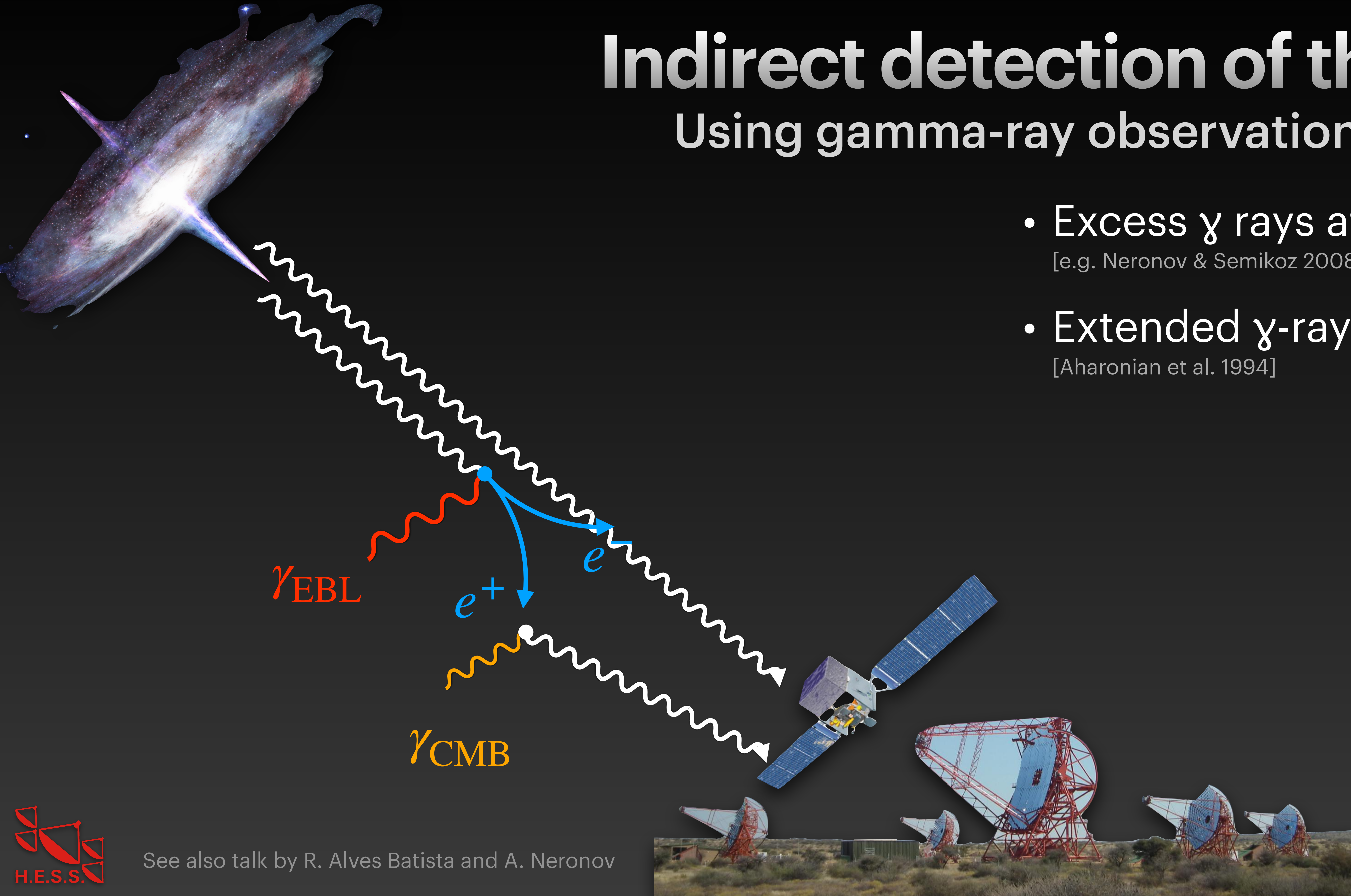


See also talk by R. Alves Batista and A. Neronov

Indirect detection of the IGMF

Using gamma-ray observations of blazars

- Excess γ rays at lower energies
[e.g. Neronov & Semikoz 2008]
- Extended γ -ray halos
[Aharonian et al. 1994]

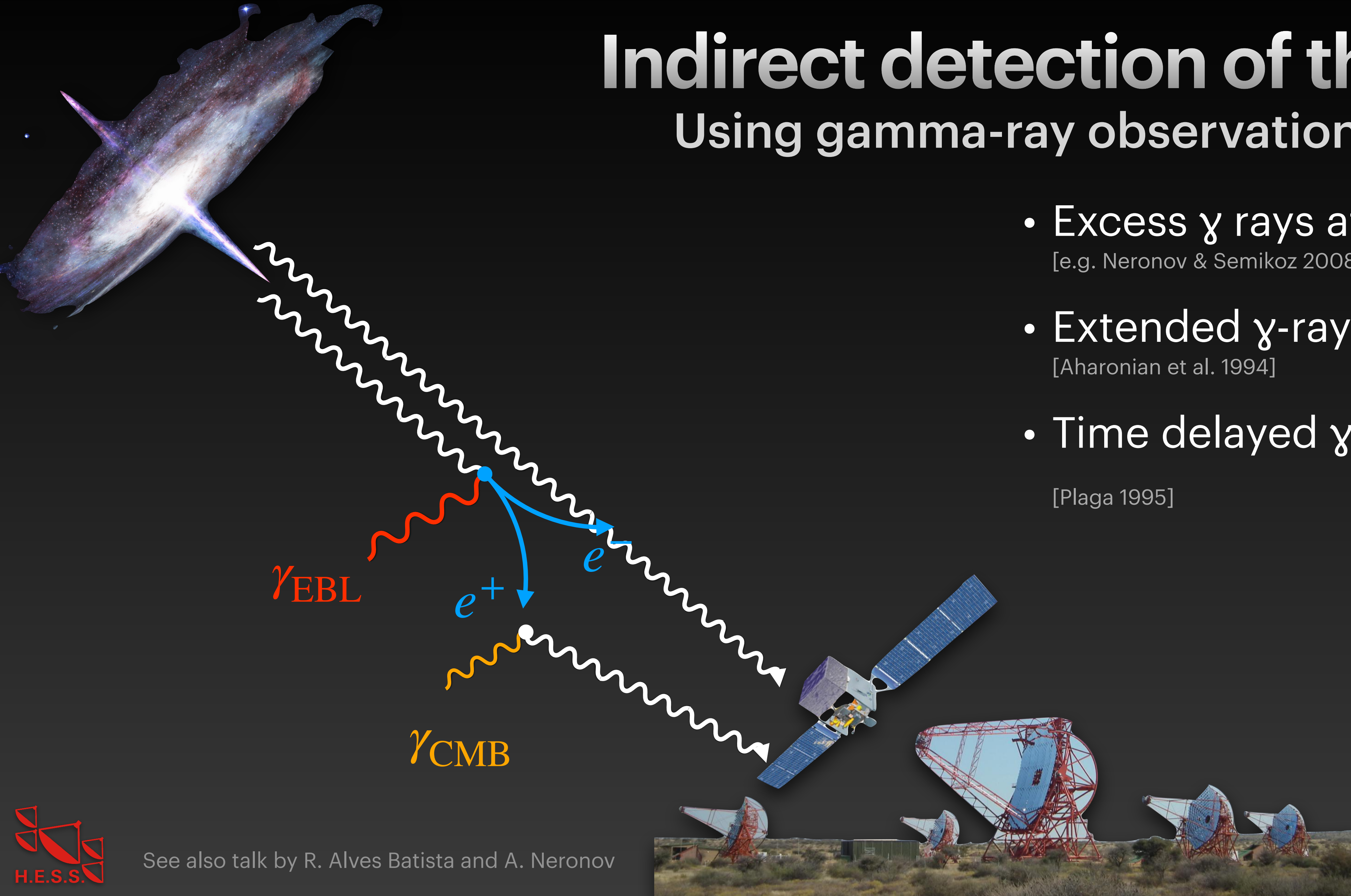


See also talk by R. Alves Batista and A. Neronov

Indirect detection of the IGMF

Using gamma-ray observations of blazars

- Excess γ rays at lower energies
[e.g. Neronov & Semikoz 2008]
- Extended γ -ray halos
[Aharonian et al. 1994]
- Time delayed γ -ray emission
[Plaga 1995]

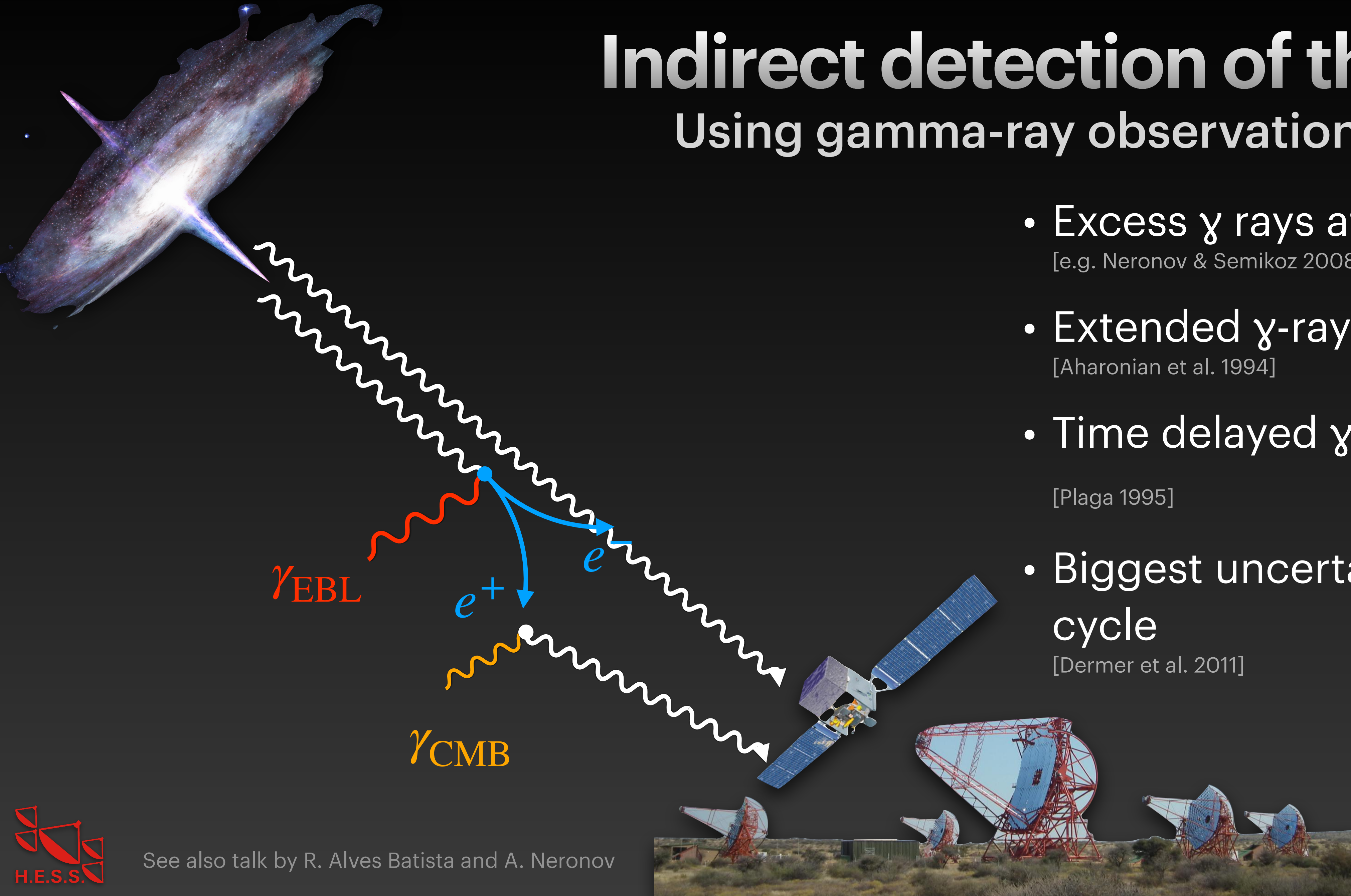


See also talk by R. Alves Batista and A. Neronov

Indirect detection of the IGMF

Using gamma-ray observations of blazars

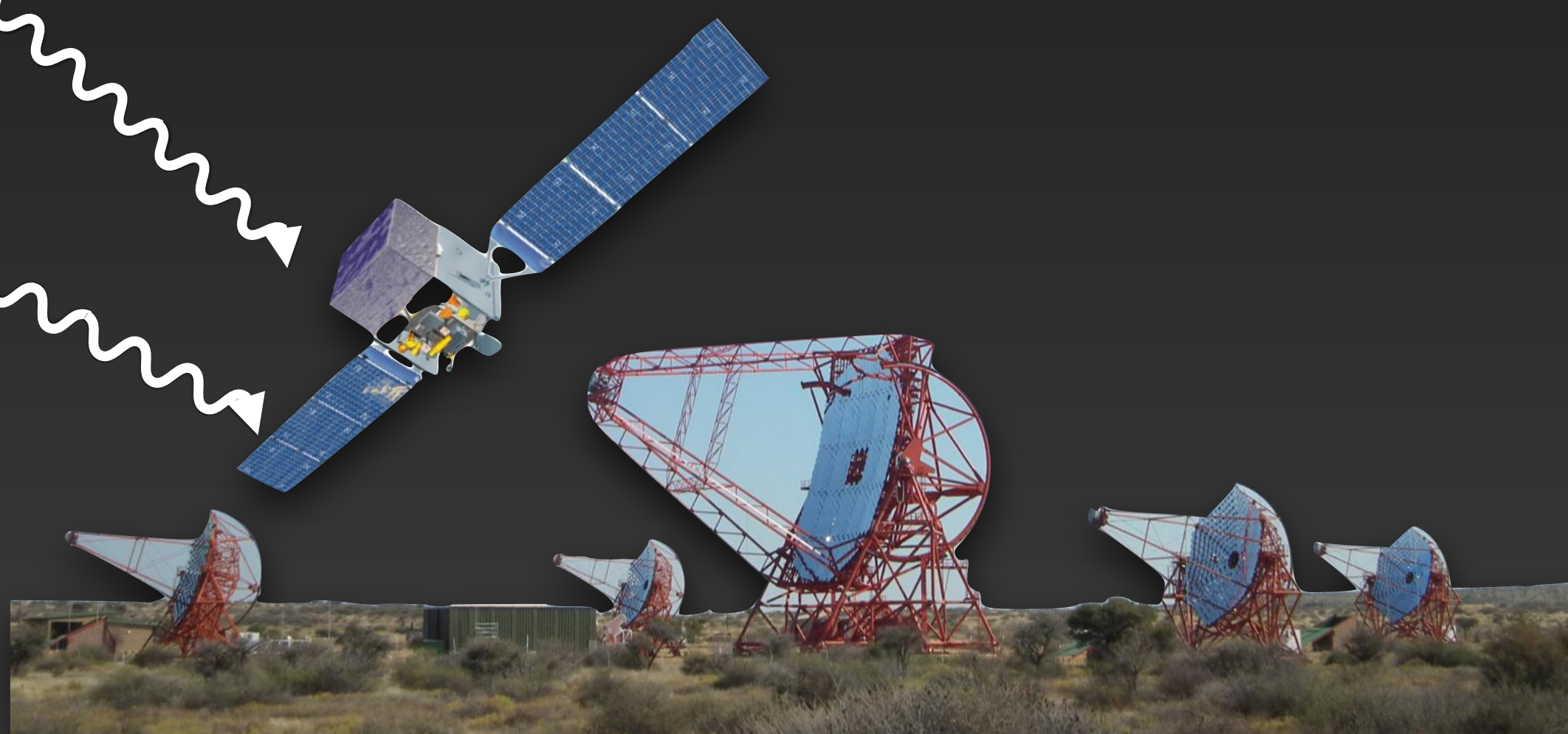
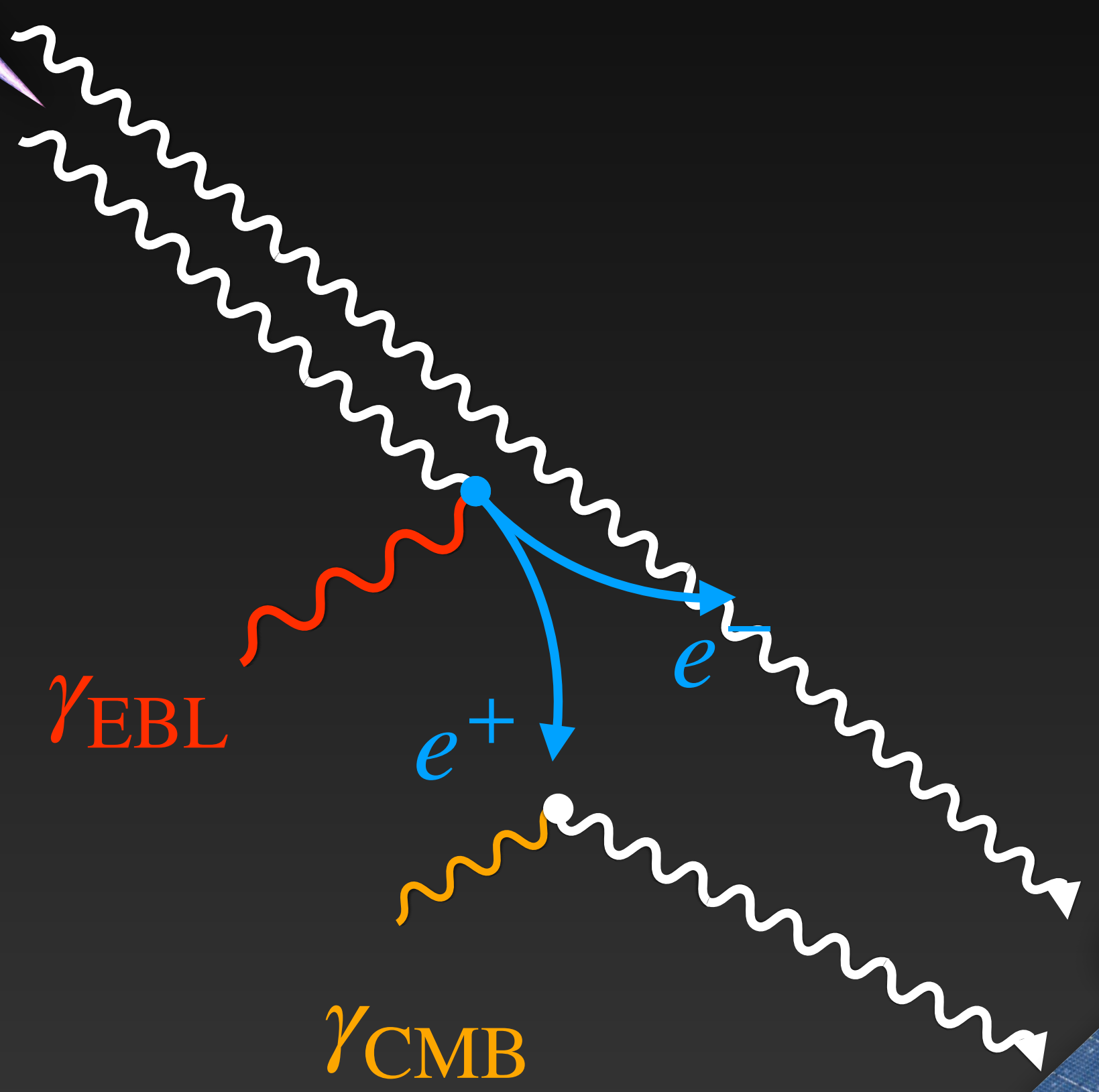
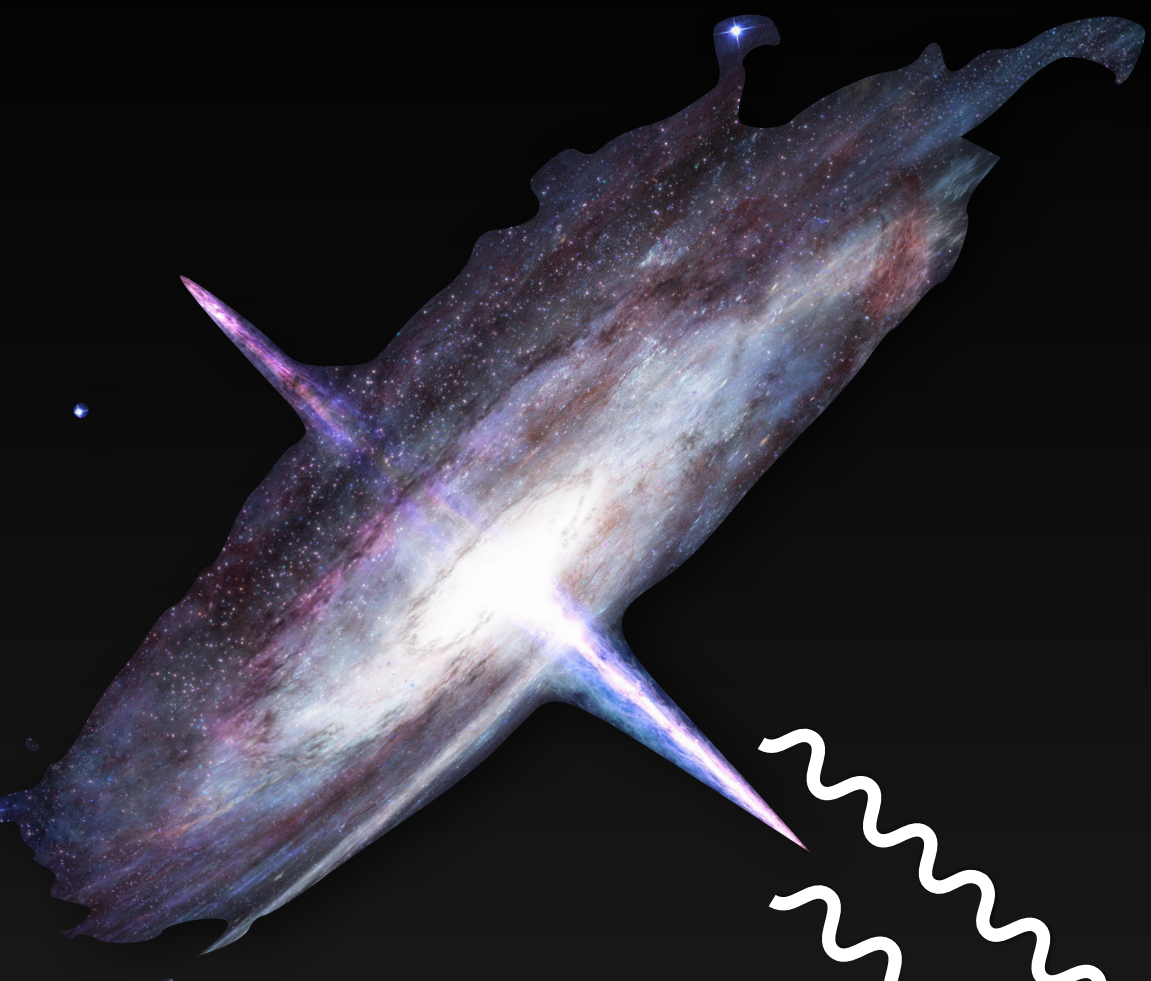
- Excess γ rays at lower energies
[e.g. Neronov & Semikoz 2008]
- Extended γ -ray halos
[Aharonian et al. 1994]
- Time delayed γ -ray emission
[Plaga 1995]
- Biggest uncertainty: blazar duty cycle
[Dermer et al. 2011]



See also talk by R. Alves Batista and A. Neronov

Goal: new constraints on the IGMF

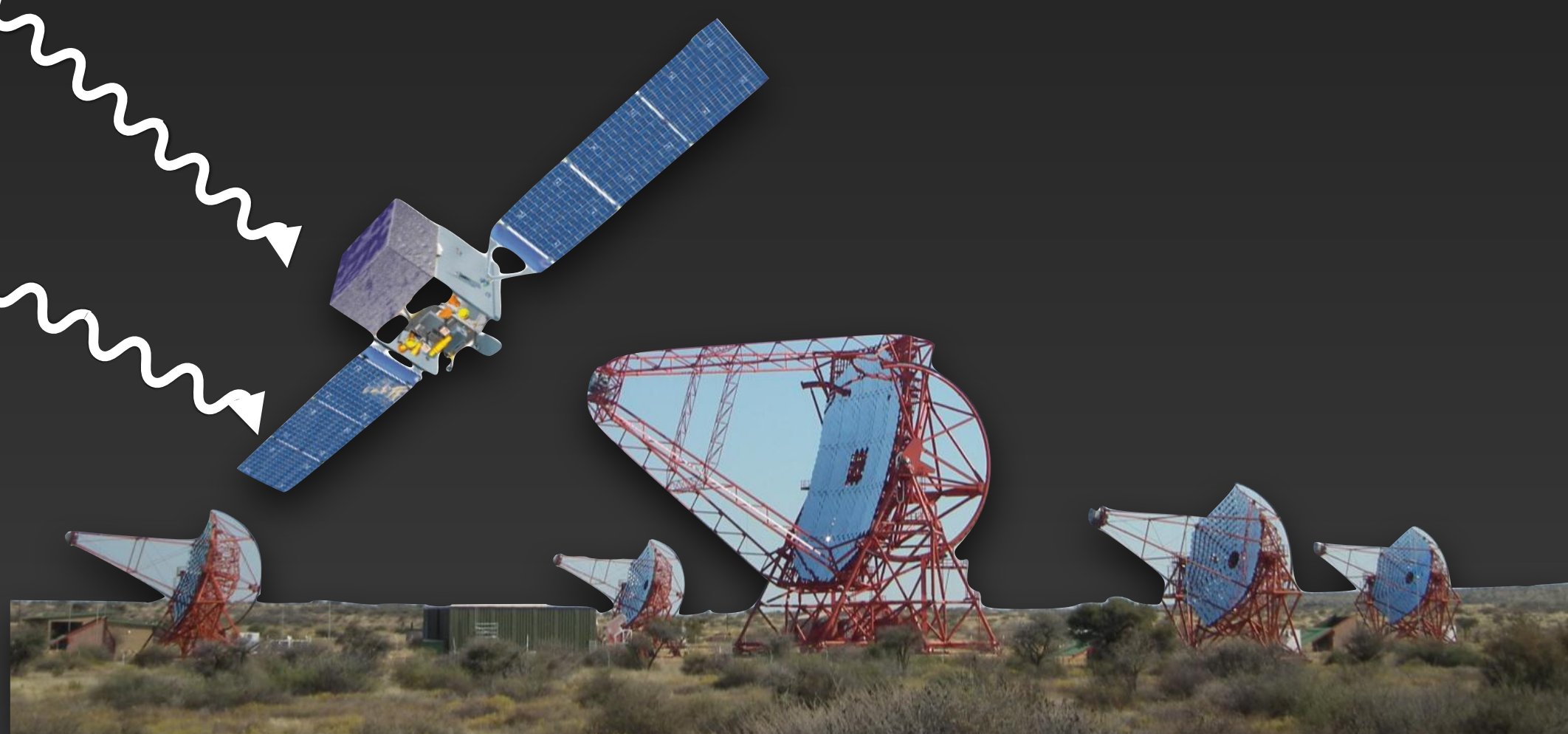
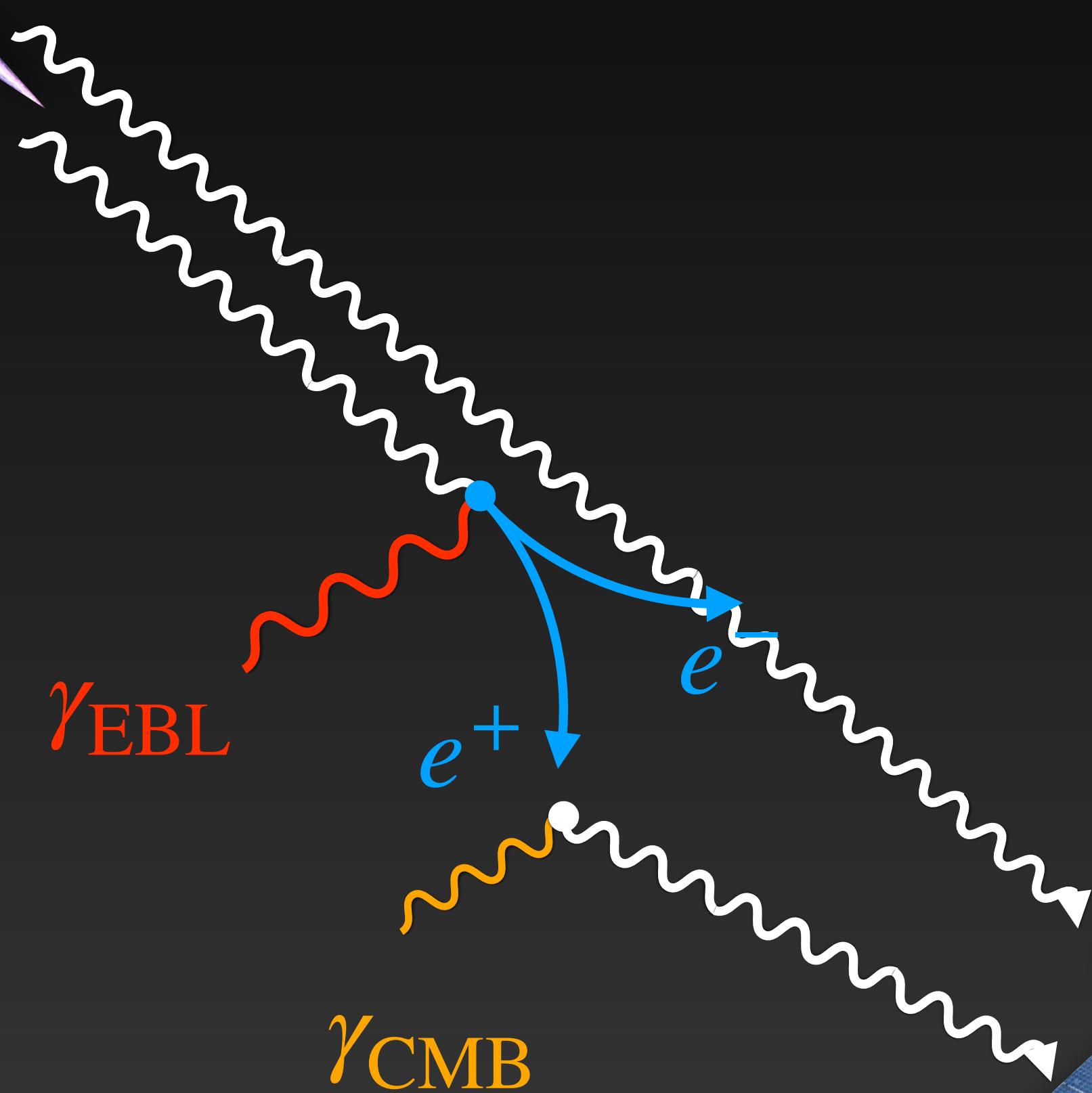
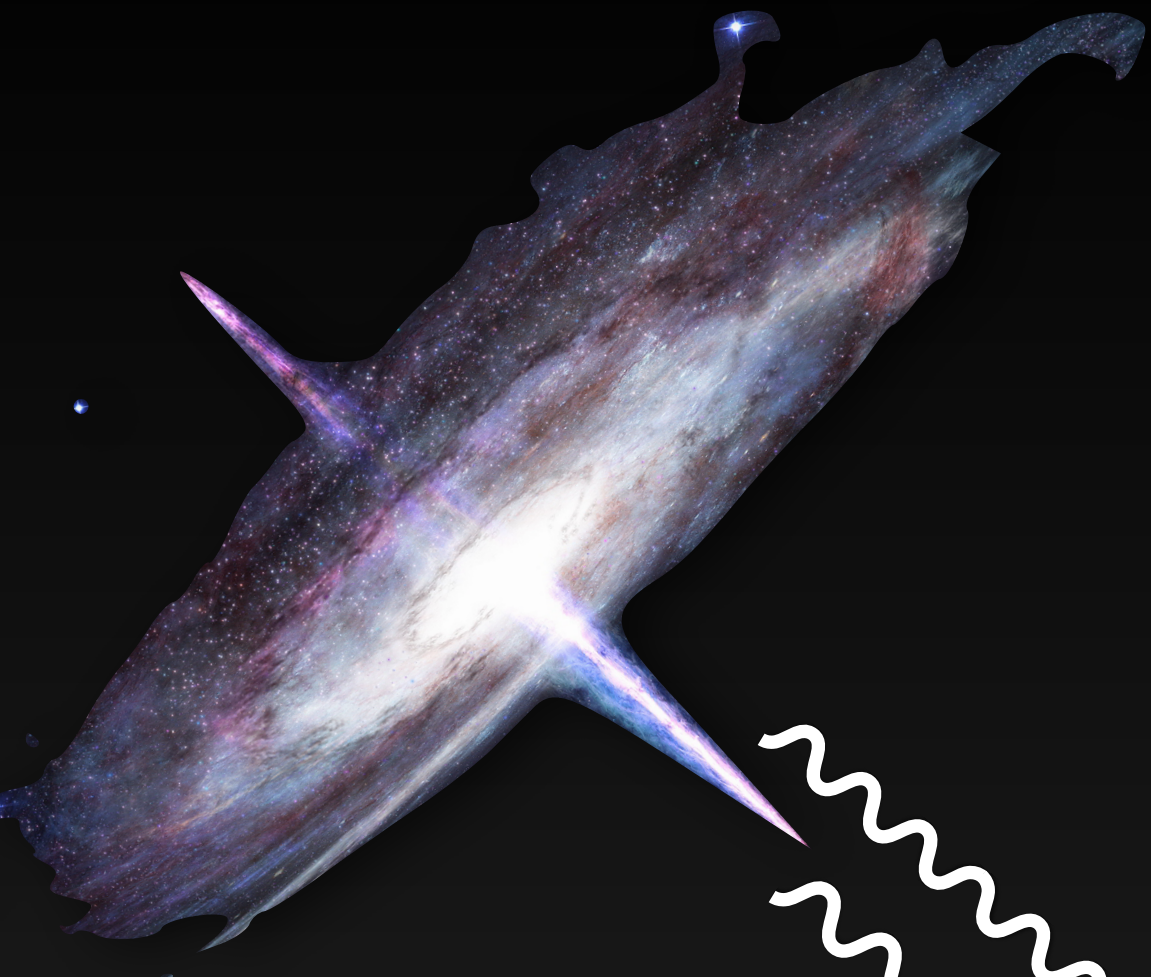
Using a combined maximum likelihood approach of H.E.S.S. and LAT data



Goal: new constraints on the IGMF

Using a combined maximum likelihood approach of H.E.S.S. and LAT data

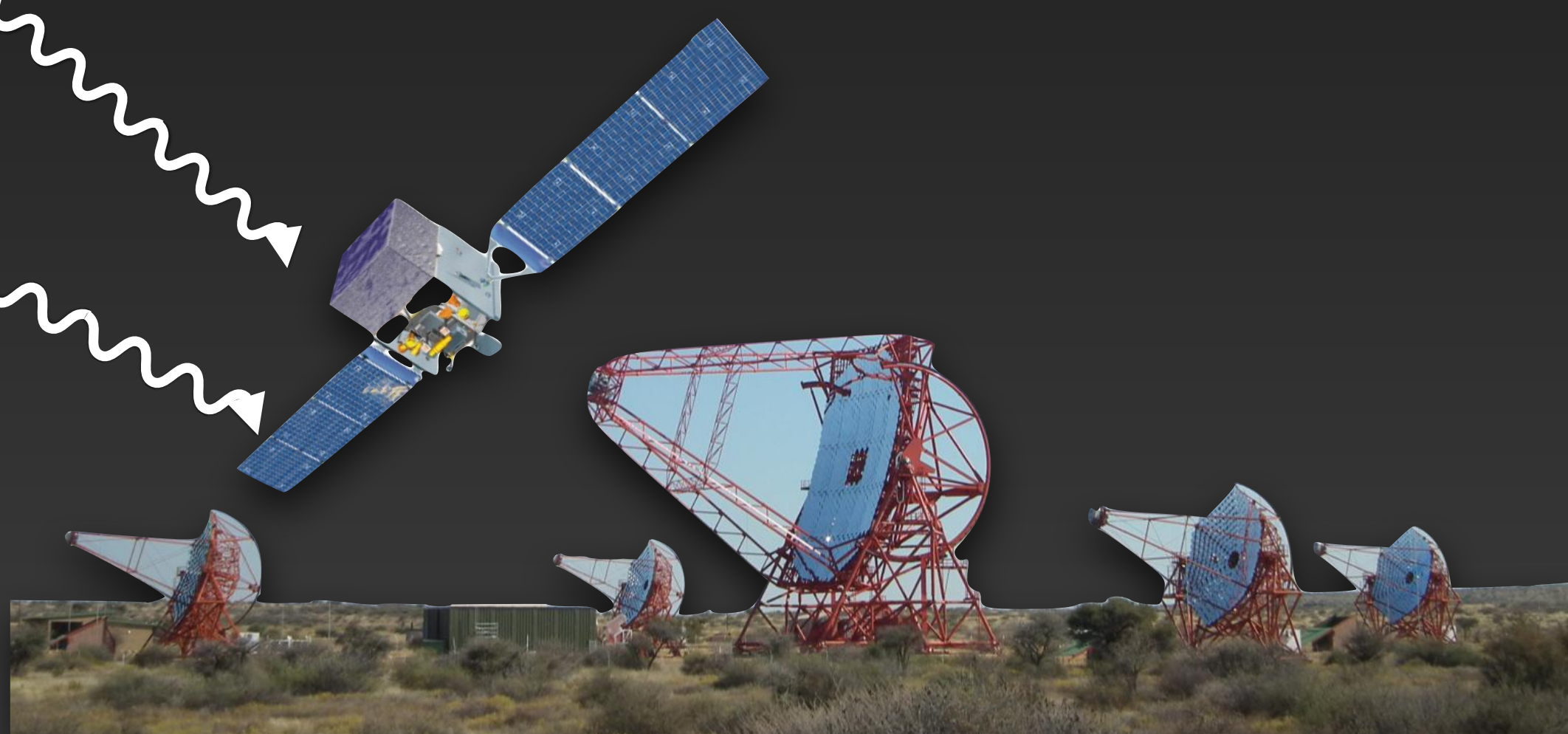
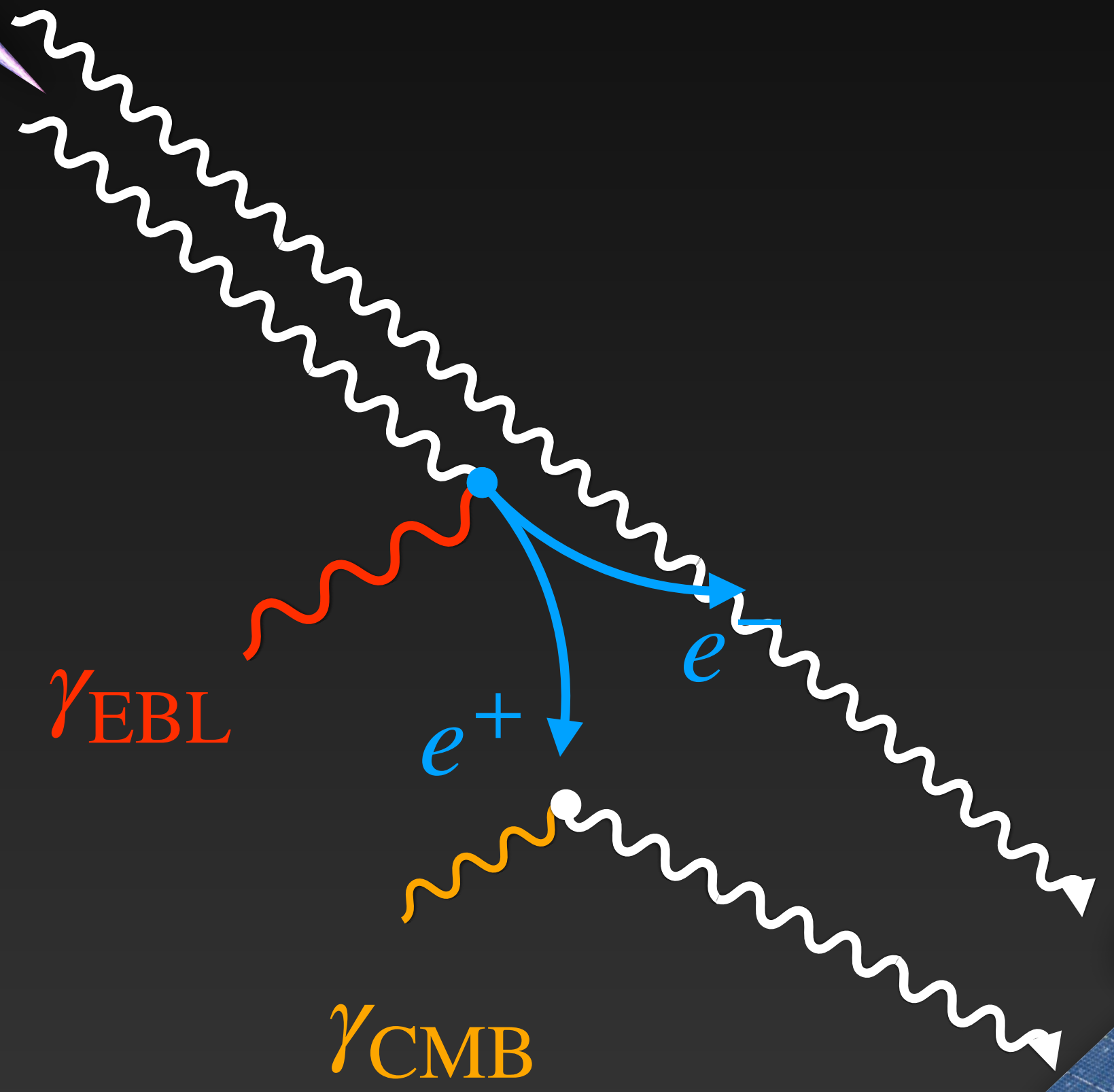
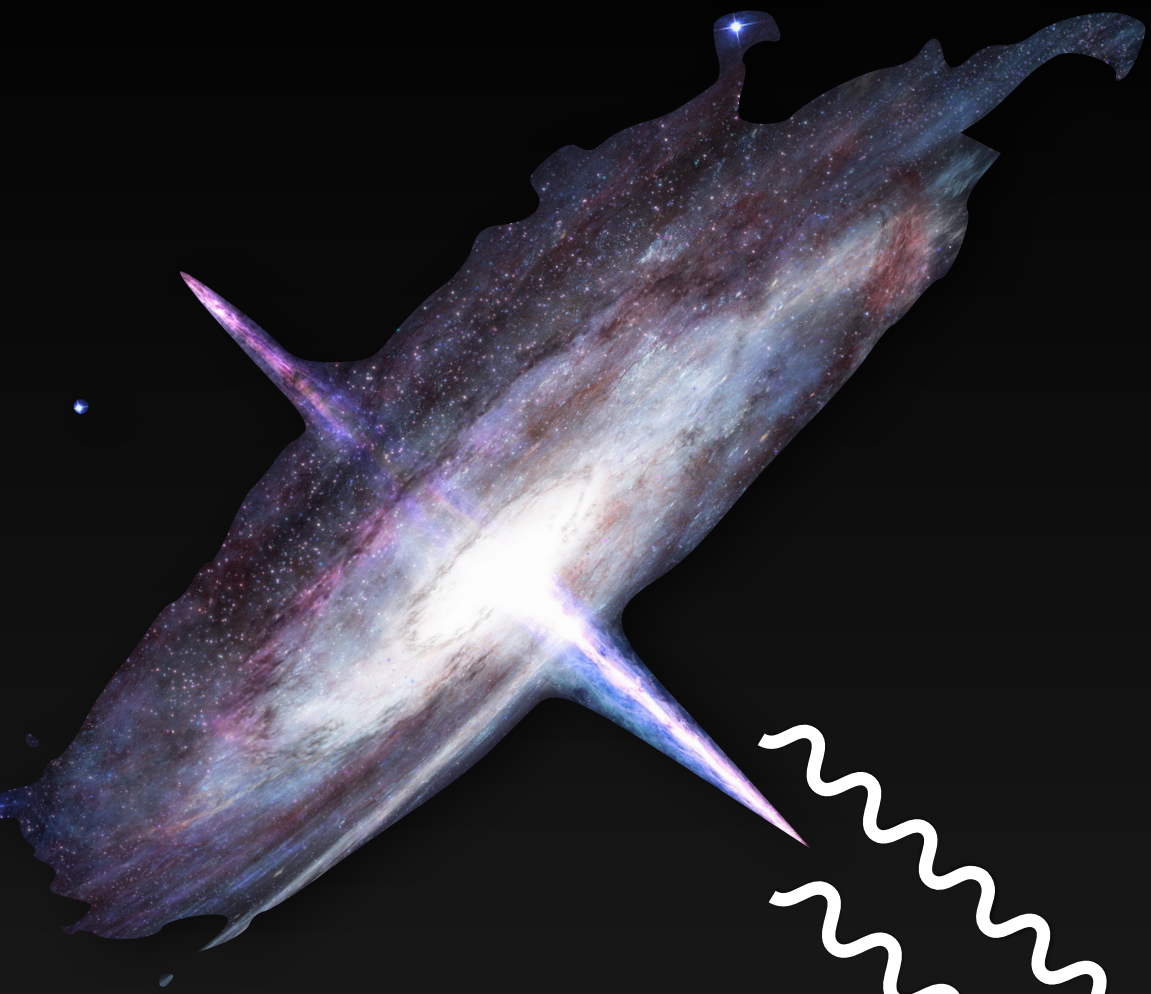
- Search for spatial and spectral halo signature



Goal: new constraints on the IGMF

Using a combined maximum likelihood approach of H.E.S.S. and LAT data

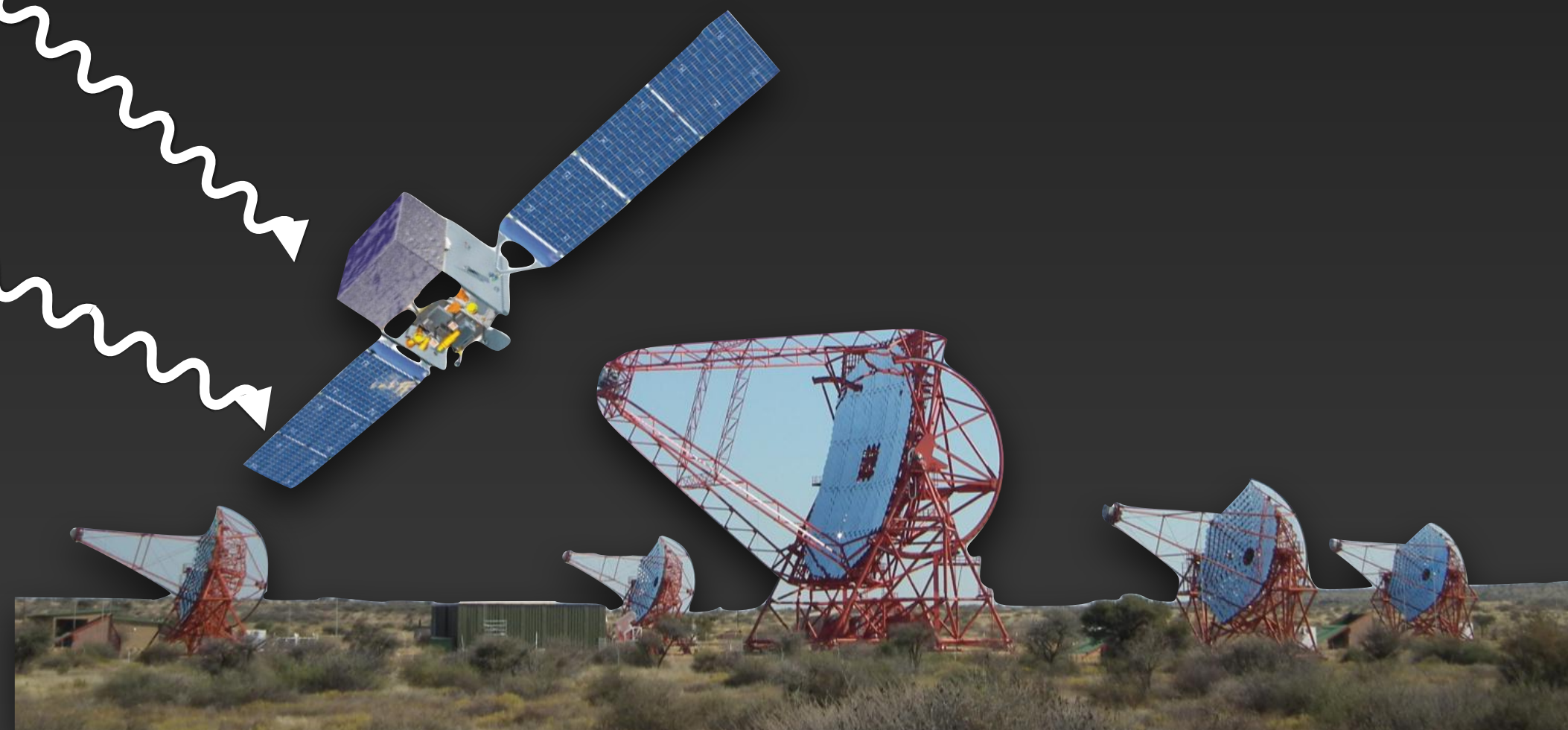
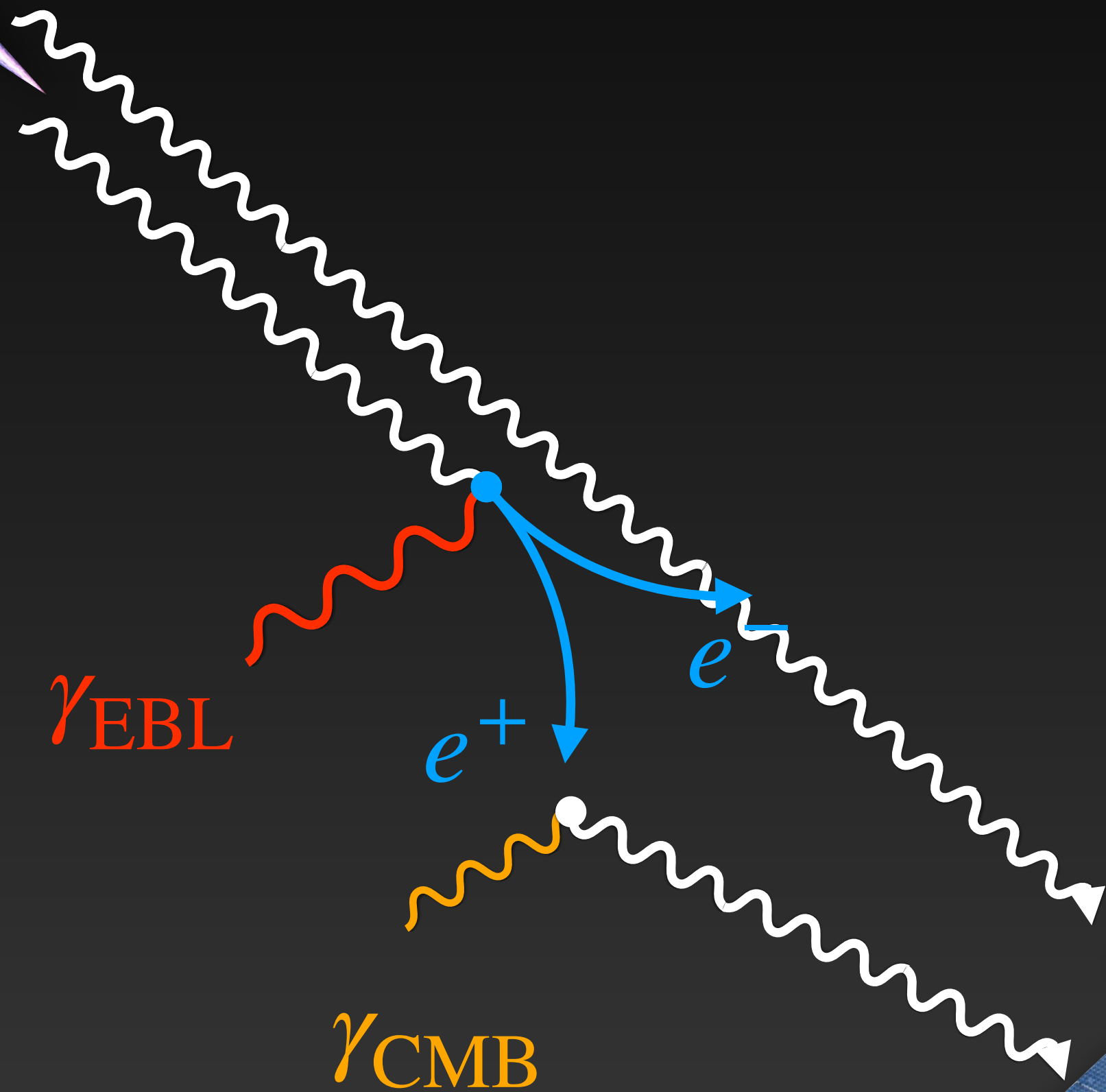
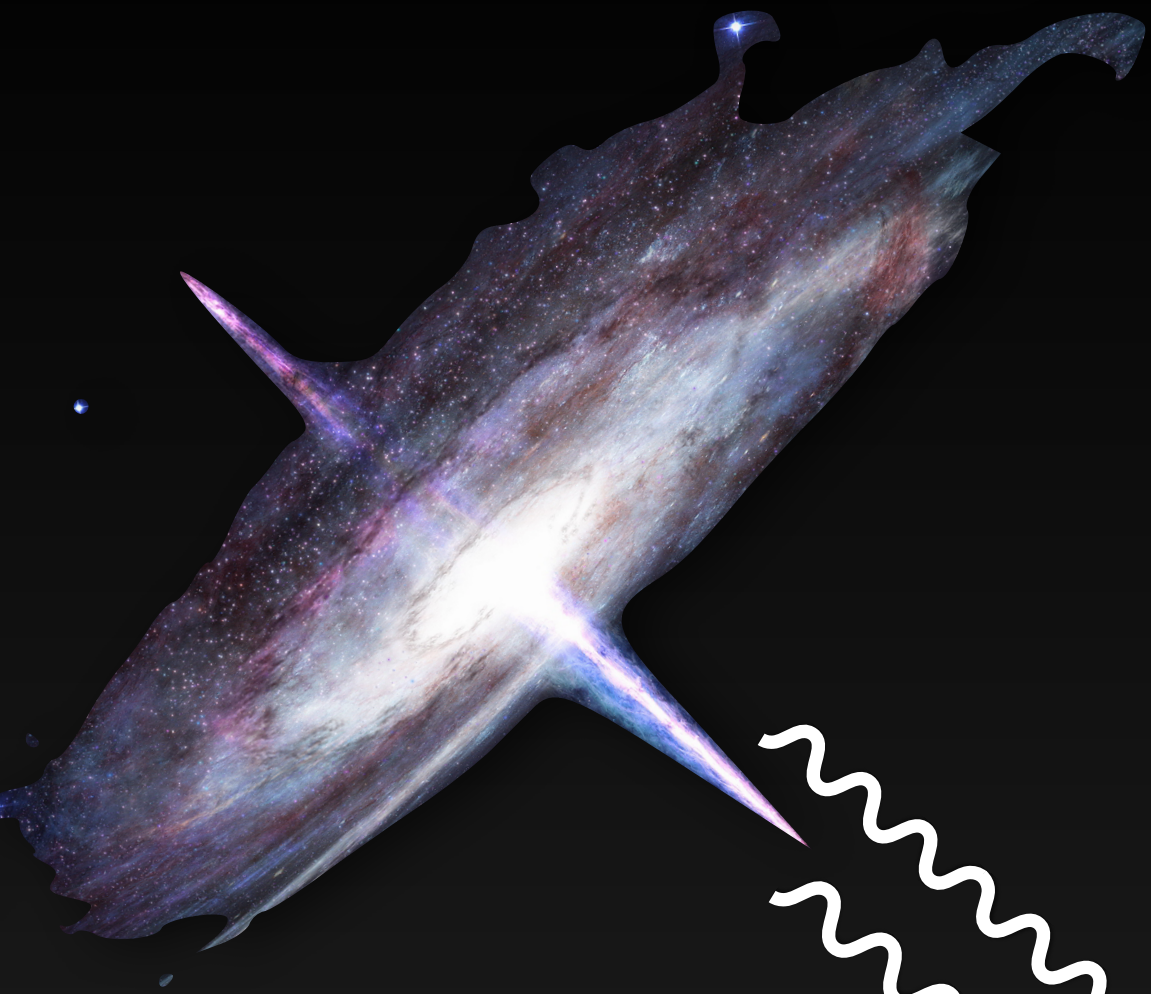
- Search for spatial and spectral halo signature
- Realistic predictions for halo from Monte Carlo Simulations



Goal: new constraints on the IGMF

Using a combined maximum likelihood approach of H.E.S.S. and LAT data

- Search for spatial and spectral halo signature
- Realistic predictions for halo from Monte Carlo Simulations
- Combining H.E.S.S. and Fermi-LAT data on the likelihood level

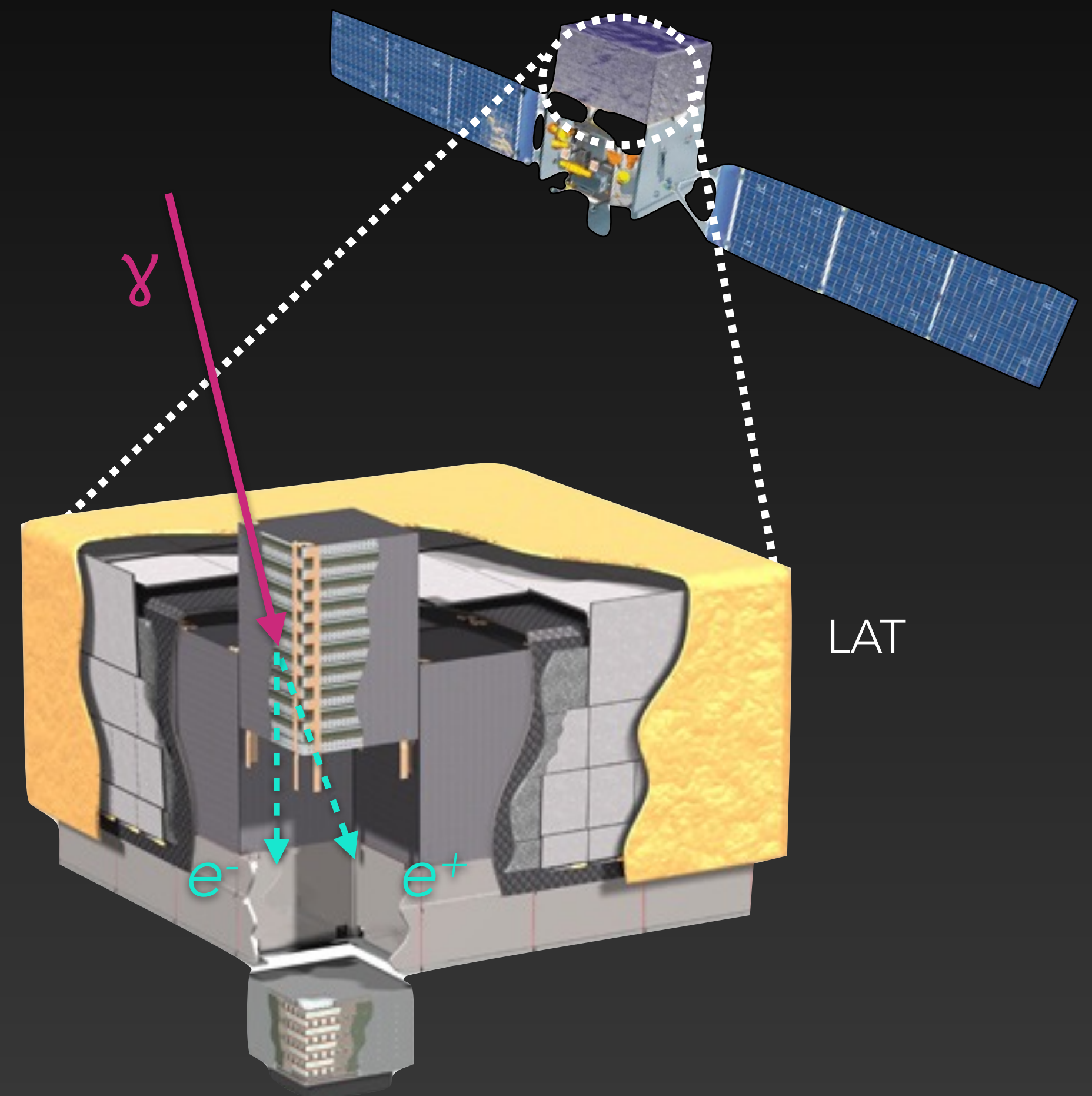


The *Fermi* Large Area Telescope (LAT)

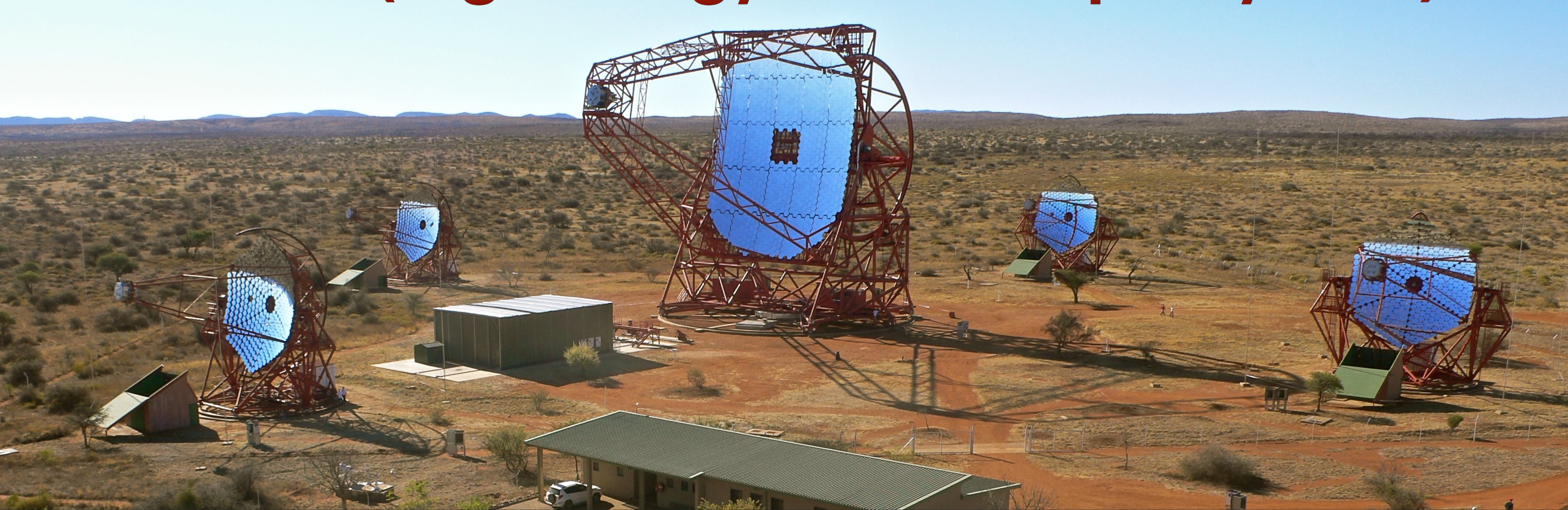
Observing the gamma-ray sky since June 11, 2008

| | |
|-------------------------------|----------------------------------|
| Energy range | 20 MeV - over 300 GeV |
| Effective Area ($E > 1$ GeV) | $\sim 1 \text{ m}^2$ |
| Point spread function (PSF) | $0.8^\circ @ 1 \text{ GeV}$ |
| Field of view | 2.4 sr ($\sim 20\%$ of the sky) |
| Orbital period | 91 minutes |
| Altitude | 565 km |

- **Survey mode:** full sky observed every 3 hours
- **Public data,** available within 12 hours

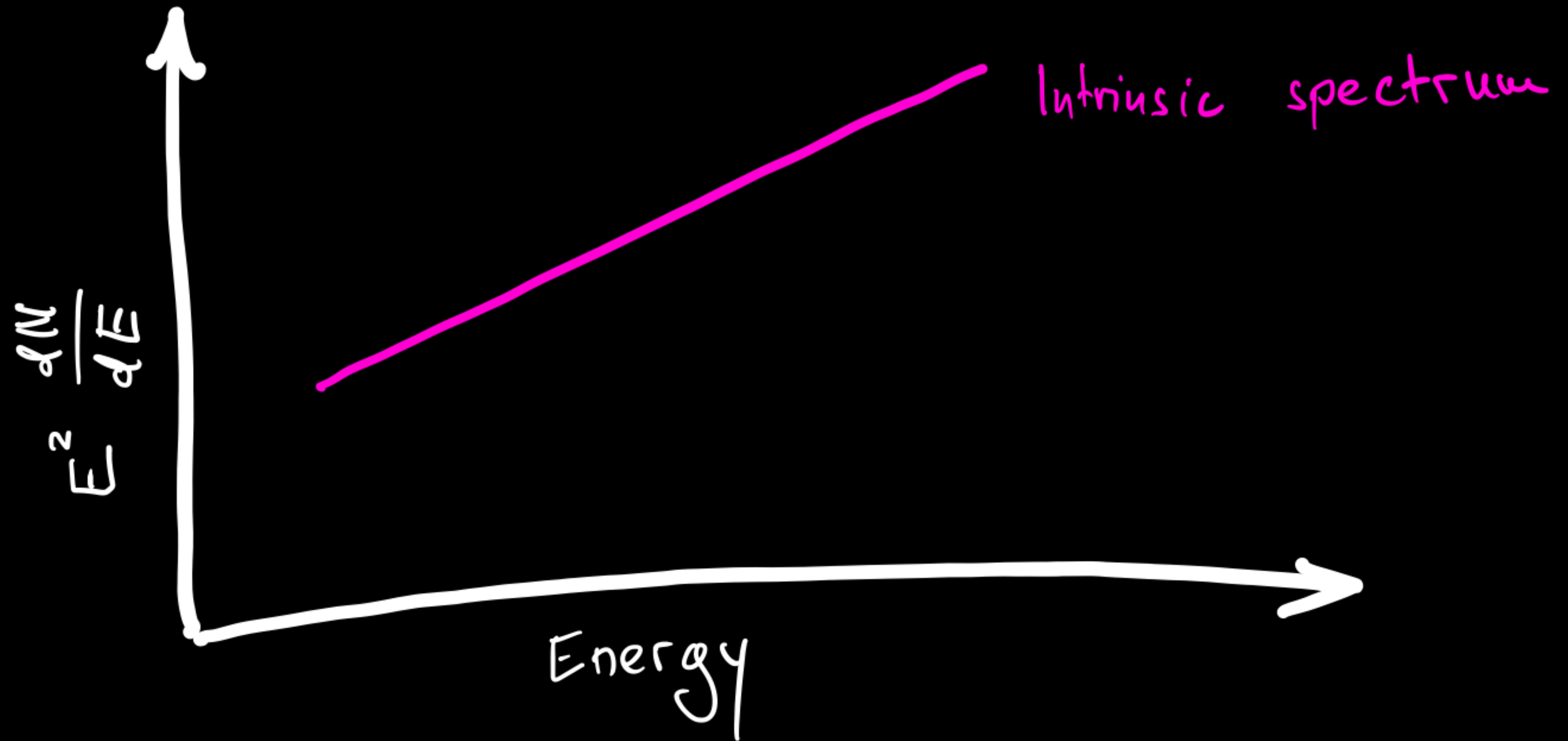


H.E.S.S. (High energy Stereoscopic System)

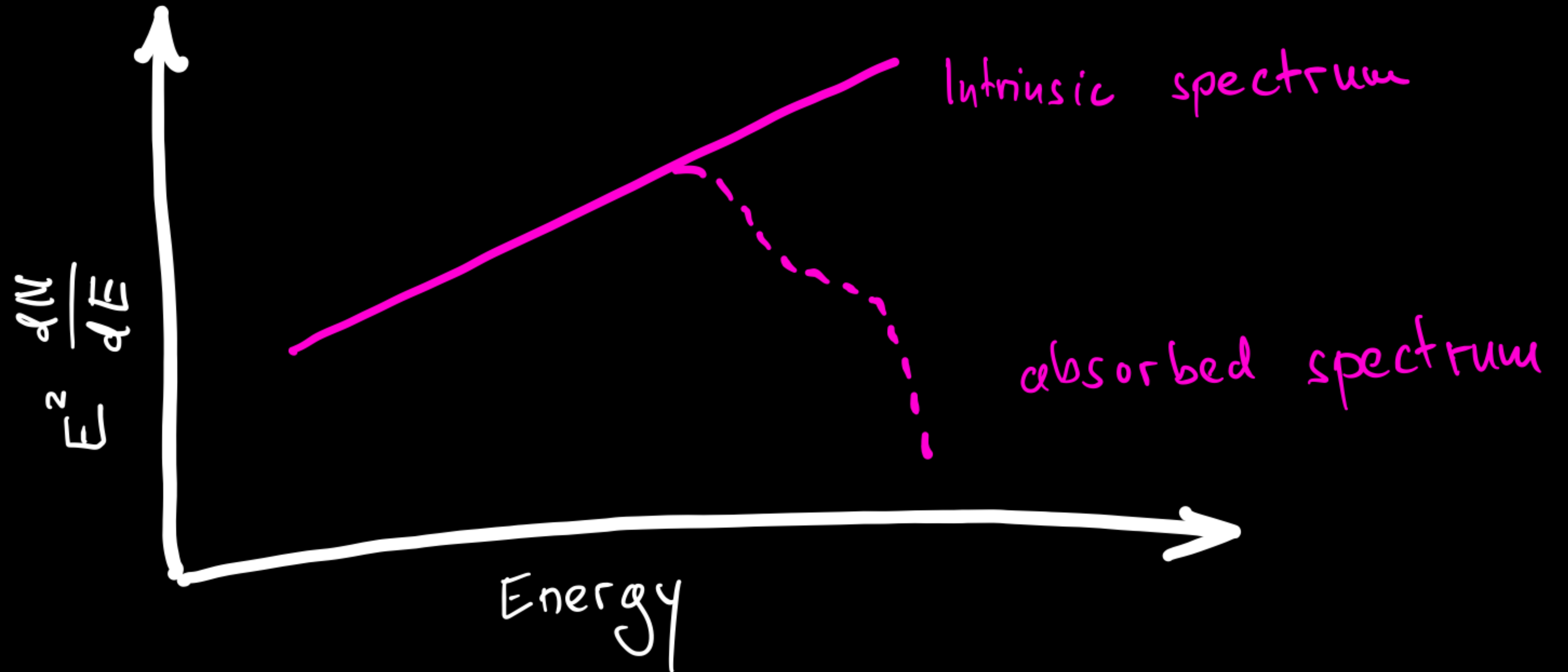


- Located in Khomas Highland in Namibia (22° S)
- Commenced operations in 2002
- Operations extended at least until 2025
- Energy coverage: above 50 GeV up to 100 TeV
- Field of view: 3° - 5°
- Angular resolution: 3 to 6 arcsin

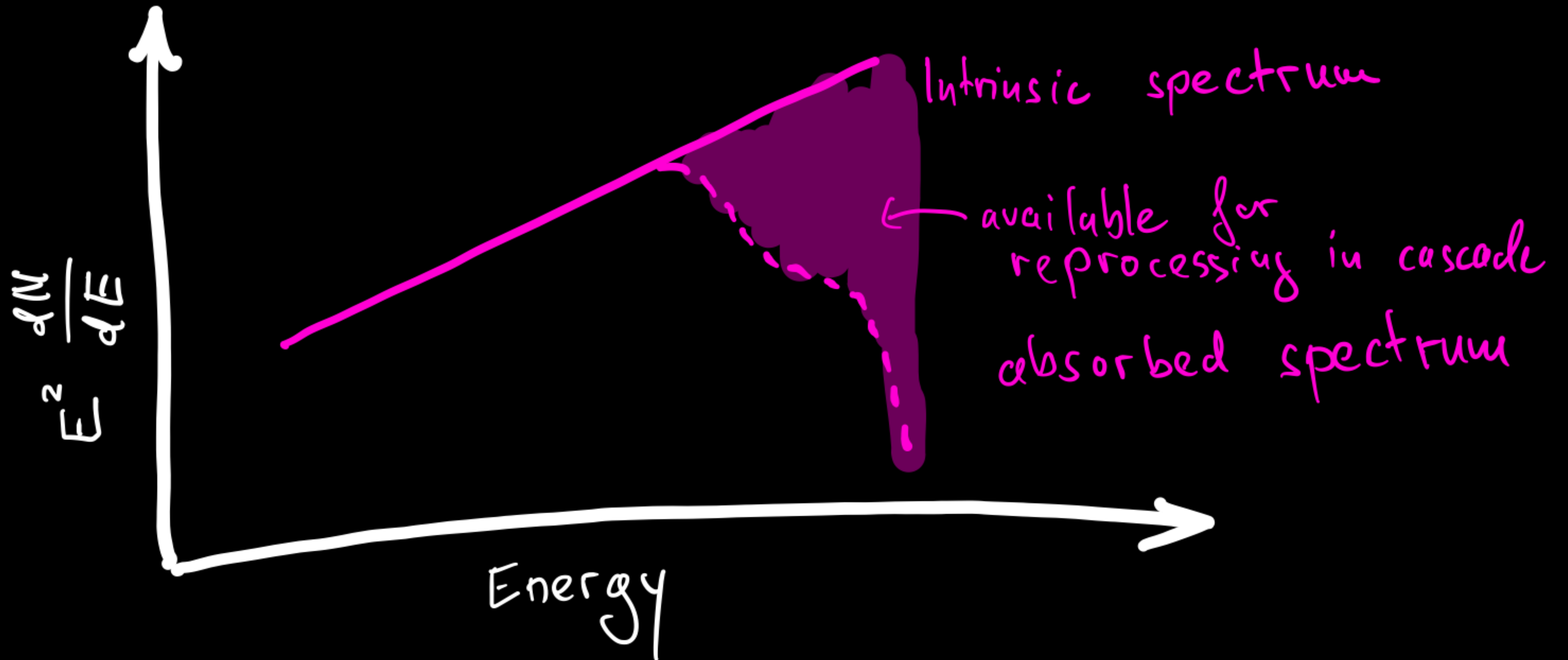
Basic idea



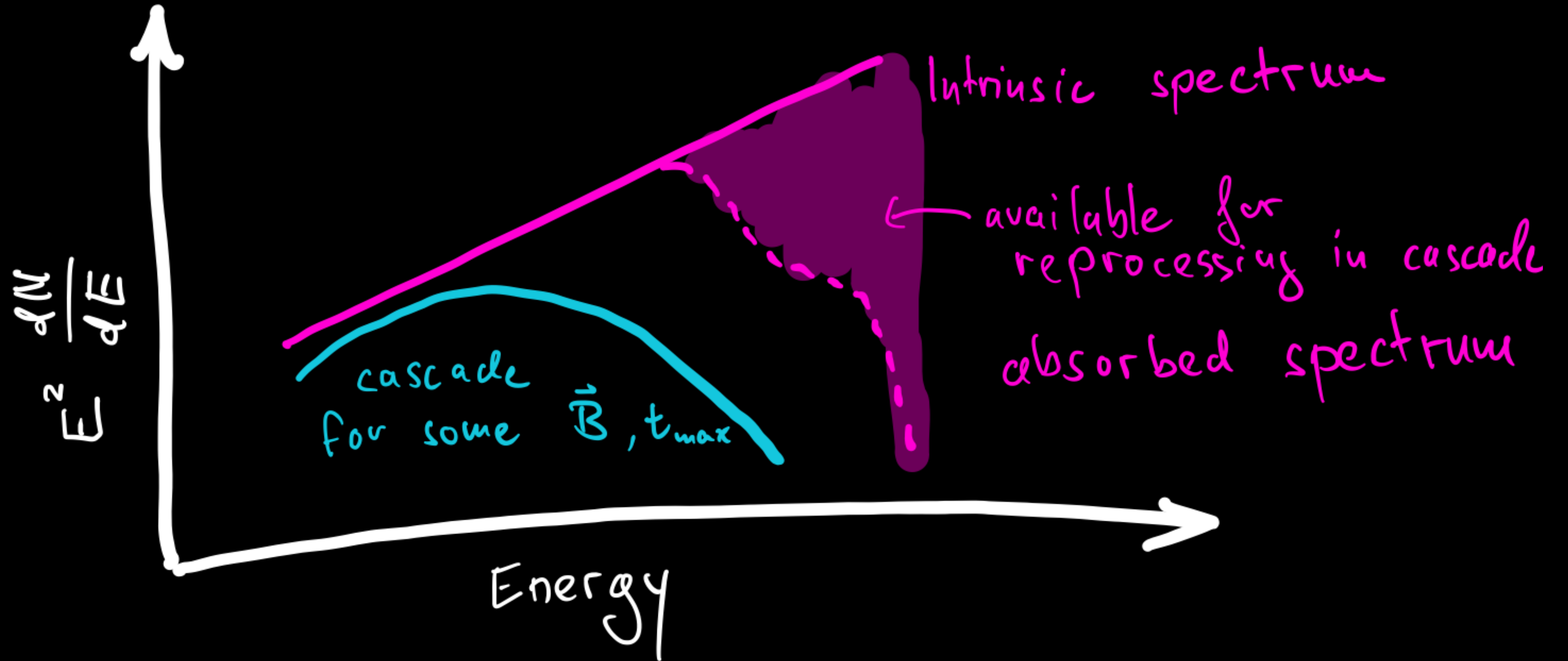
Basic idea



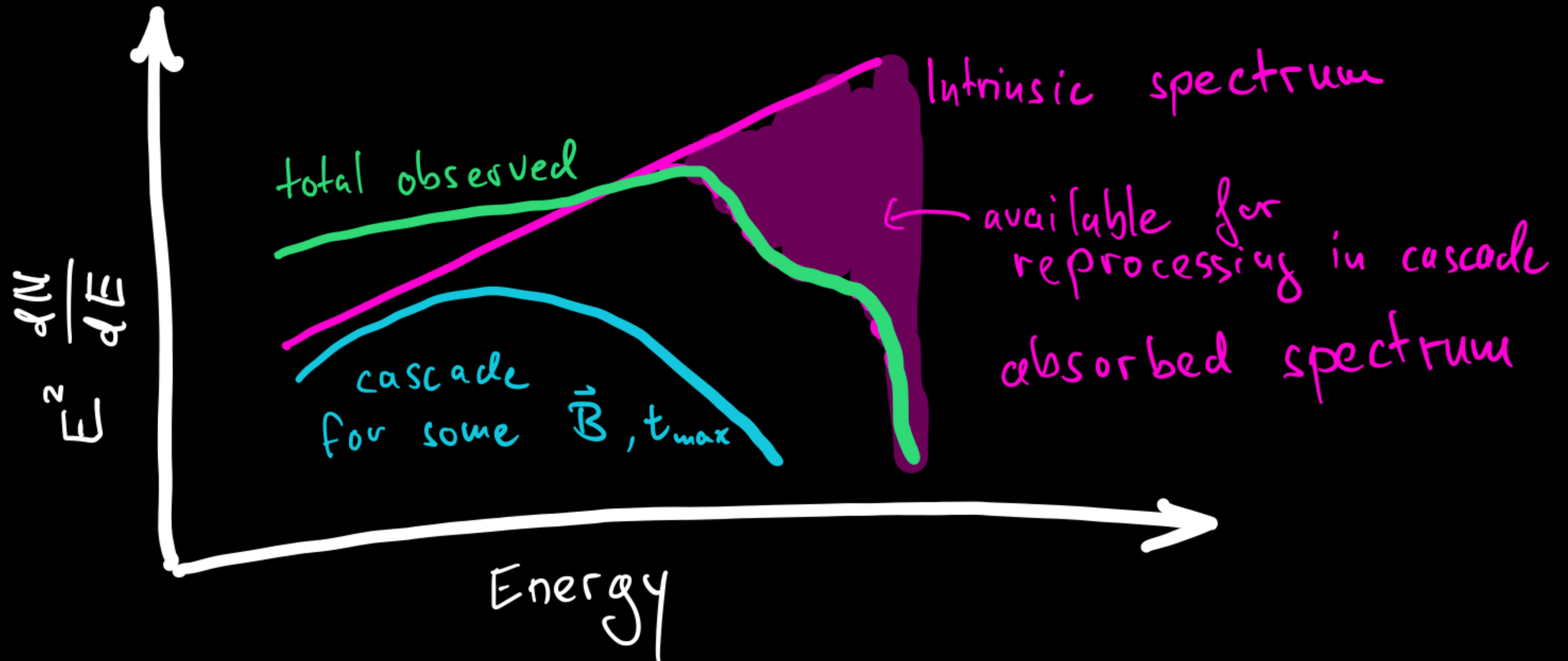
Basic idea



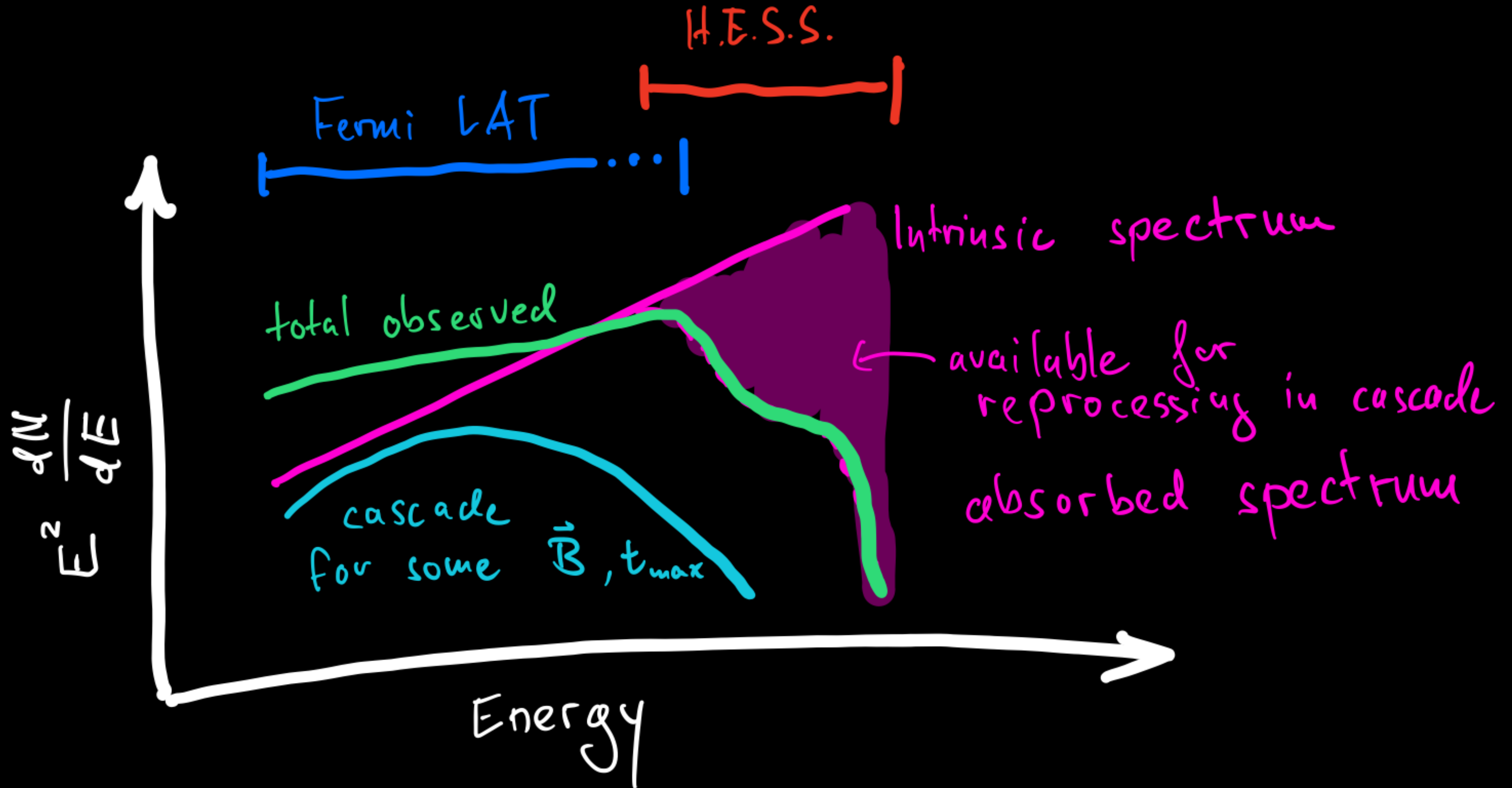
Basic idea



Basic idea



Basic idea



Source Selection

Source Selection

- **Demands:**

Source Selection

- **Demands:**
 - Emission at energies corresponding to high optical depth

Source Selection

- **Demands:**
 - Emission at energies corresponding to high optical depth
 - Stable gamma-ray emission in time as seen with the LAT

Source Selection

- **Demands:**
 - Emission at energies corresponding to high optical depth
 - Stable gamma-ray emission in time as seen with the LAT
 - \Rightarrow extreme HBL sources

Source Selection

- **Demands:**
 - Emission at energies corresponding to high optical depth
 - Stable gamma-ray emission in time as seen with the LAT
 - \Rightarrow extreme HBL sources
- **Source selection from 4LAC-DR2 catalog:**

Source Selection

- **Demands:**
 - Emission at energies corresponding to high optical depth
 - Stable gamma-ray emission in time as seen with the LAT
 - \Rightarrow extreme HBL sources
- **Source selection from 4LAC-DR2 catalog:**
 - Spectral type: power law & $\Gamma + \sigma_{\Gamma} < 2$

Source Selection

- **Demands:**
 - Emission at energies corresponding to high optical depth
 - Stable gamma-ray emission in time as seen with the LAT
 - \Rightarrow extreme HBL sources
- **Source selection from 4LAC-DR2 catalog:**
 - Spectral type: power law & $\Gamma + \sigma_{\Gamma} < 2$
 - Redshift known

Source Selection

- **Demands:**
 - Emission at energies corresponding to high optical depth
 - Stable gamma-ray emission in time as seen with the LAT
 - \Rightarrow extreme HBL sources
- **Source selection from 4LAC-DR2 catalog:**
 - Spectral type: power law & $\Gamma + \sigma_{\Gamma} < 2$
 - Redshift known
 - BL Lac source type with synchrotron peak $\nu_{\text{Synch}} > 10^{17}$ Hz

Source Selection

- **Demands:**
 - Emission at energies corresponding to high optical depth
 - Stable gamma-ray emission in time as seen with the LAT
 - \Rightarrow extreme HBL sources
- **Source selection from 4LAC-DR2 catalog:**
 - Spectral type: power law & $\Gamma + \sigma_{\Gamma} < 2$
 - Redshift known
 - BL Lac source type with synchrotron peak $\nu_{\text{Synch}} > 10^{17}$ Hz
 - Chance probability < 99% that source is variable

Source Selection

- **Demands:**
 - Emission at energies corresponding to high optical depth
 - Stable gamma-ray emission in time as seen with the LAT
 - \Rightarrow extreme HBL sources
- **Source selection from 4LAC-DR2 catalog:**
 - Spectral type: power law & $\Gamma + \sigma_{\Gamma} < 2$
 - Redshift known
 - BL Lac source type with synchrotron peak $\nu_{\text{sync}} > 10^{17}$ Hz
 - Chance probability < 99% that source is variable
 - Sources with TeV counterpart observed with H.E.S.S.

Source Selection

- **Demands:**
 - Emission at energies corresponding to high optical depth
 - Stable gamma-ray emission in time as seen with the LAT
 - \Rightarrow extreme HBL sources
- **Source selection from 4LAC-DR2 catalog:**
 - Spectral type: power law & $\Gamma + \sigma_{\Gamma} < 2$
 - Redshift known
 - BL Lac source type with synchrotron peak $\nu_{\text{Sync}} > 10^{17}$ Hz
 - Chance probability < 99% that source is variable
 - Sources with TeV counterpart observed with H.E.S.S.

Resulting sources:

| Source Name | Redshift |
|---------------------|----------|
| 1ES 0229+200 | 0,139 |
| 1ES 0347-121 | 0,188 |
| PKS 0548-322 | 0,069 |
| 1ES 1101-232 | 0,186 |
| H 2356-309 | 0,165 |

Modeling the halo with CRPropa3

Modeling the halo with CRPropa3

- CRPropa 3 Monte Carlo Code used to generate 4D (spatial + energy + delay time) halo templates

Modeling the halo with CRPropa3

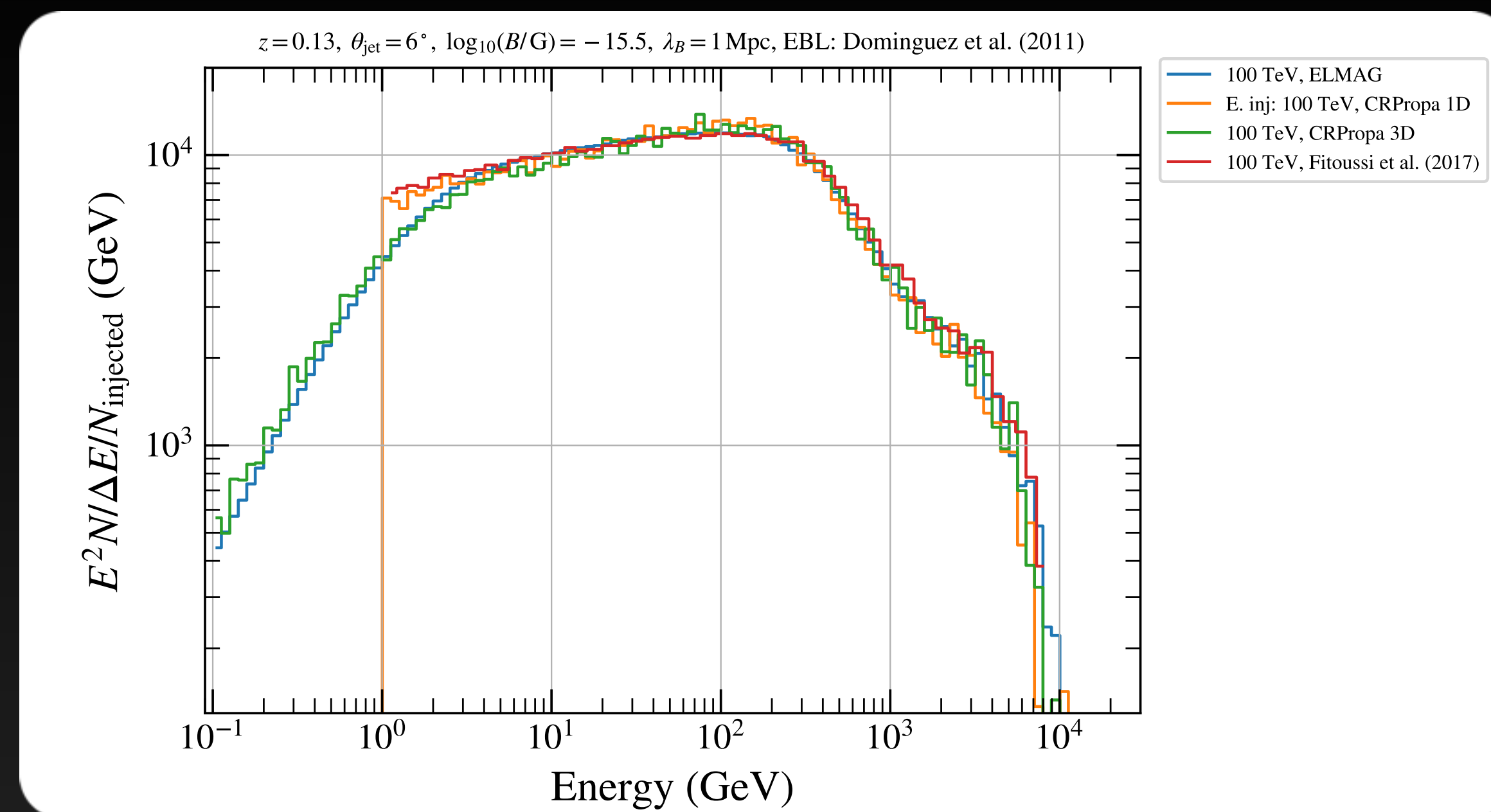
- CRPropa 3 Monte Carlo Code used to generate 4D (spatial + energy + delay time) halo templates
- Assumed magnetic field:
 - $B = 10^{-16} \text{ G}, \dots, 10^{-13} \text{ G}$
 - $\lambda_B = 1 \text{ Mpc}$

Modeling the halo with CRPropa3

- CRPropa 3 Monte Carlo Code used to generate 4D (spatial + energy + delay time) halo templates
- Assumed magnetic field:
 - $B = 10^{-16} \text{ G}, \dots, 10^{-13} \text{ G}$
 - $\lambda_B = 1 \text{ Mpc}$
- EBL model of Dominguez et al. (2011)

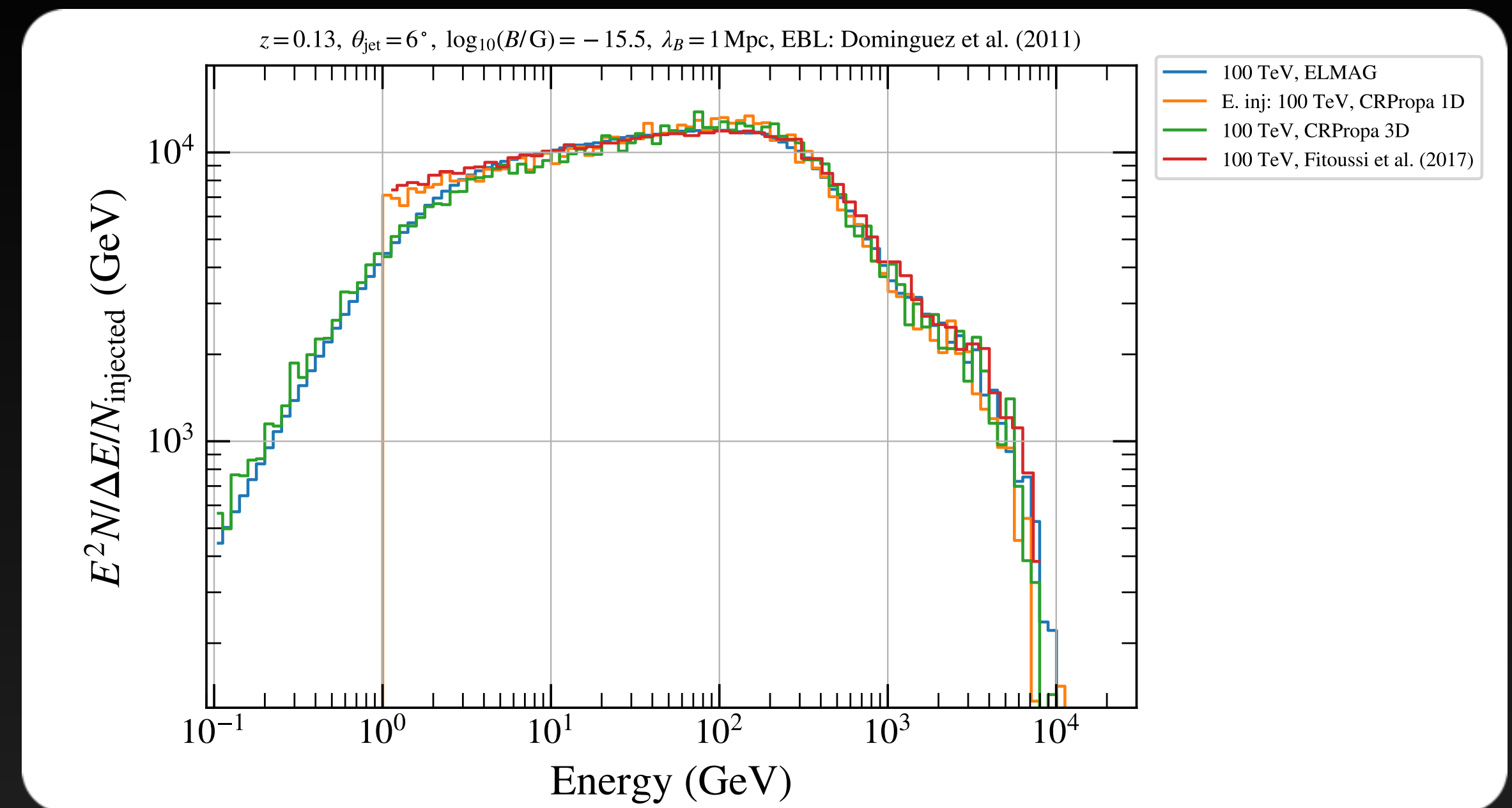
Modeling the halo with CRPropa3

- CRPropa 3 Monte Carlo Code used to generate 4D (spatial + energy + delay time) halo templates
- Assumed magnetic field:
 - $B = 10^{-16} \text{ G}, \dots, 10^{-13} \text{ G}$
 - $\lambda_B = 1 \text{ Mpc}$
- EBL model of Dominguez et al. (2011)



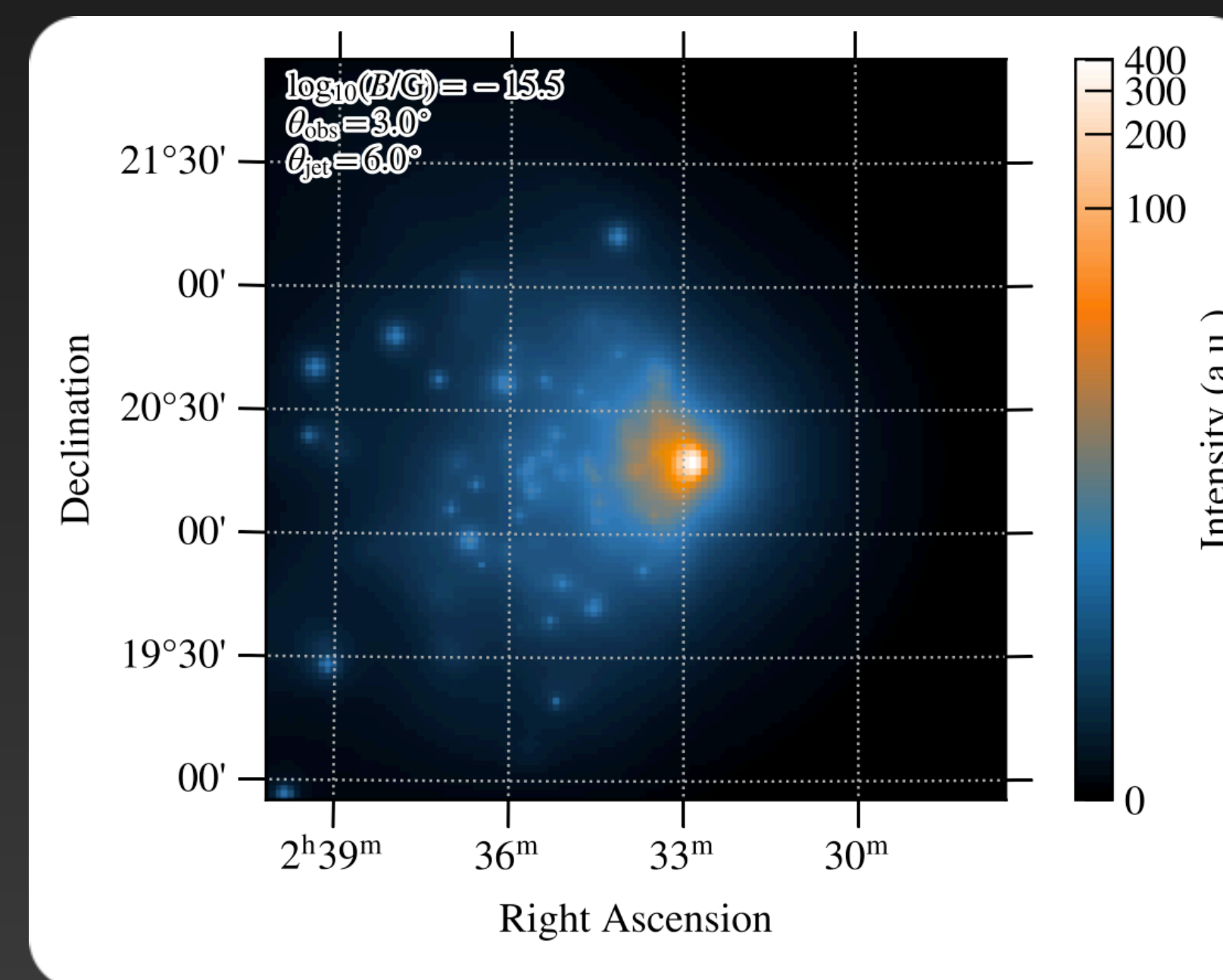
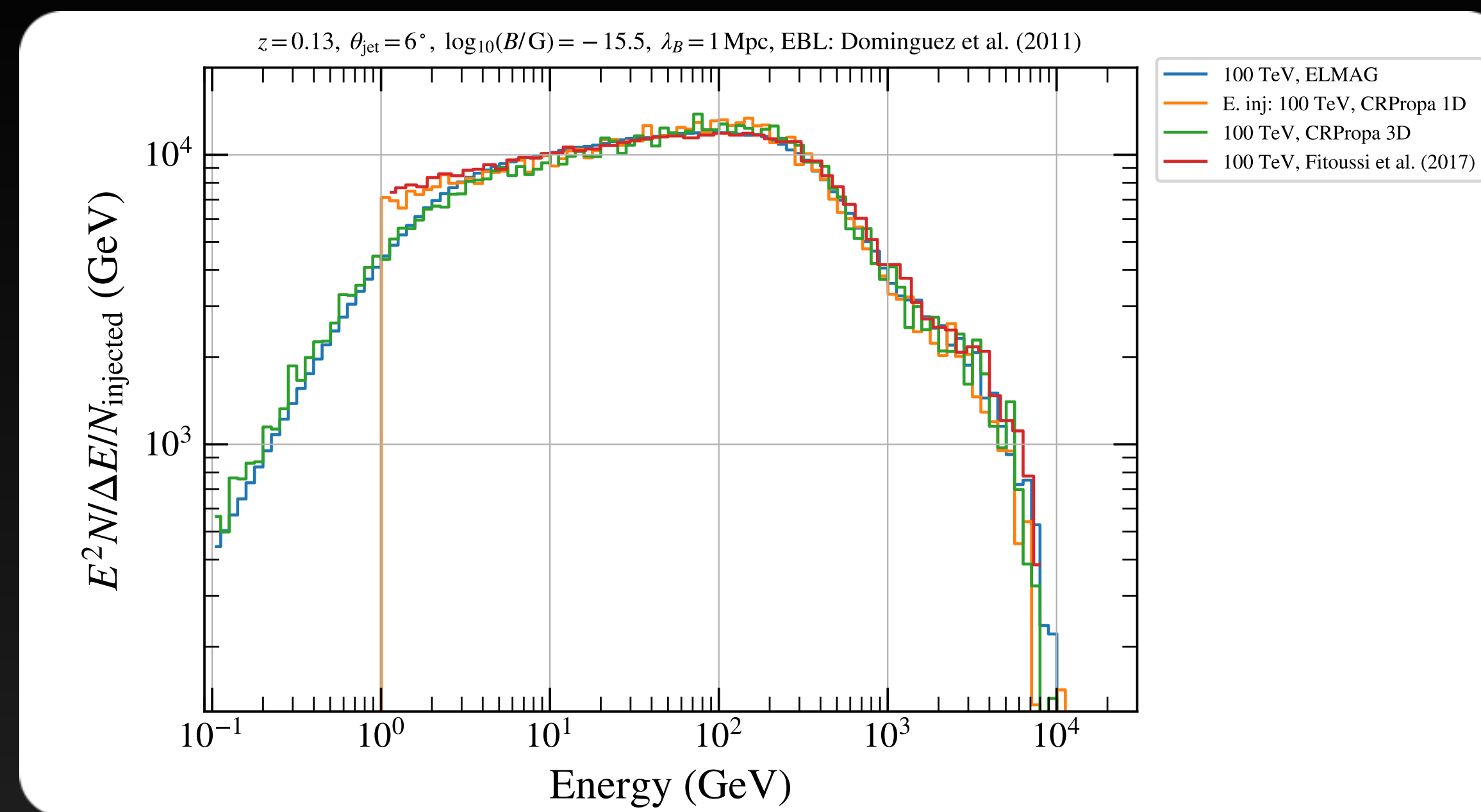
Modeling the halo with CRPropa3

- CRPropa 3 Monte Carlo Code used to generate 4D (spatial + energy + delay time) halo templates
- Assumed magnetic field:
 - $B = 10^{-16} \text{ G}, \dots, 10^{-13} \text{ G}$
 - $\lambda_B = 1 \text{ Mpc}$
- EBL model of Dominguez et al. (2011)
- Developed python wrapper in order to:
 - Reweight simulations for different input spectra [Ackermann et al. 2018]
 - Smooth sky maps adaptively [Ebeling et al. 2006]
 - Change orientation between source and observer in post processing [Alves Batista et al. 2016]
 - Change blazar activity time



Modeling the halo with CRPropa3

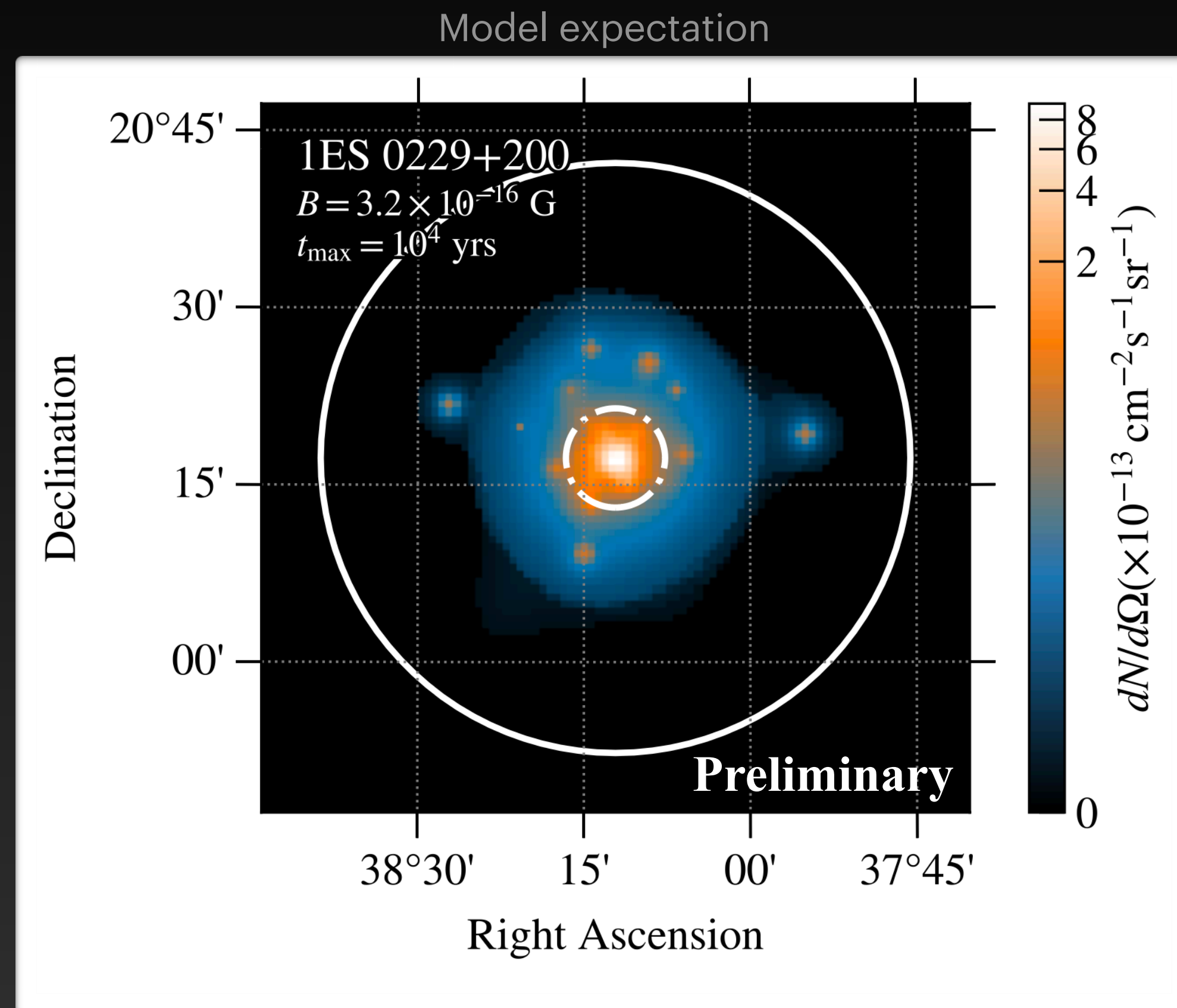
- CRPropa 3 Monte Carlo Code used to generate 4D (spatial + energy + delay time) halo templates
- Assumed magnetic field:
 - $B = 10^{-16} \text{ G}, \dots, 10^{-13} \text{ G}$
 - $\lambda_B = 1 \text{ Mpc}$
- EBL model of Dominguez et al. (2011)
- Developed [python wrapper](#) in order to:
 - Reweight simulations for different input spectra [Ackermann et al. 2018]
 - Smooth sky maps adaptively [Ebeling et al. 2006]
 - Change orientation between source and observer in post processing [Alves Batista et al. 2016]
 - Change blazar activity time



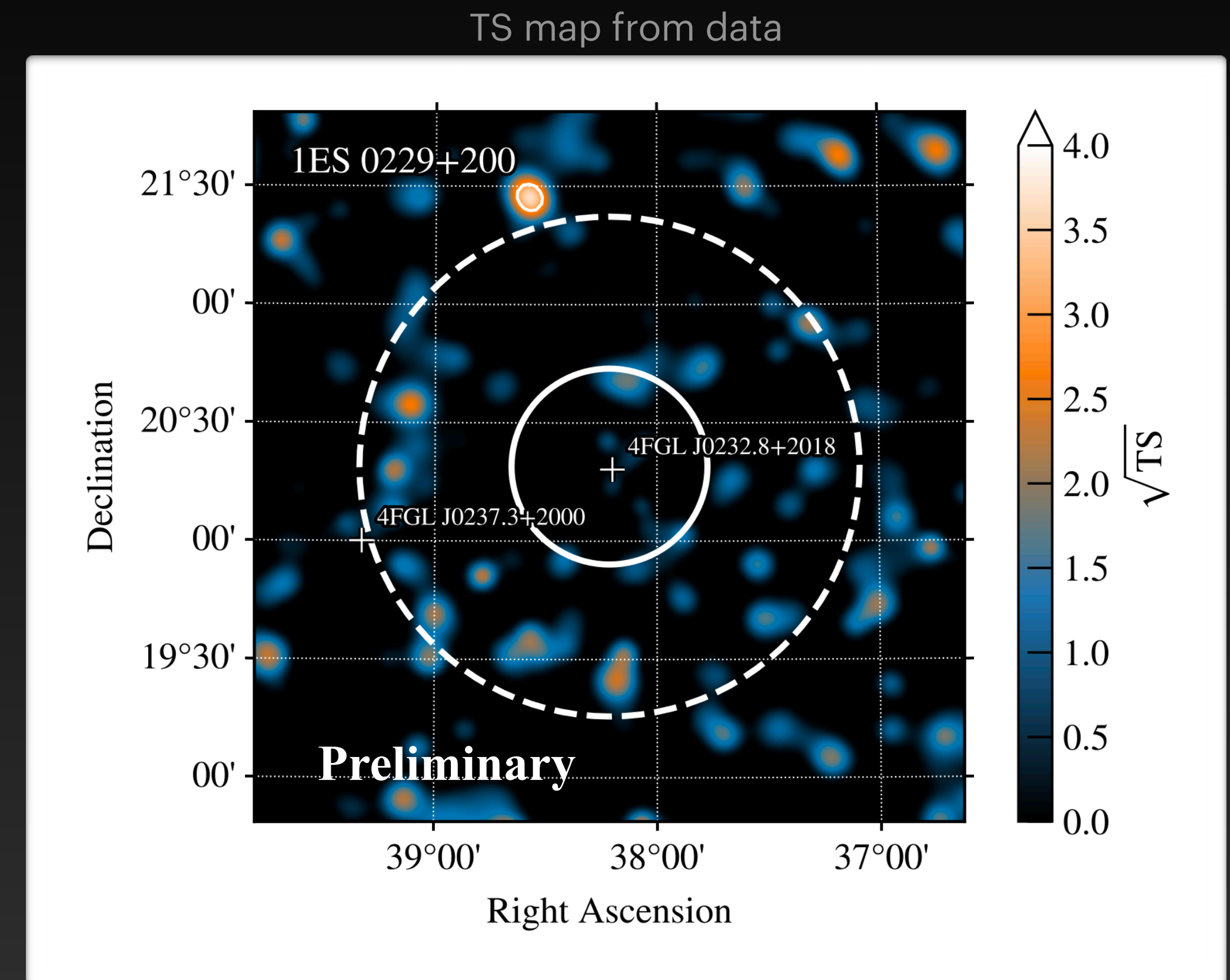
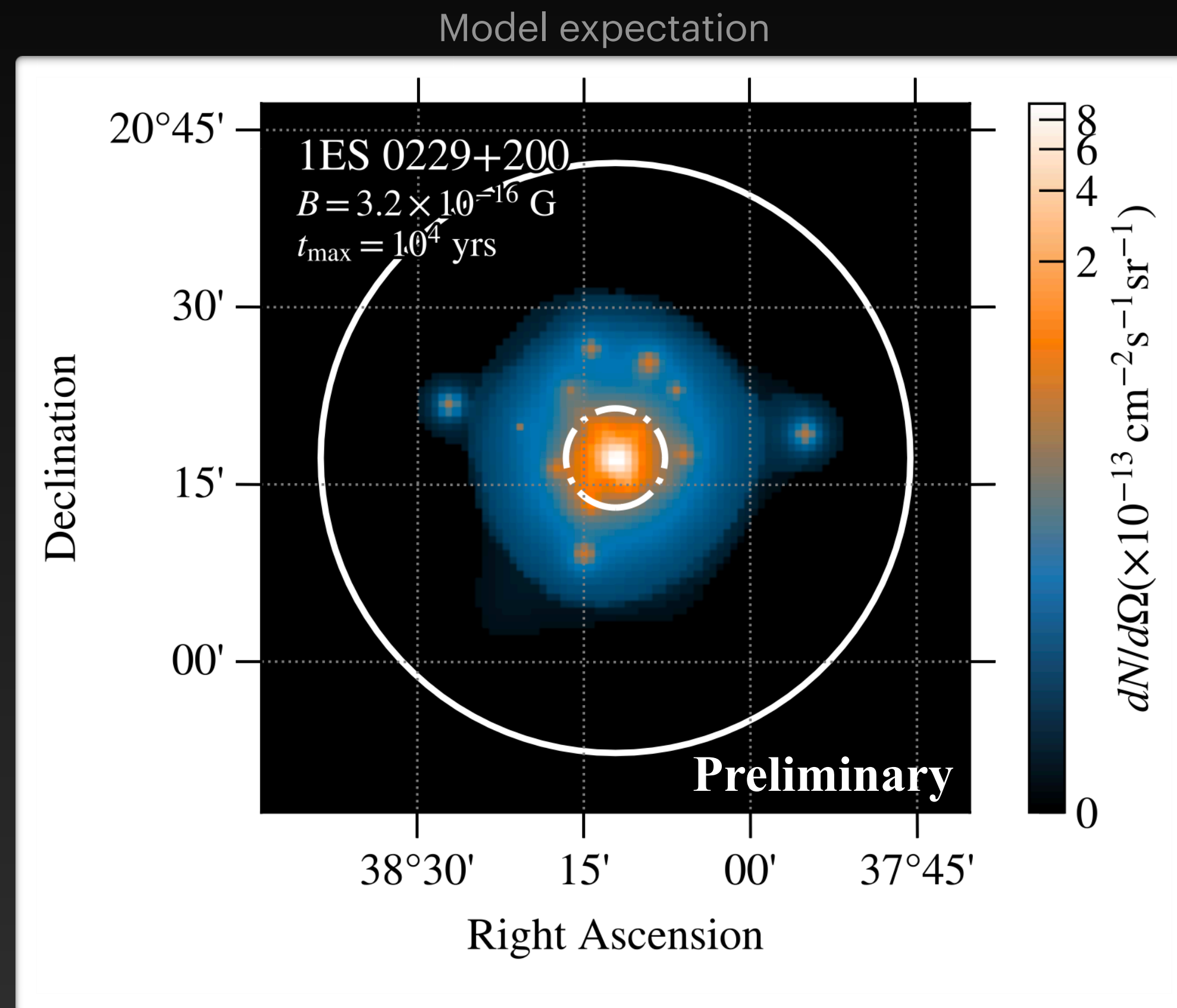
Fermi-LAT data selection

| Parameter | Selection |
|--------------------|------------------------------|
| Time range | 11.5 years |
| Energy Range | > 1 GeV |
| ROI size | 6° x 6° |
| Max. Zenith angle | 100° |
| Filter | DATA_QUAL>0 && LAT_CONFIG==1 |
| Spatial binning | 0.025° / pixel |
| Energy binning | 8 bins per decade |
| Event Class / IRFs | P8R3_SOURCE_V3, inflight PSF |
| Event types | PSF0-2, PSF3 |

Searching for cascade emission in LAT data

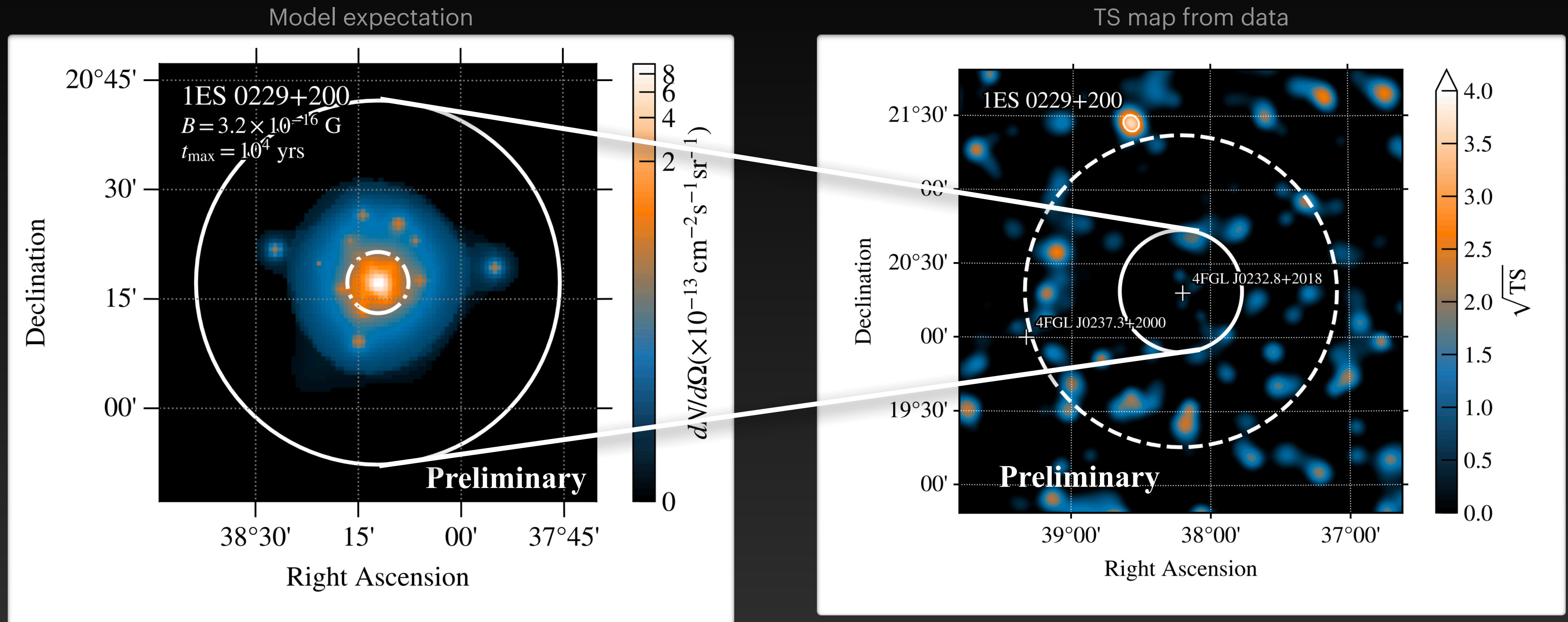


Searching for cascade emission in LAT data



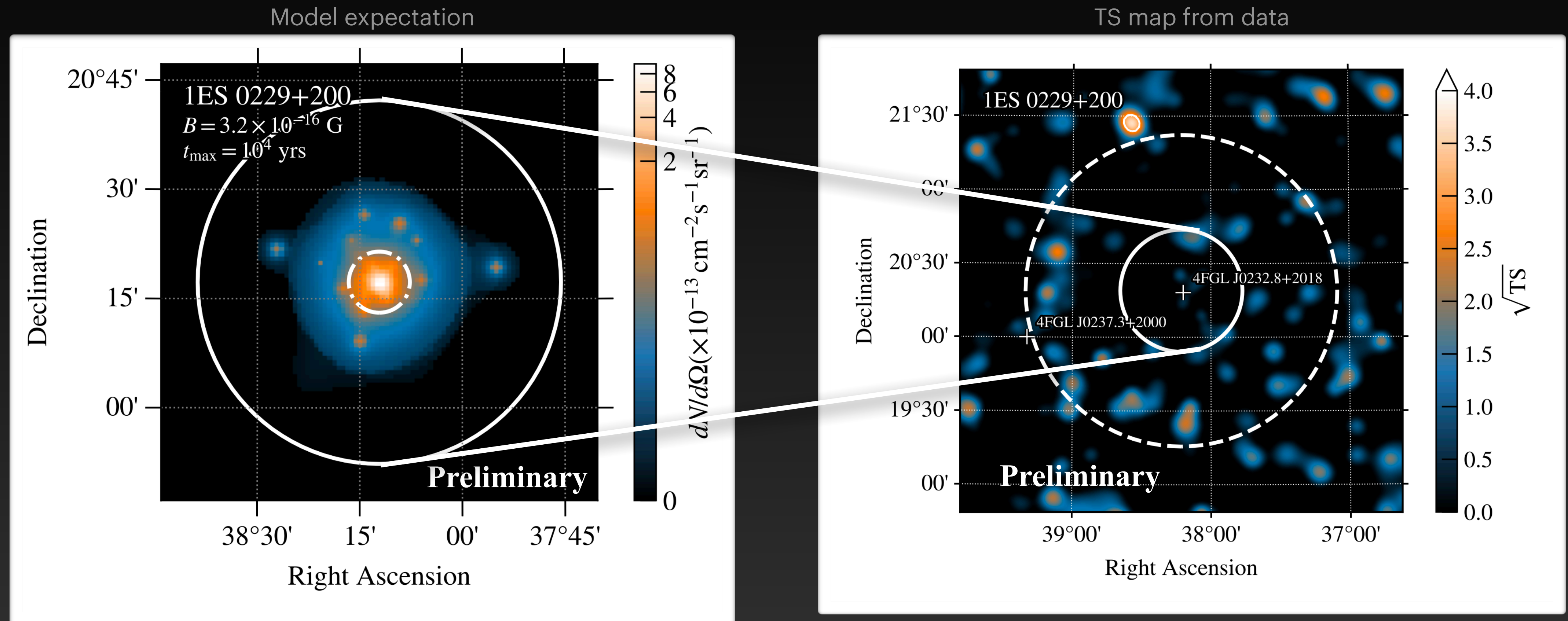
- TS map tests at each pixel if additional emission is present

Searching for cascade emission in LAT data



- TS map tests at each pixel if additional emission is present

Searching for cascade emission in LAT data



- TS map tests at each pixel if additional emission is present
- No un-modeled excess emission in vicinity of sources observed

Extracting LAT likelihoods in the presence of a halo

Some technical details

Extracting LAT likelihoods in the presence of a halo

Some technical details

- First step: standard LAT point source analysis (previous slide)

Extracting LAT likelihoods in the presence of a halo

Some technical details

- First step: standard LAT point source analysis (previous slide)
- For each simulated IGMF strength:

Extracting LAT likelihoods in the presence of a halo

Some technical details

- First step: standard LAT point source analysis (previous slide)
- For each simulated IGMF strength:
 - Change point source model to $\phi_{\text{obs}} = N(E/E_0)^{-\Gamma} \exp(-E/E_{\text{cut}}) \exp(-\tau)$

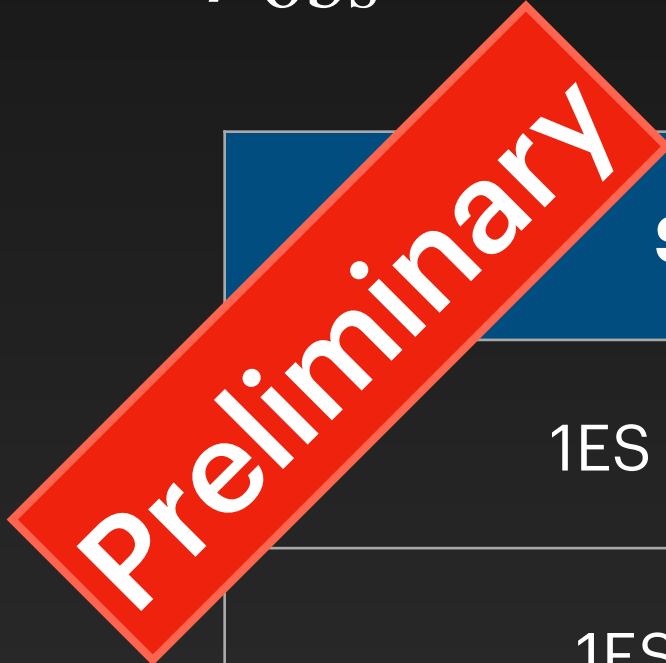
Extracting LAT likelihoods in the presence of a halo

Some technical details

- First step: standard LAT point source analysis (previous slide)
- For each simulated IGMF strength:
 - Change point source model to $\phi_{\text{obs}} = N(E/E_0)^{-\Gamma} \exp(-E/E_{\text{cut}}) \exp(-\tau)$
 - Loop over spectral parameters, add corresponding halo template, extract likelihood of fit, $\ln \mathcal{L}_{\text{LAT}}$

H.E.S.S. Data sets

- Data taken with small telescopes up to 2018 considered here
- Analysis performed using gammapy [Deil et al. 2017]
- Source spectra ϕ_{obs} well described by power law including EBL absorption,
$$\phi_{\text{obs}} = N(E/E_0)^{-\Gamma} \exp(-\tau)$$



| Source | Life time (hours) | Detection significance | Power law index Γ |
|--------------|-------------------|------------------------|--------------------------|
| 1ES 0229+200 | 144,1 | 16.5 σ | 1.76 \pm 0.12 |
| 1ES 0347-121 | 59,2 | 16.1 σ | 2.12 \pm 0.15 |
| PKS 0548-322 | 53,9 | 10.2 σ | 1.92 \pm 0.12 |
| 1ES 1101-232 | 71,9 | 18.7 σ | 1.66 \pm 0.09 |
| H 2356-309 | 150,5 | 23.4 σ | 2.10 \pm 0.09 |

Combined H.E.S.S. and LAT analysis

Combined H.E.S.S. and LAT analysis

- Intrinsic blazar model:

$$\phi(E) = N \left(\frac{E}{E_0} \right)^{-\Gamma} \exp \left(-\frac{E}{E_{\text{cut}}} \right)$$

Combined H.E.S.S. and LAT analysis

- Intrinsic blazar model:

$$\phi(E) = N \left(\frac{E}{E_0} \right)^{-\Gamma} \exp \left(-\frac{E}{E_{\text{cut}}} \right)$$

- Total source model:

$$\phi_{\text{tot}}(E, B) = \phi(E) \exp(-\tau) + \phi_{\text{halo}}(E, B)$$

Combined H.E.S.S. and LAT analysis

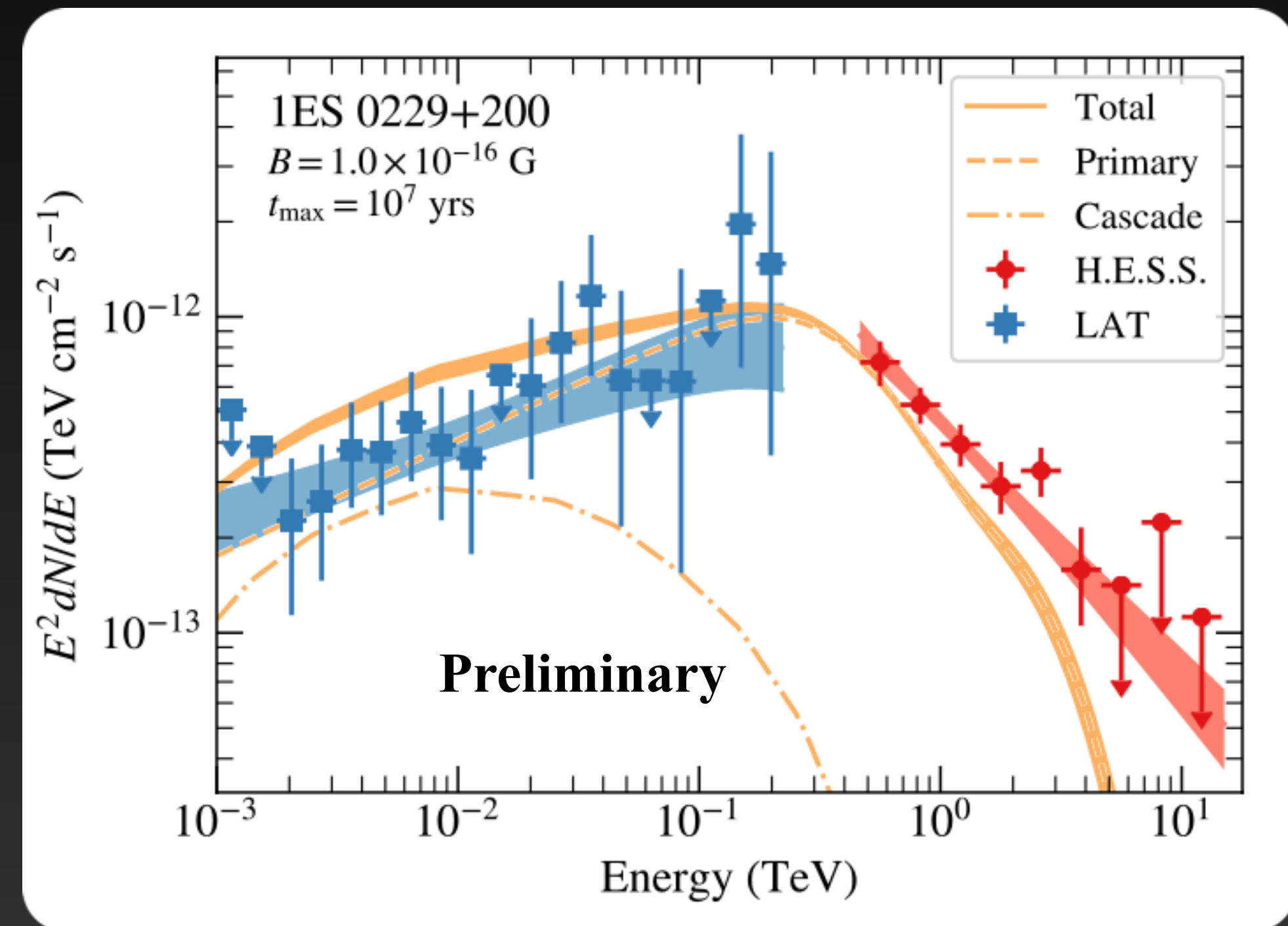
- Intrinsic blazar model:

$$\phi(E) = N \left(\frac{E}{E_0} \right)^{-\Gamma} \exp \left(-\frac{E}{E_{\text{cut}}} \right)$$

- Total source model:

$$\phi_{\text{tot}}(E, B) = \phi(E) \exp(-\tau) + \phi_{\text{halo}}(E, B)$$

- Halo flux taken from CRPropa3 simulation; depends on spectral parameters, blazar activity time...



Combined H.E.S.S. and LAT analysis

- Intrinsic blazar model:

$$\phi(E) = N \left(\frac{E}{E_0} \right)^{-\Gamma} \exp \left(-\frac{E}{E_{\text{cut}}} \right)$$

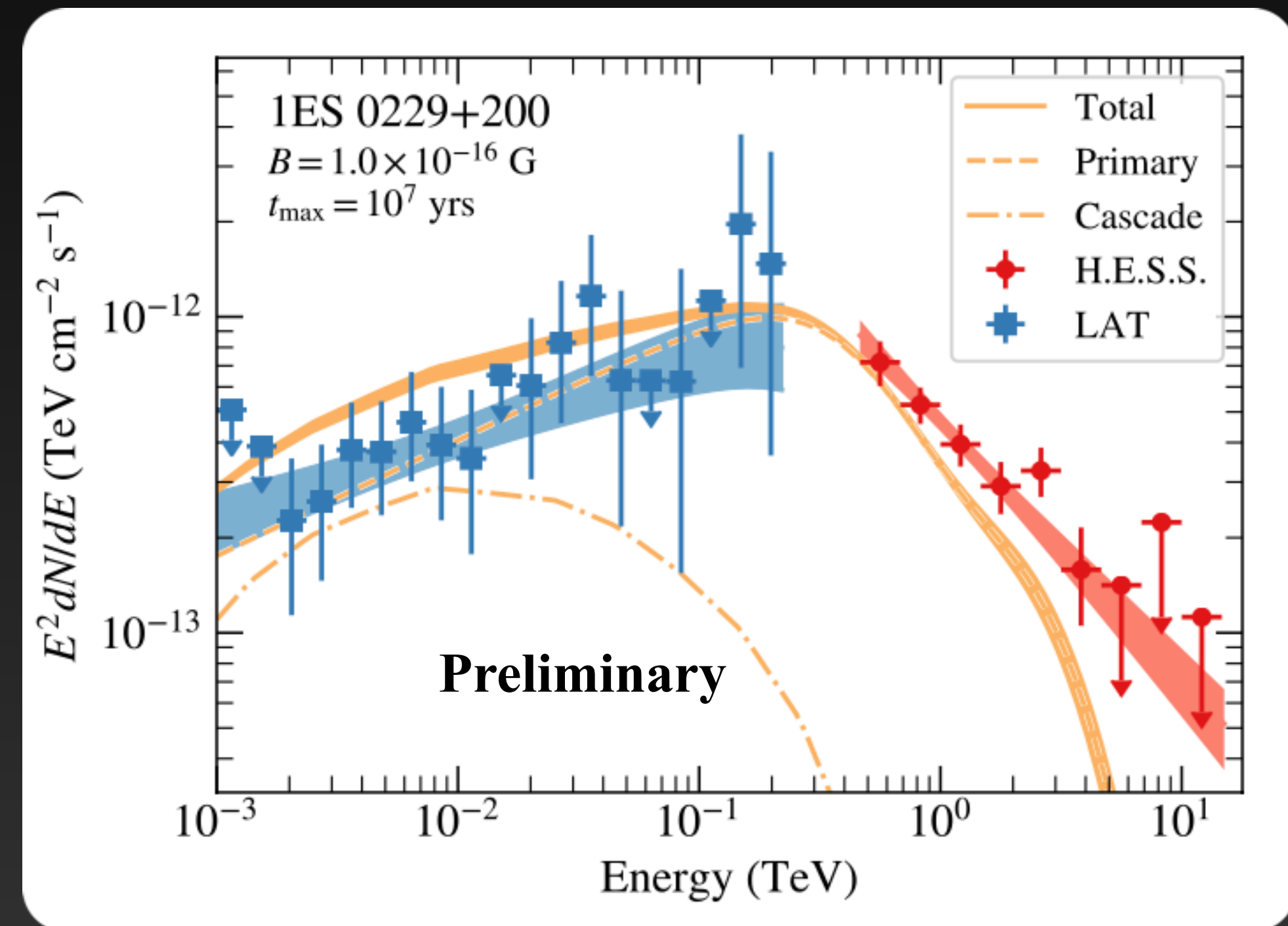
- Total source model:

$$\phi_{\text{tot}}(E, B) = \phi(E) \exp(-\tau) + \phi_{\text{halo}}(E, B)$$

- Halo flux taken from CRPropa3 simulation; depends on spectral parameters, blazar activity time...

- Spectral parameters optimized using combined H.E.S.S. and LAT likelihoods:

$$\ln \mathcal{L} = \ln \mathcal{L}_{\text{LAT}} + \ln \mathcal{L}_{\text{H.E.S.S.}}$$



Combined H.E.S.S. and LAT analysis

- Intrinsic blazar model:

$$\phi(E) = N \left(\frac{E}{E_0} \right)^{-\Gamma} \exp \left(-\frac{E}{E_{\text{cut}}} \right)$$

- Total source model:

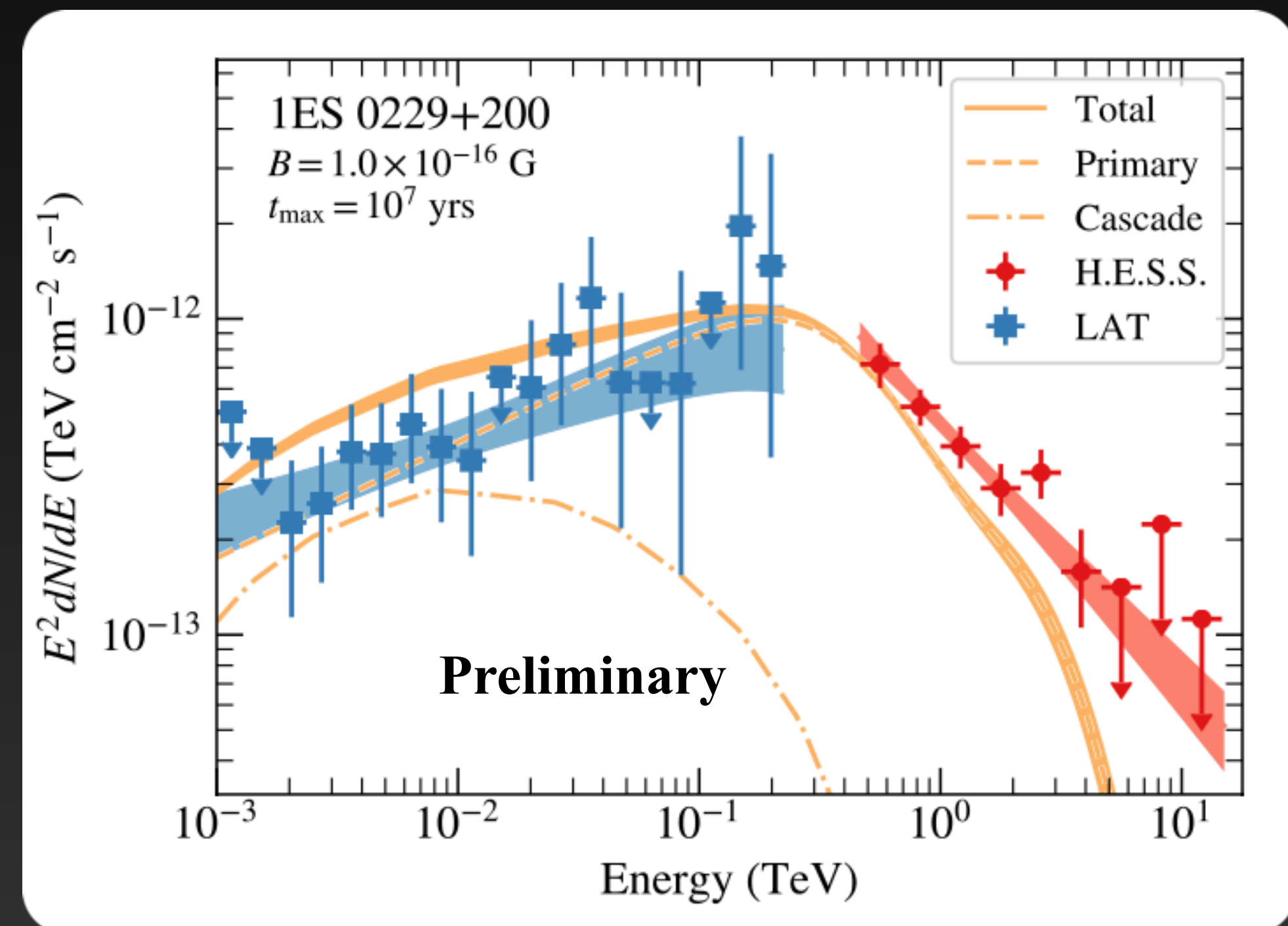
$$\phi_{\text{tot}}(E, B) = \phi(E) \exp(-\tau) + \phi_{\text{halo}}(E, B)$$

- Halo flux taken from CRPropa3 simulation; depends on spectral parameters, blazar activity time...

- Spectral parameters optimized using combined H.E.S.S. and LAT likelihoods:

$$\ln \mathcal{L} = \ln \mathcal{L}_{\text{LAT}} + \ln \mathcal{L}_{\text{H.E.S.S.}}$$

- Takes both spectral and spatial (for LAT) information into account



Combined H.E.S.S. and LAT analysis

- Intrinsic blazar model:

$$\phi(E) = N \left(\frac{E}{E_0} \right)^{-\Gamma} \exp \left(-\frac{E}{E_{\text{cut}}} \right)$$

- Total source model:

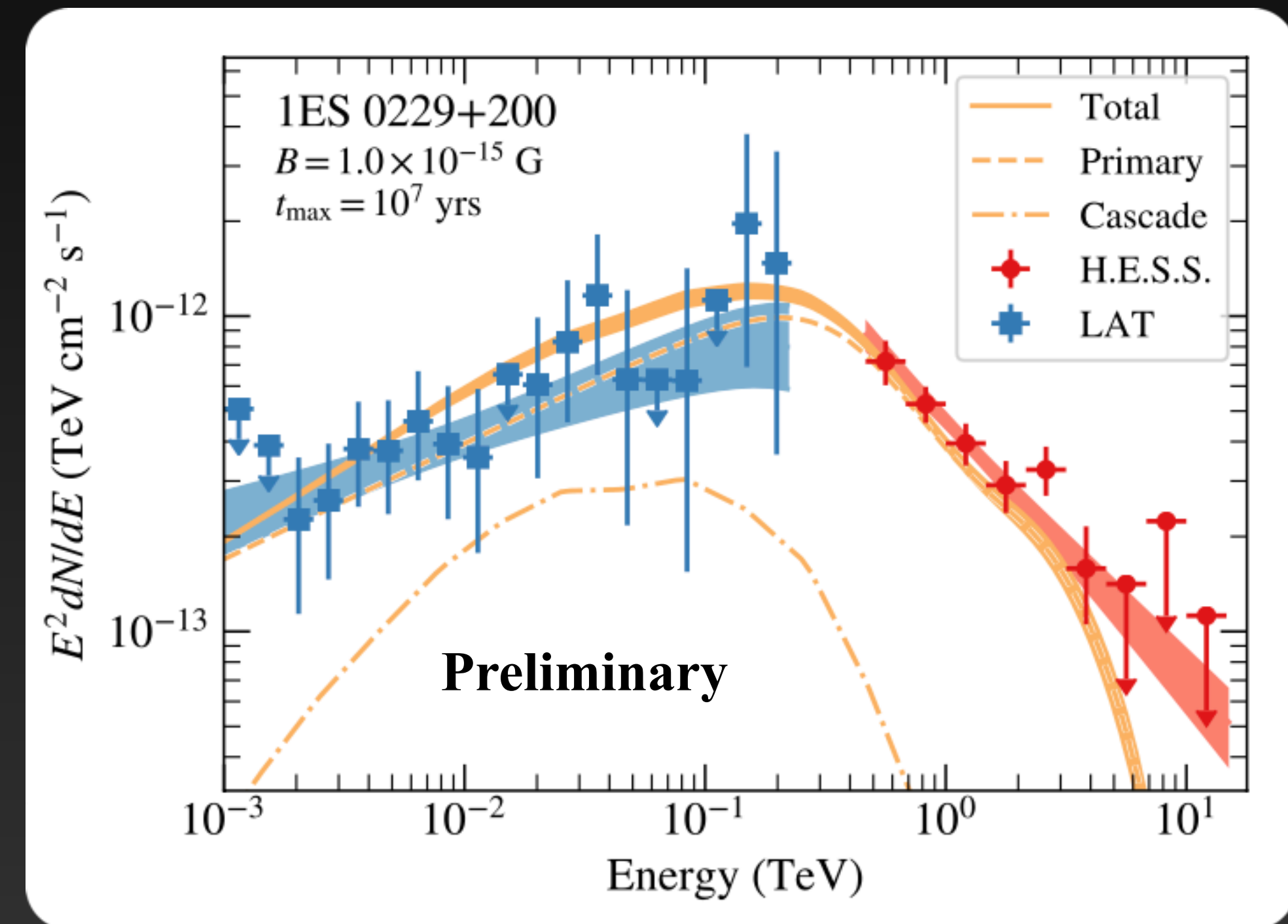
$$\phi_{\text{tot}}(E, B) = \phi(E) \exp(-\tau) + \phi_{\text{halo}}(E, B)$$

- Halo flux taken from CRPropa3 simulation; depends on spectral parameters, blazar activity time...

- Spectral parameters optimized using combined H.E.S.S. and LAT likelihoods:

$$\ln \mathcal{L} = \ln \mathcal{L}_{\text{LAT}} + \ln \mathcal{L}_{\text{H.E.S.S.}}$$

- Takes both spectral and spatial (for LAT) information into account



Combined H.E.S.S. and LAT analysis

- Intrinsic blazar model:

$$\phi(E) = N \left(\frac{E}{E_0} \right)^{-\Gamma} \exp \left(-\frac{E}{E_{\text{cut}}} \right)$$

- Total source model:

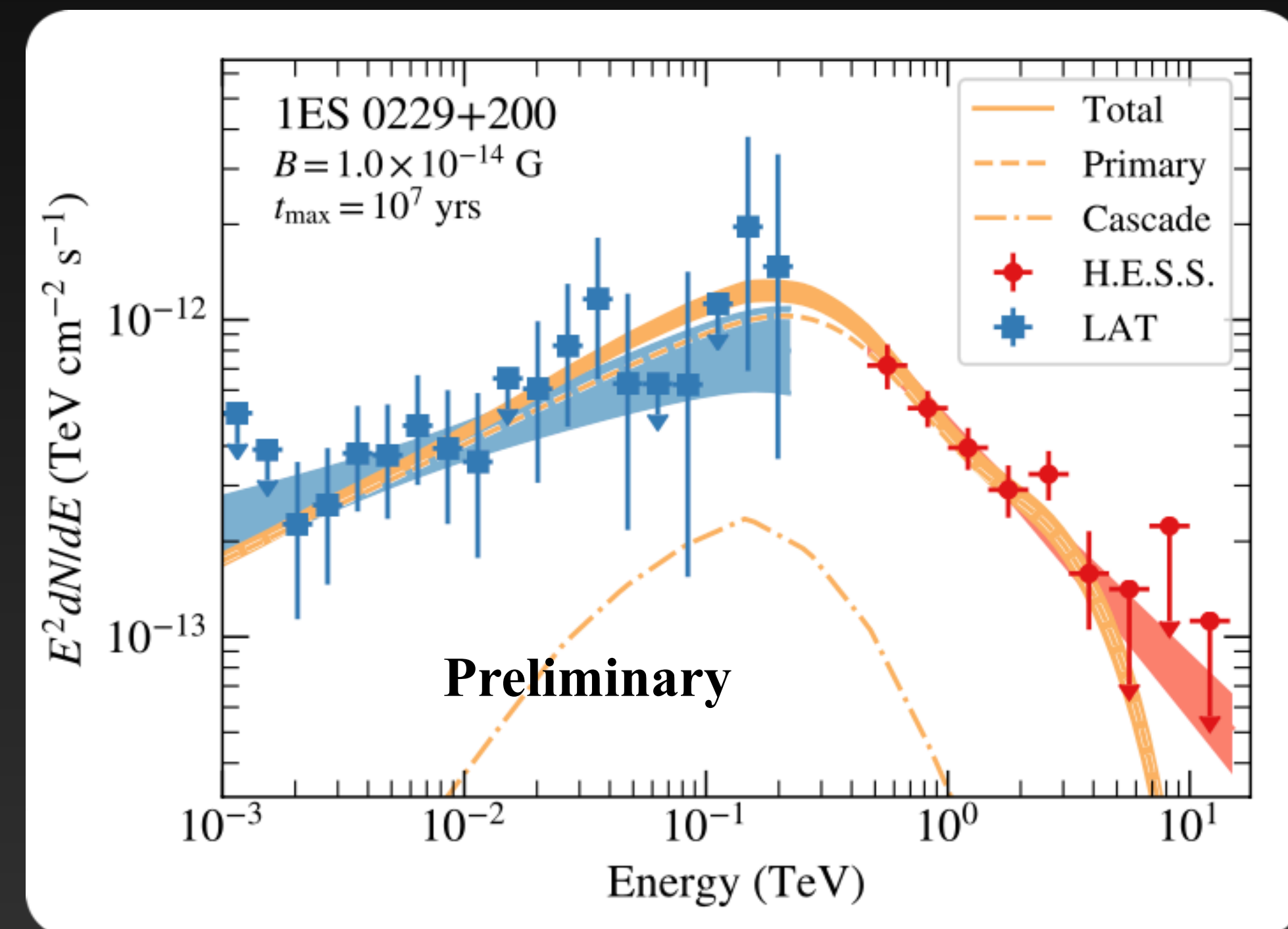
$$\phi_{\text{tot}}(E, B) = \phi(E) \exp(-\tau) + \phi_{\text{halo}}(E, B)$$

- Halo flux taken from CRPropa3 simulation; depends on spectral parameters, blazar activity time...

- Spectral parameters optimized using combined H.E.S.S. and LAT likelihoods:

$$\ln \mathcal{L} = \ln \mathcal{L}_{\text{LAT}} + \ln \mathcal{L}_{\text{H.E.S.S.}}$$

- Takes both spectral and spatial (for LAT) information into account



Combined H.E.S.S. and LAT analysis

- Intrinsic blazar model:

$$\phi(E) = N \left(\frac{E}{E_0} \right)^{-\Gamma} \exp \left(-\frac{E}{E_{\text{cut}}} \right)$$

- Total source model:

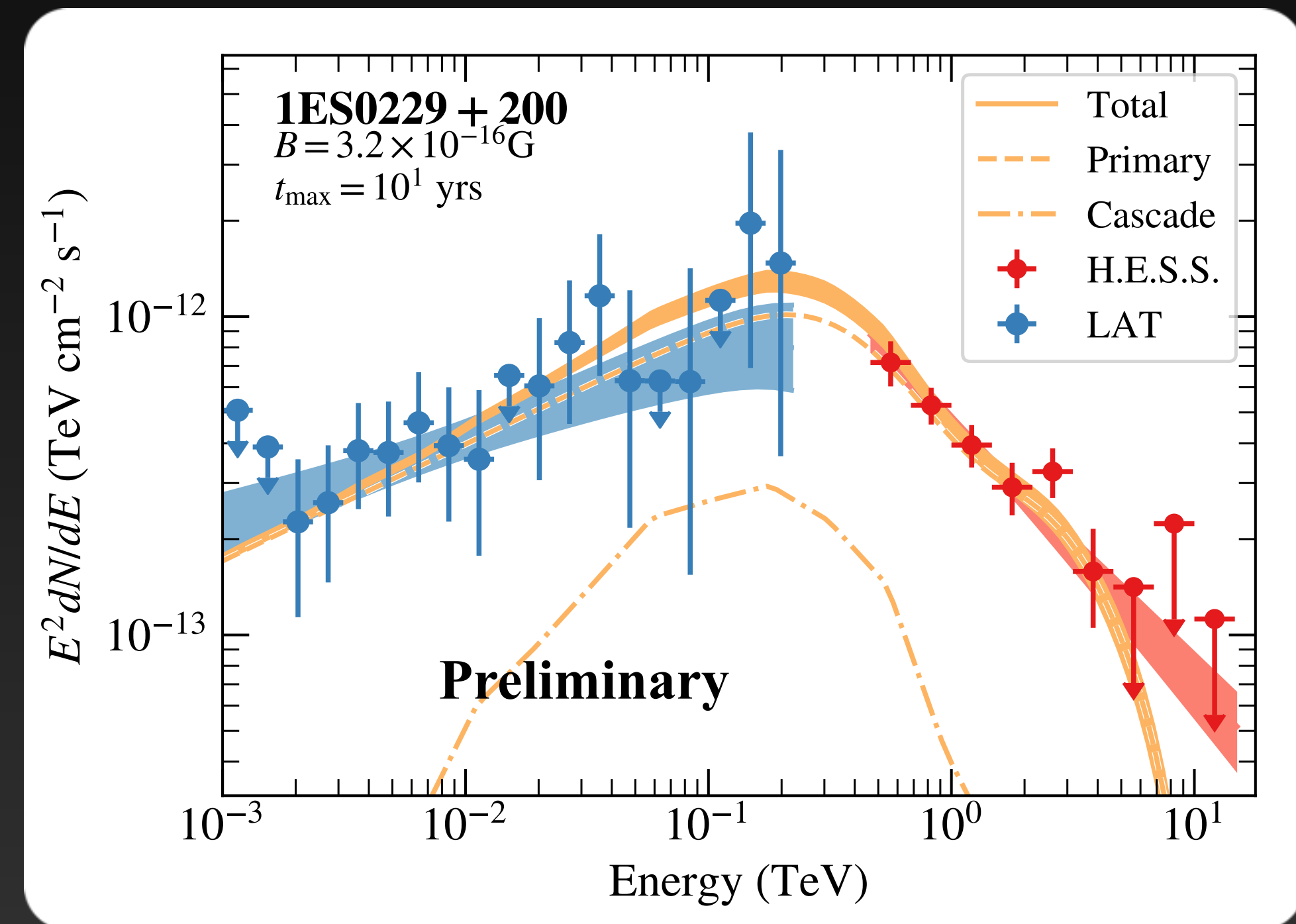
$$\phi_{\text{tot}}(E, B) = \phi(E) \exp(-\tau) + \phi_{\text{halo}}(E, B)$$

- Halo flux taken from CRPropa3 simulation; depends on spectral parameters, blazar activity time...

- Spectral parameters optimized using combined H.E.S.S. and LAT likelihoods:

$$\ln \mathcal{L} = \ln \mathcal{L}_{\text{LAT}} + \ln \mathcal{L}_{\text{H.E.S.S.}}$$

- Takes both spectral and spatial (for LAT) information into account



Combined H.E.S.S. and LAT analysis

- Intrinsic blazar model:

$$\phi(E) = N \left(\frac{E}{E_0} \right)^{-\Gamma} \exp \left(-\frac{E}{E_{\text{cut}}} \right)$$

- Total source model:

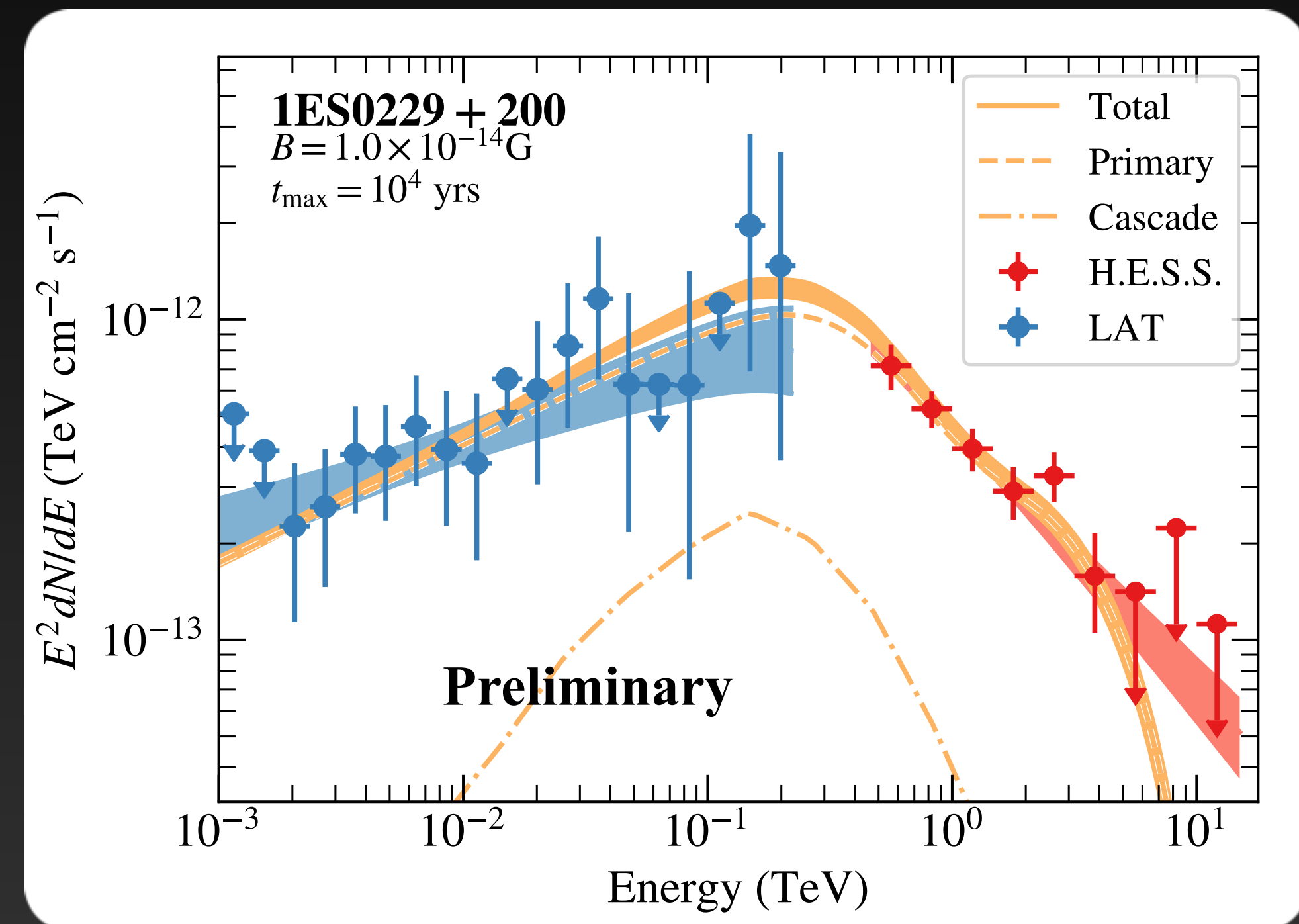
$$\phi_{\text{tot}}(E, B) = \phi(E) \exp(-\tau) + \phi_{\text{halo}}(E, B)$$

- Halo flux taken from CRPropa3 simulation; depends on spectral parameters, blazar activity time...

- Spectral parameters optimized using combined H.E.S.S. and LAT likelihoods:

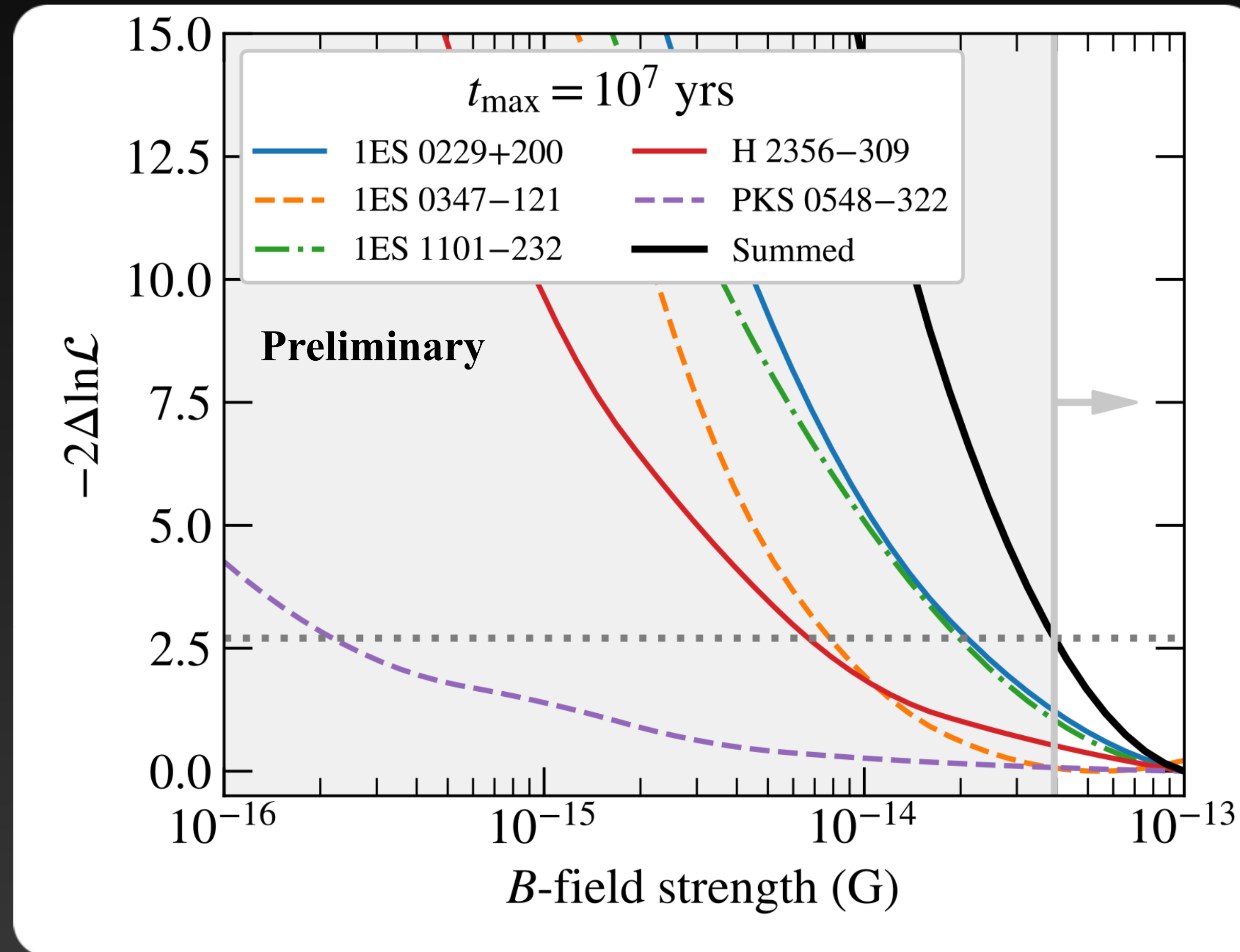
$$\ln \mathcal{L} = \ln \mathcal{L}_{\text{LAT}} + \ln \mathcal{L}_{\text{H.E.S.S.}}$$

- Takes both spectral and spatial (for LAT) information into account



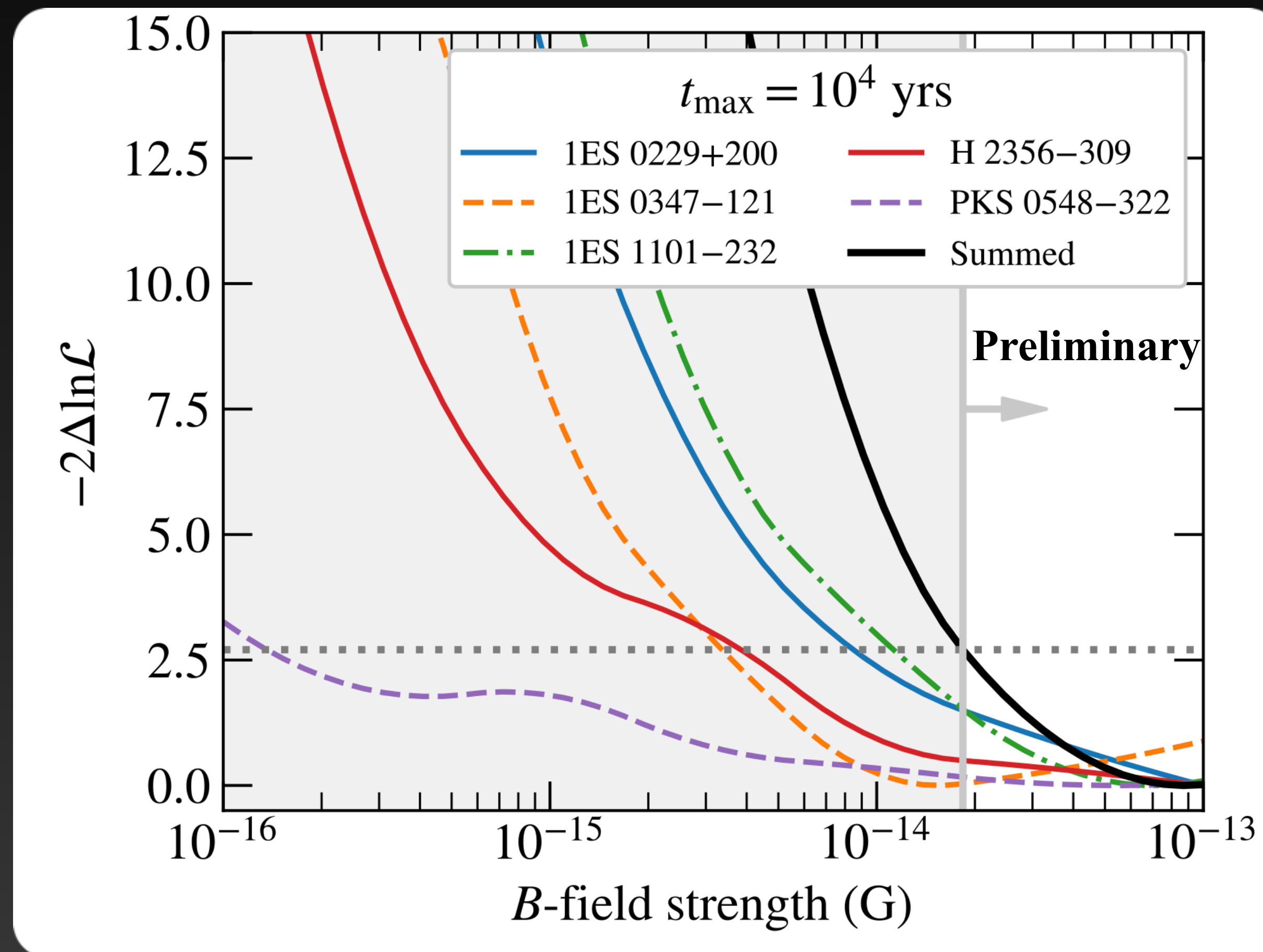
Results: lower limits on IGMF

Data does not prefer presence of halo



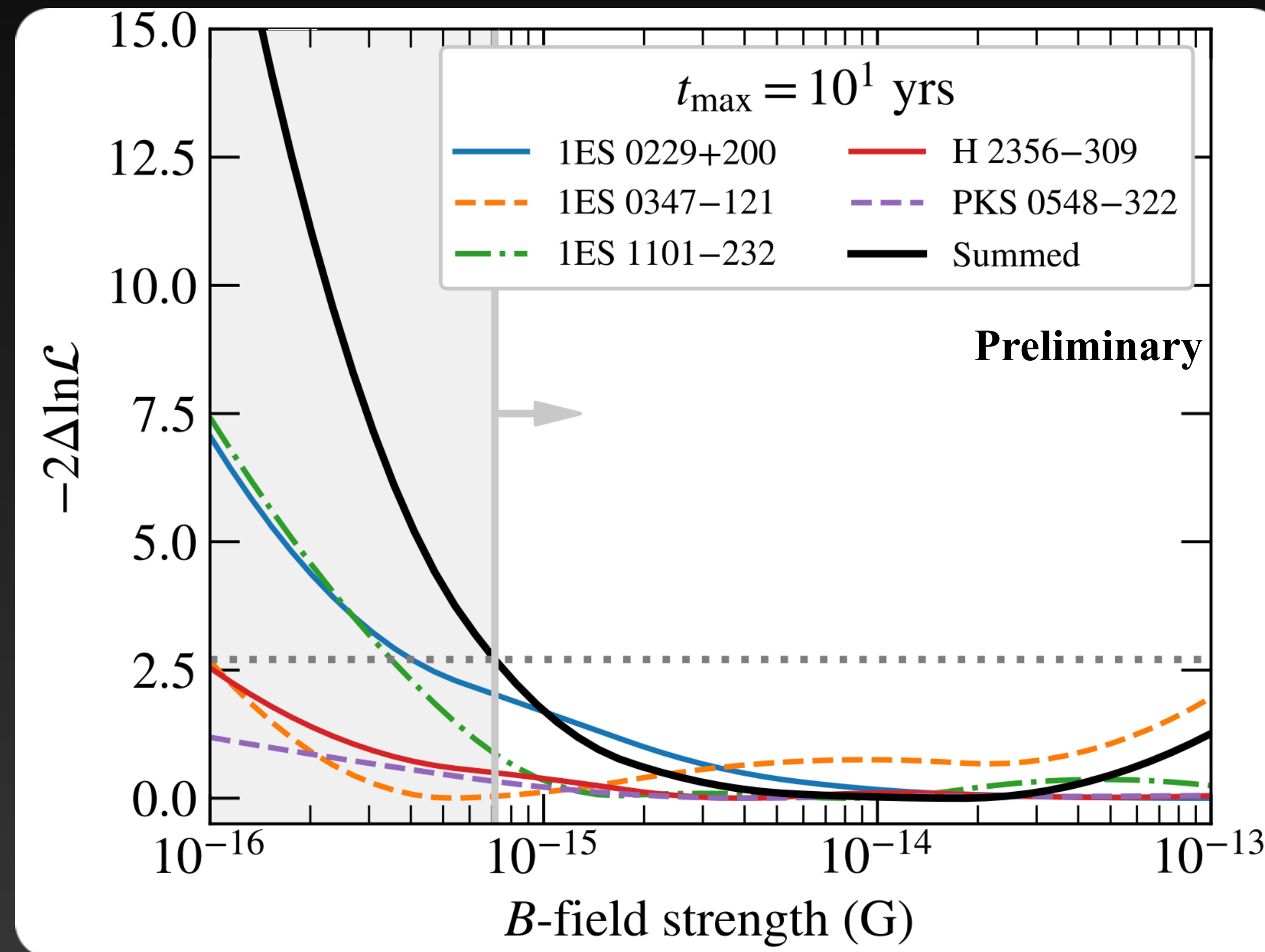
Results: lower limits on IGMF

Data does not prefer presence of halo

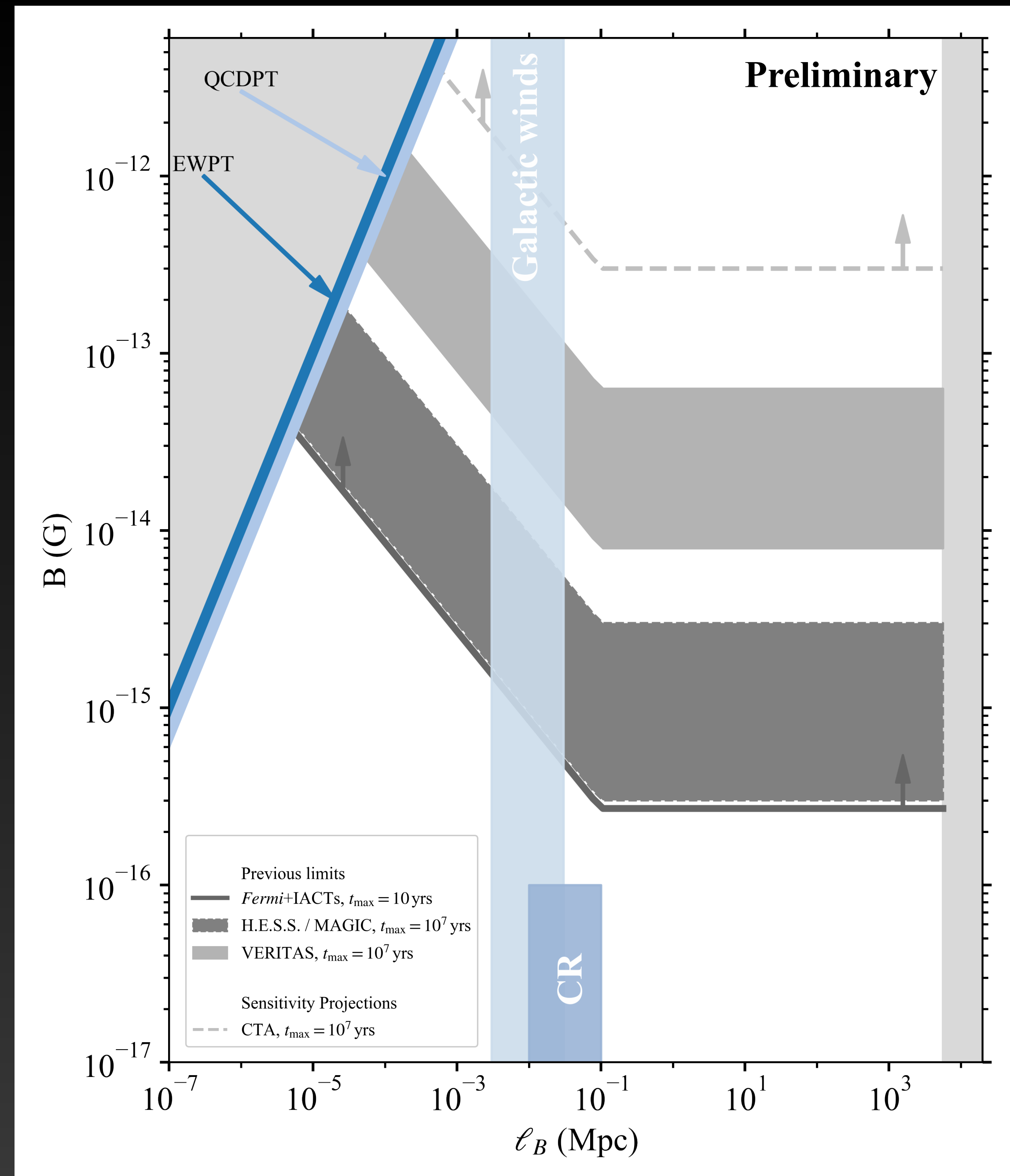


Results: lower limits on IGMF

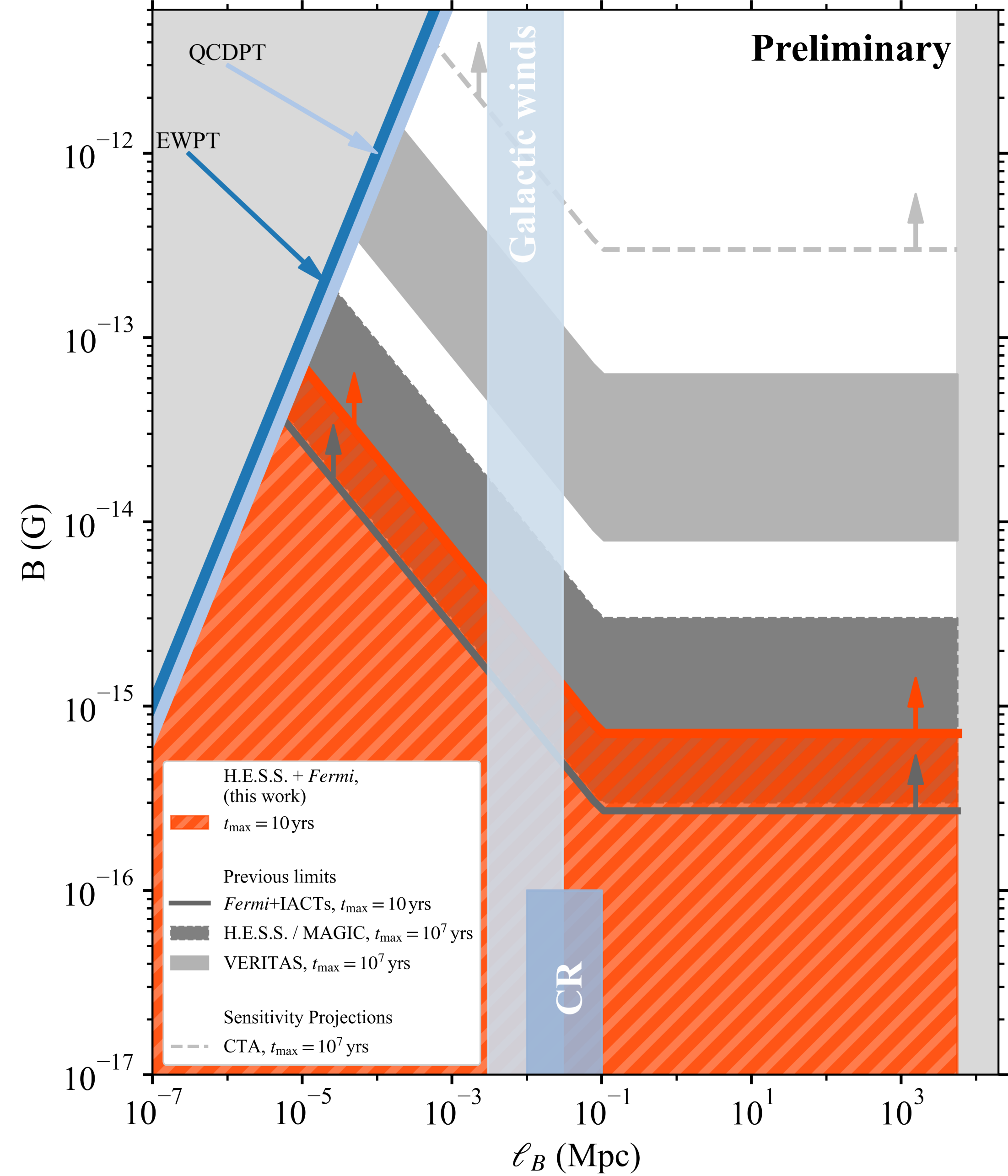
Data does not prefer presence of halo



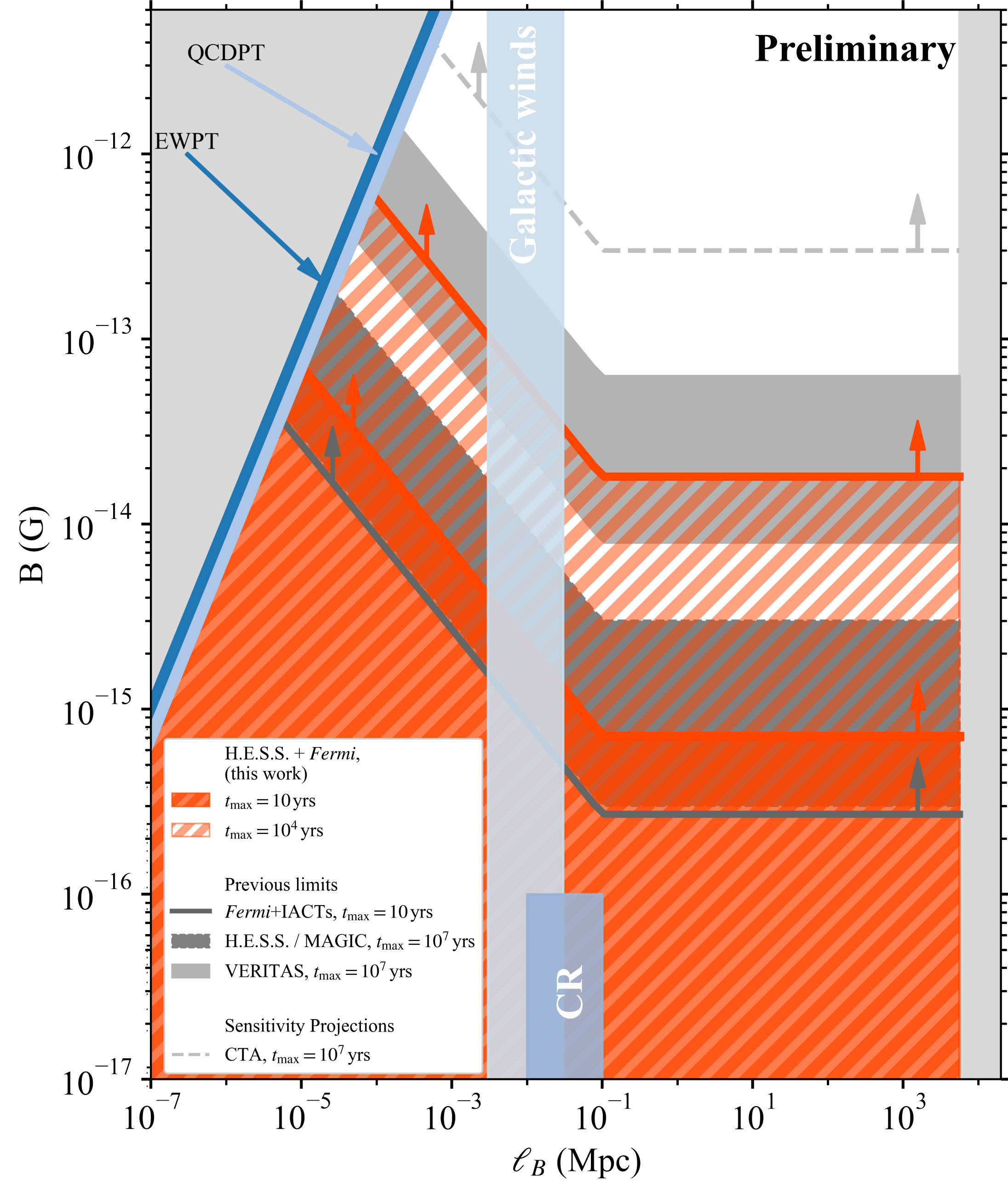
Conclusions



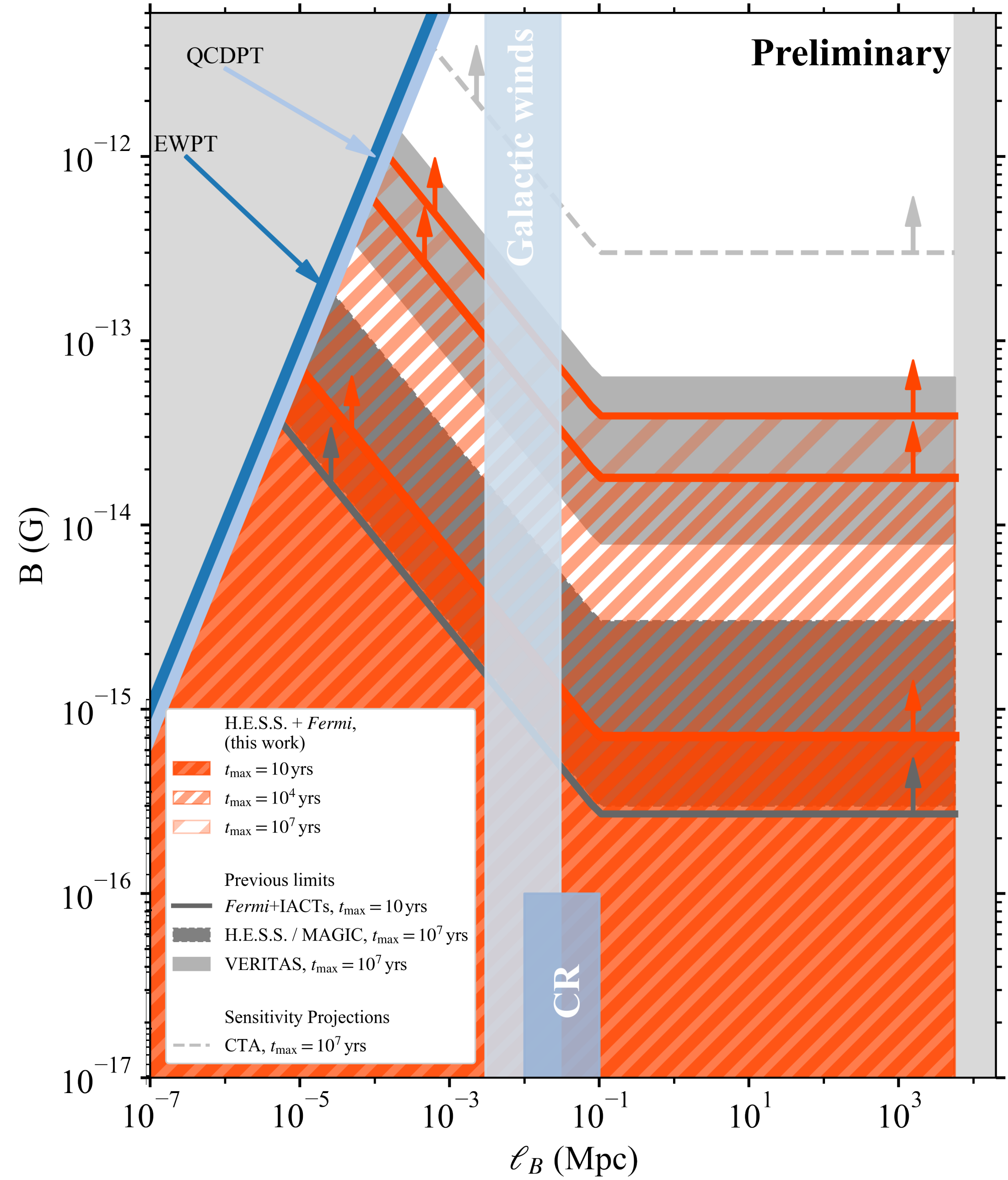
Conclusions



Conclusions

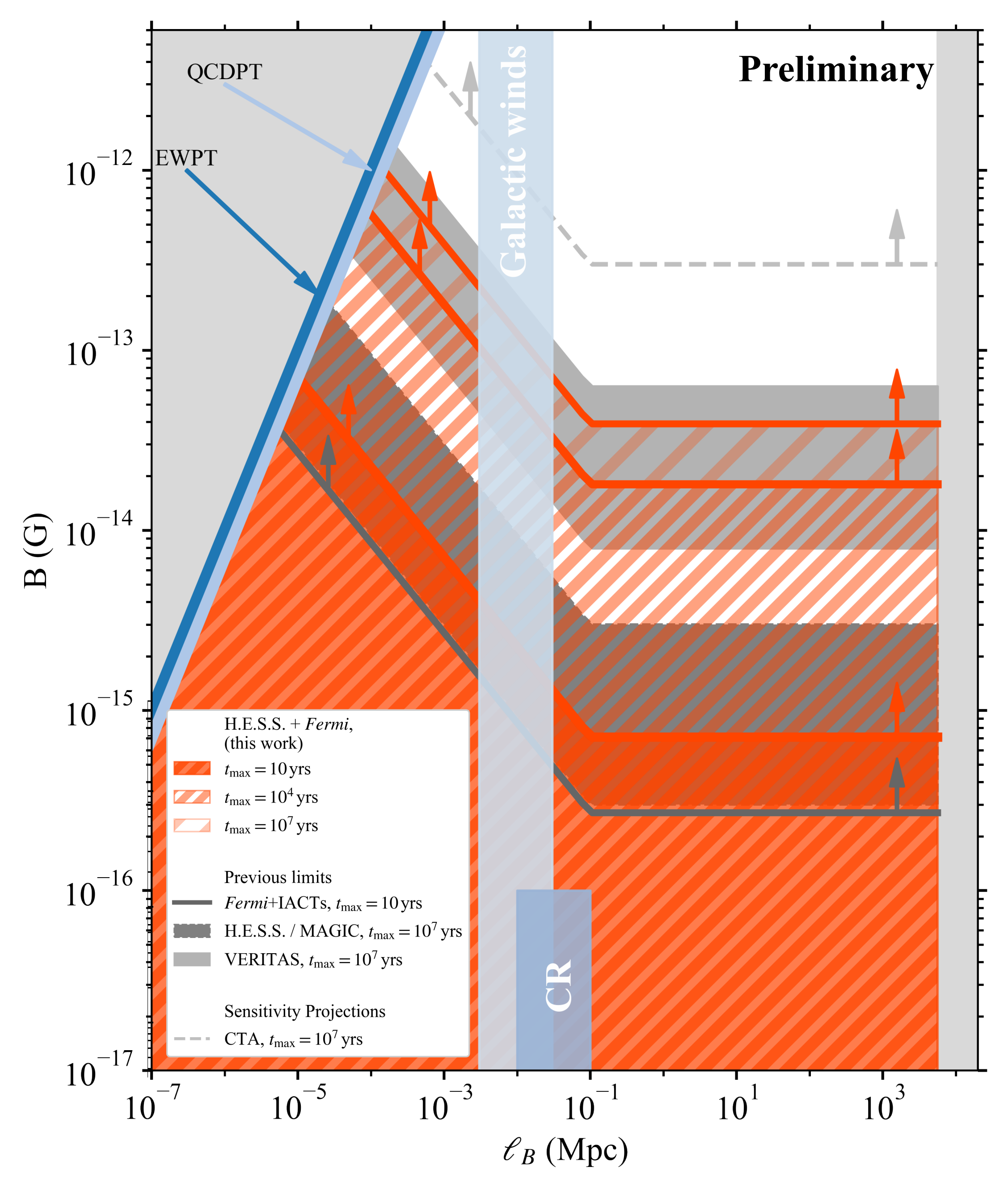


Conclusions



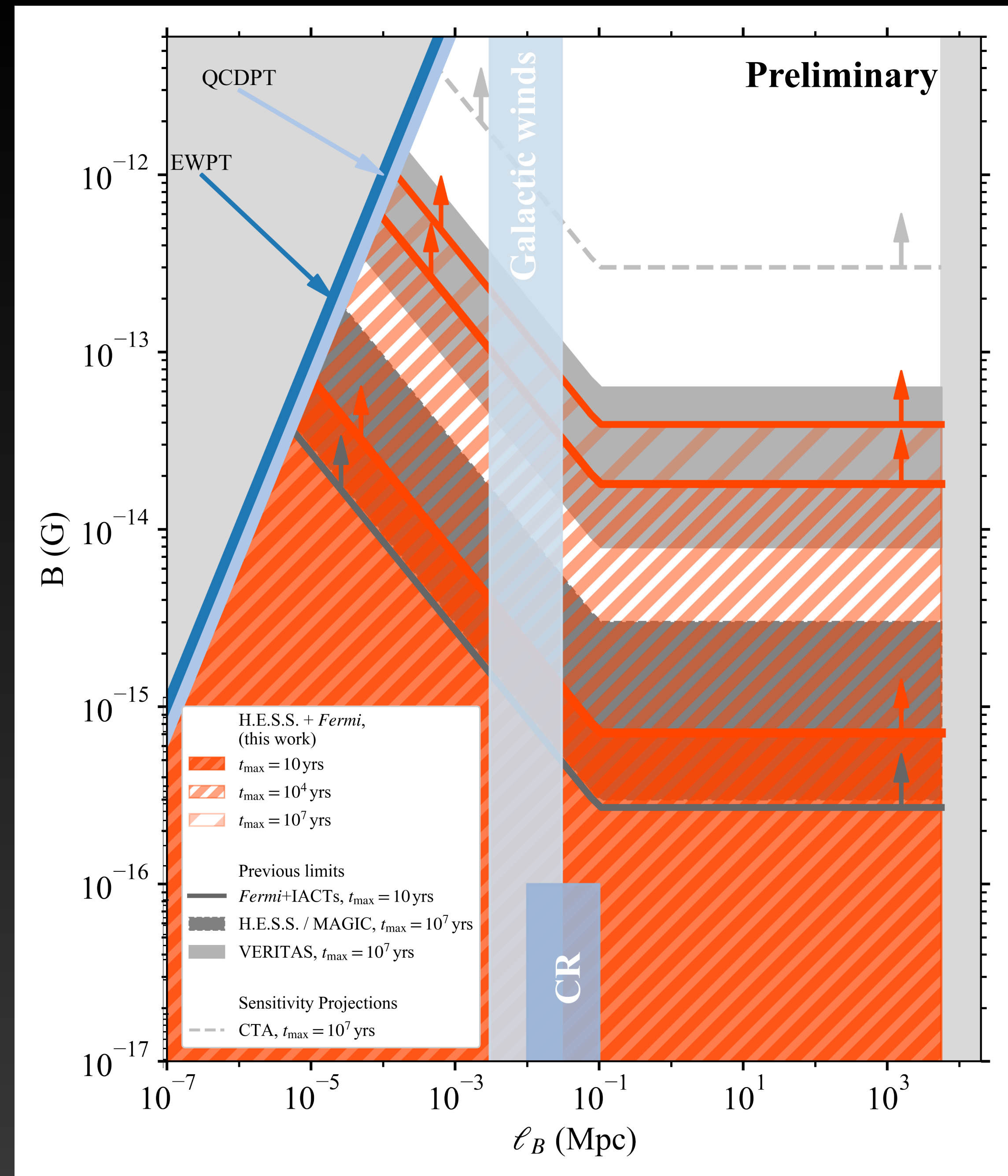
Conclusions

- CRPropa3 simulations used to generate realistic cascade templates



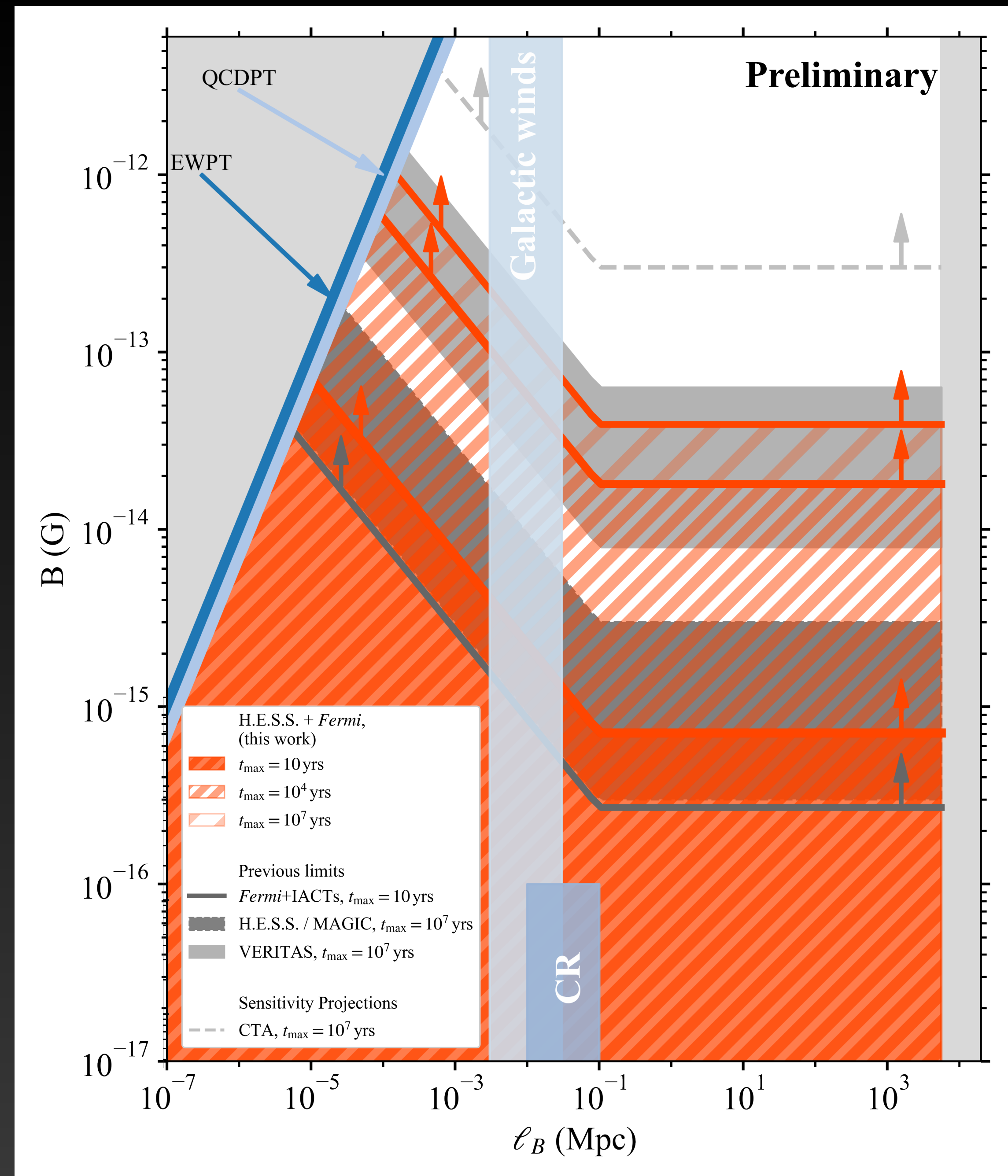
Conclusions

- CRPropa3 simulations used to generate realistic cascade templates
- No halo detected in combined LAT and H.E.S.S. data



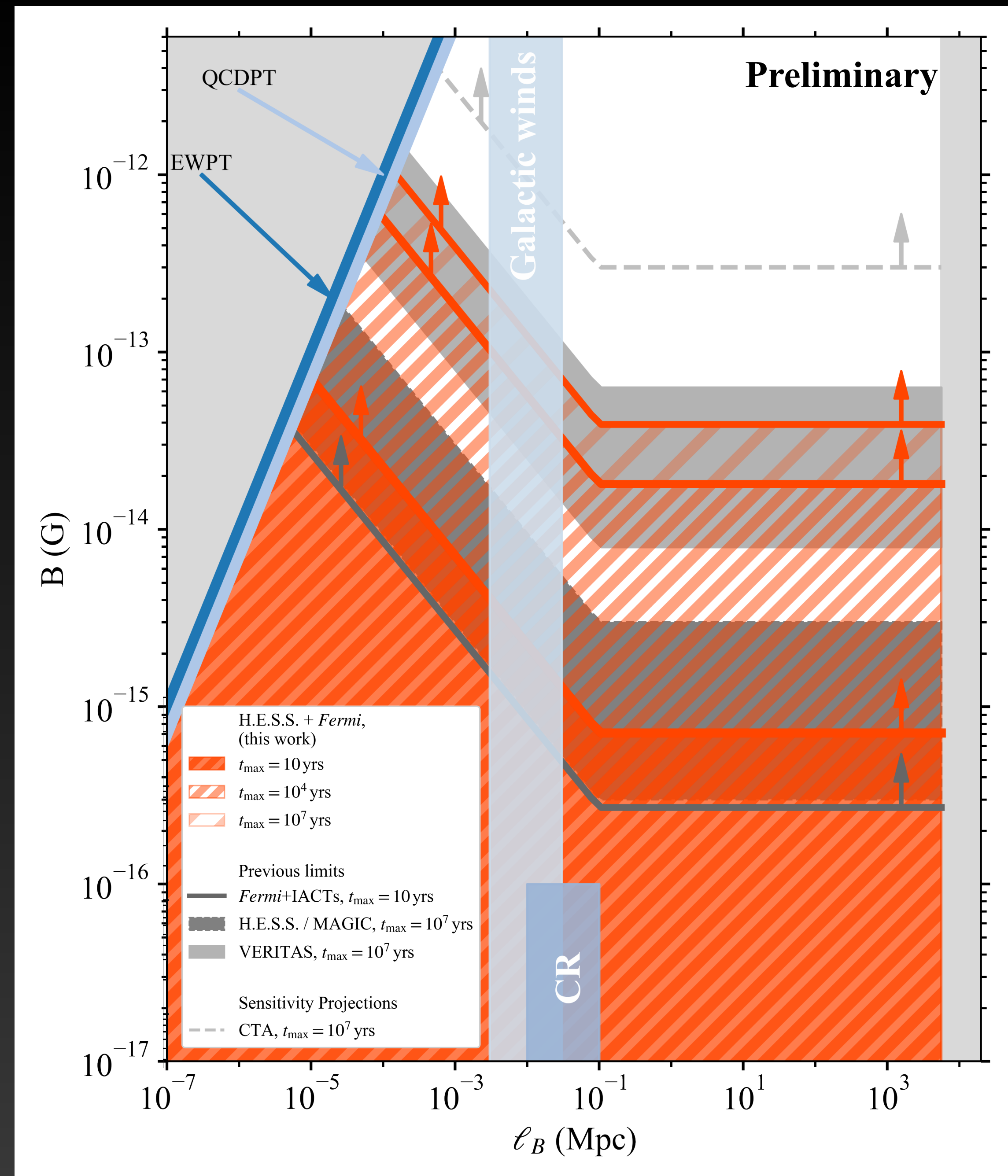
Conclusions

- CRPropa3 simulations used to generate realistic cascade templates
- No halo detected in combined LAT and H.E.S.S. data
- If pairs lose energy through scattering CMB photons, B fields weaker than $B \lesssim 7 \times 10^{-16} \text{ G}$ for $t_{\text{max}} = 10 \text{ yr}$ are ruled out



Conclusions

- CRPropa3 simulations used to generate realistic cascade templates
- No halo detected in combined LAT and H.E.S.S. data
- If pairs lose energy through scattering CMB photons, B fields weaker than $B \lesssim 7 \times 10^{-16} \text{ G}$ for $t_{\text{max}} = 10 \text{ yr}$ are ruled out
- Previous constraints improved by factor of 2



Back up

Fermi-LAT analysis with halo component

Start from optimized ROI without halo

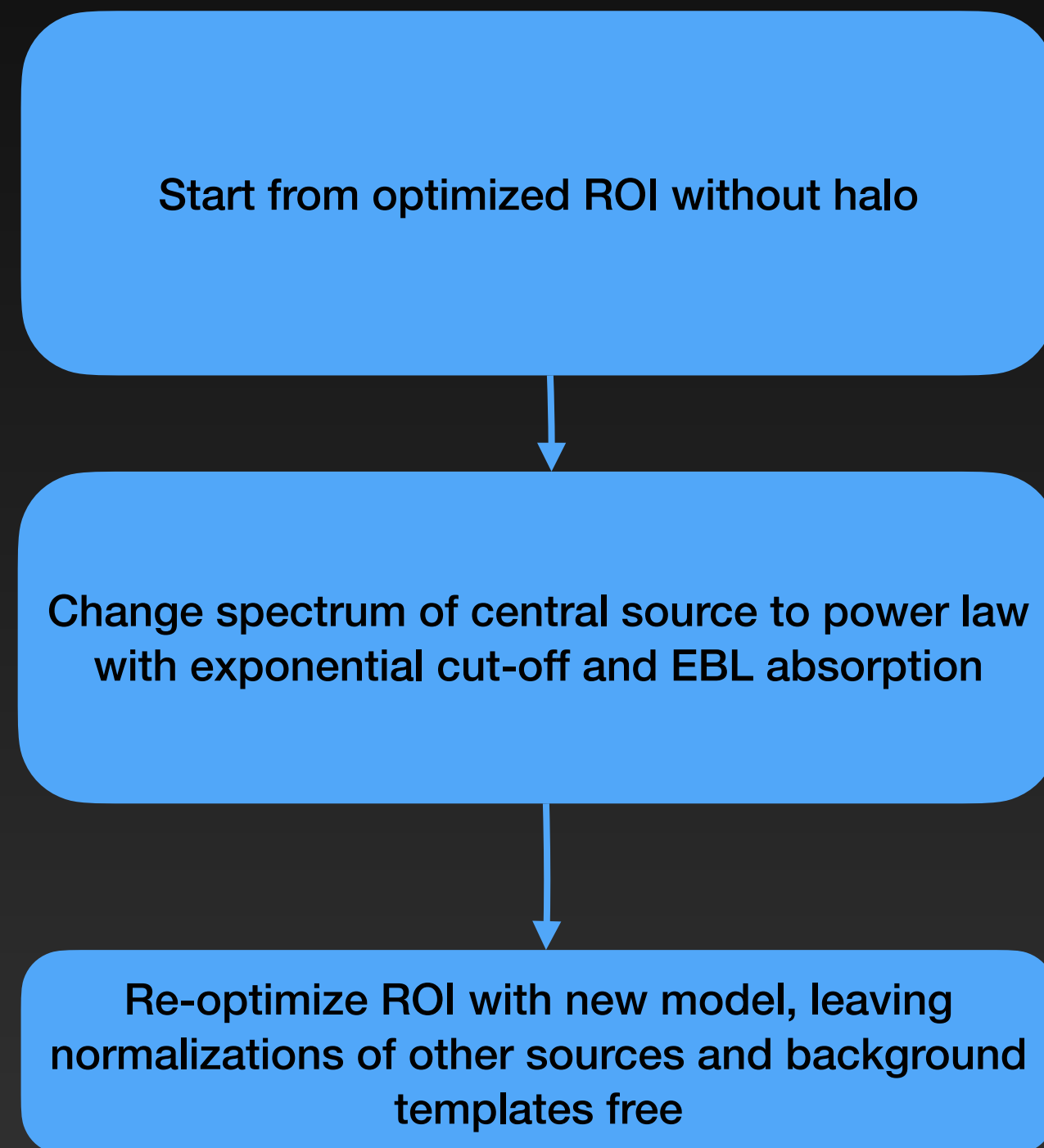
Fermi-LAT analysis with halo component

Start from optimized ROI without halo

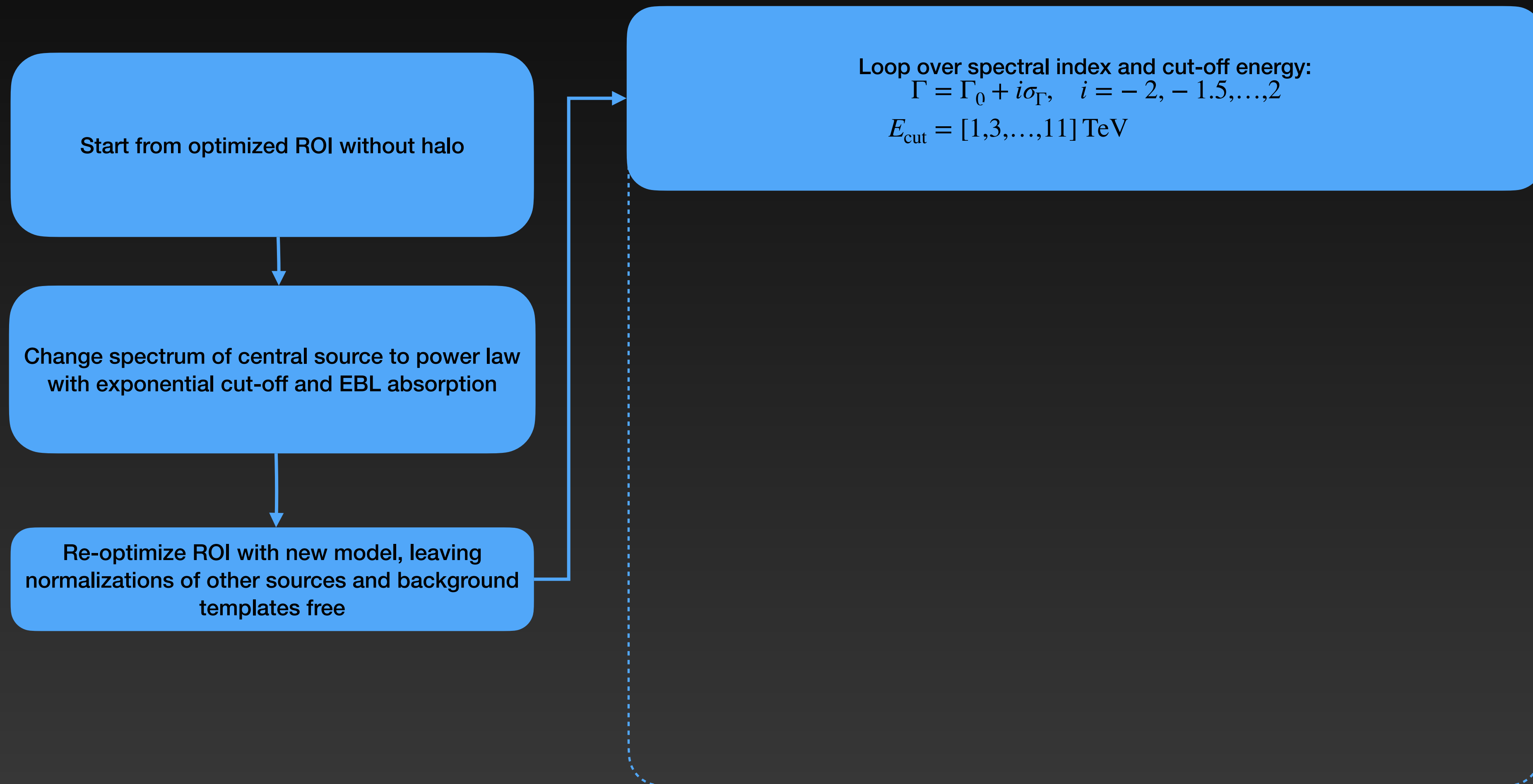


Change spectrum of central source to power law with exponential cut-off and EBL absorption

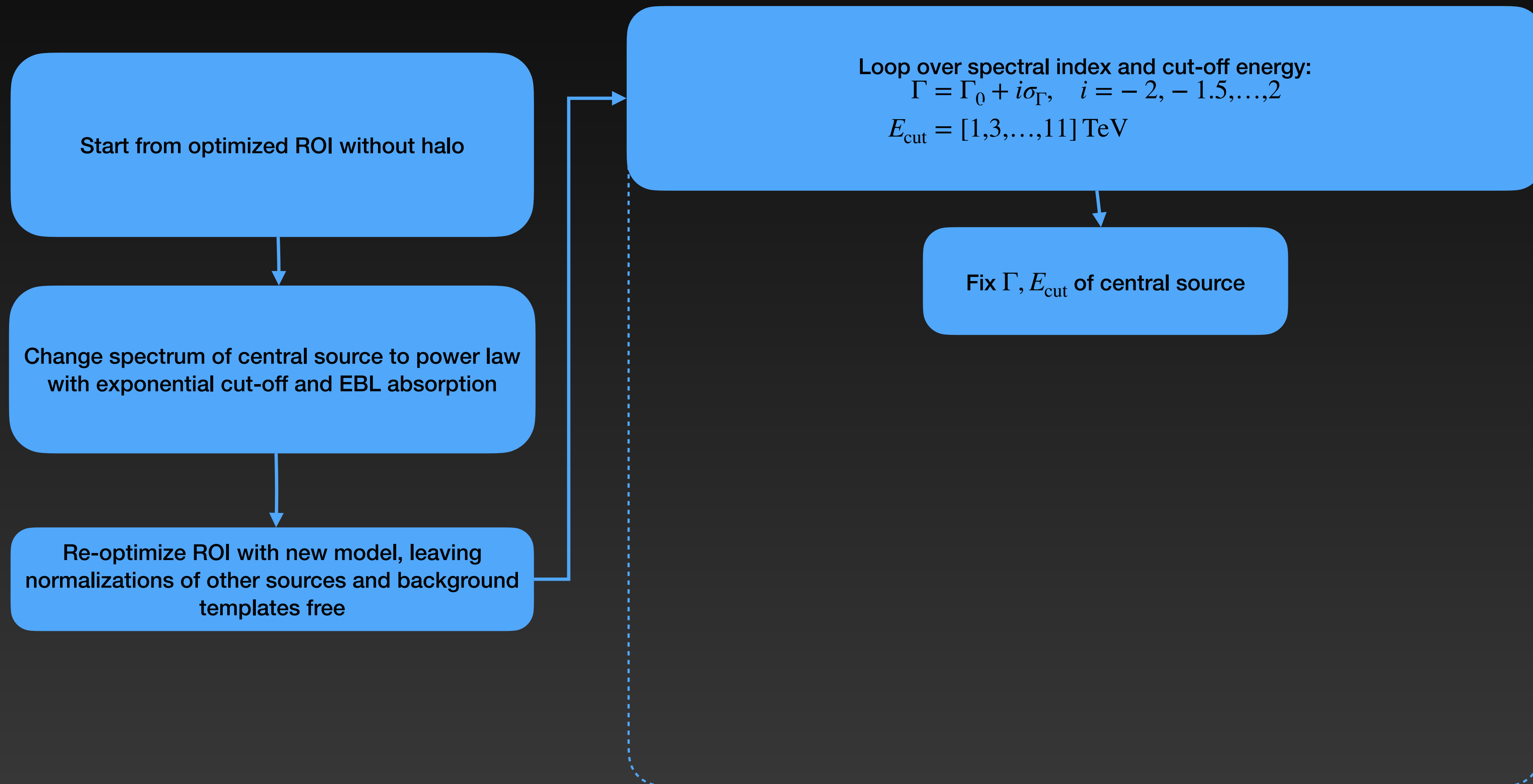
Fermi-LAT analysis with halo component



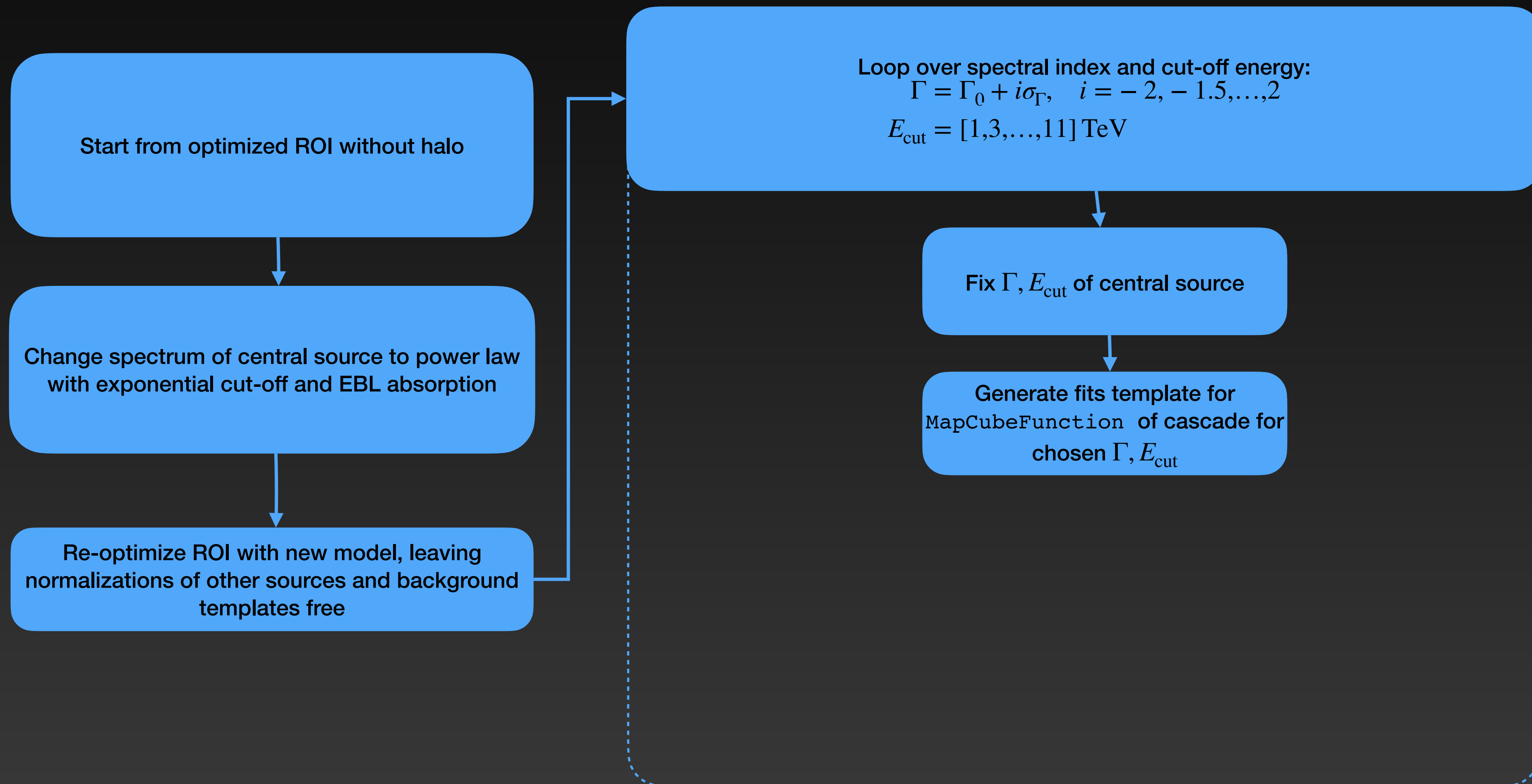
Fermi-LAT analysis with halo component



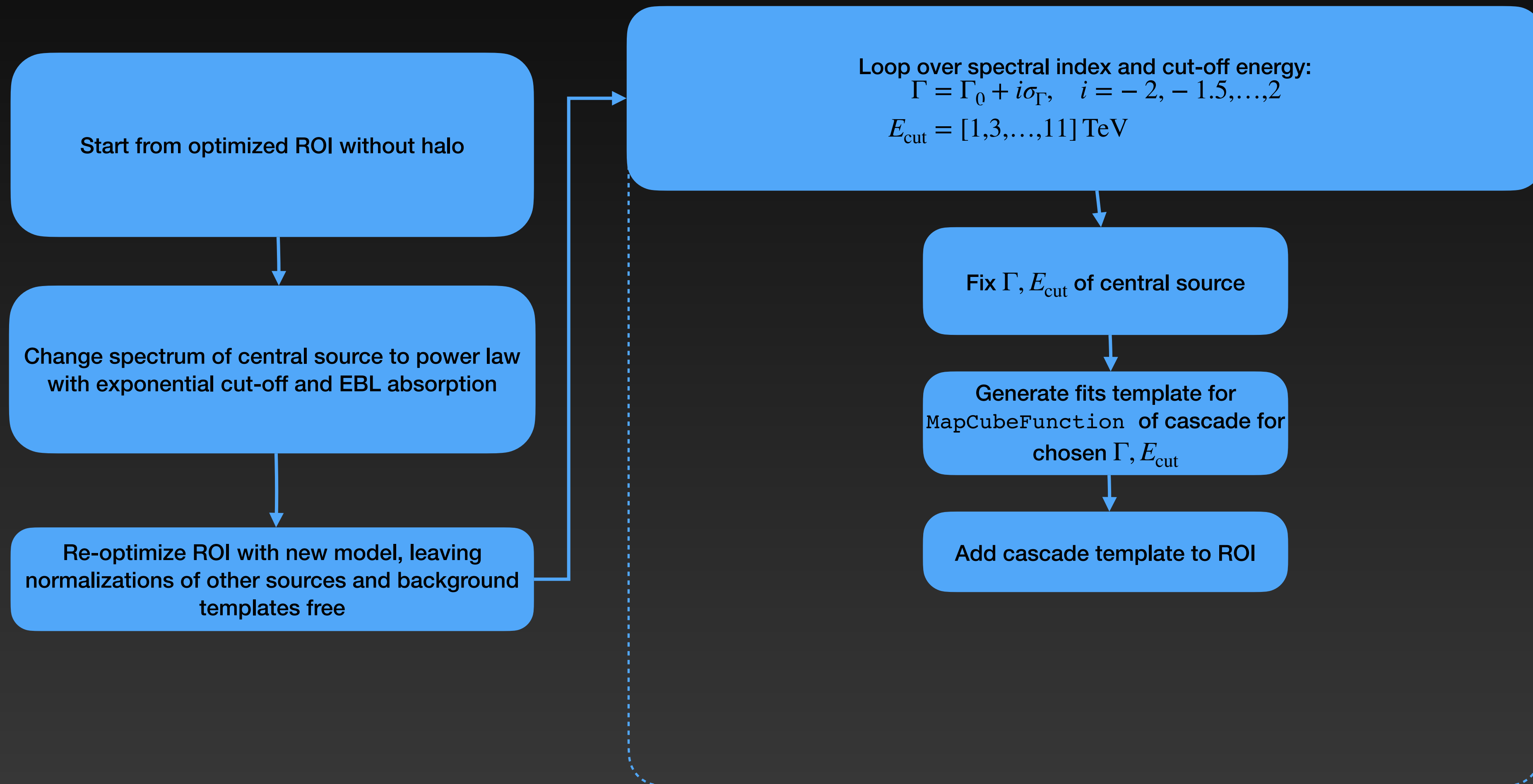
Fermi-LAT analysis with halo component



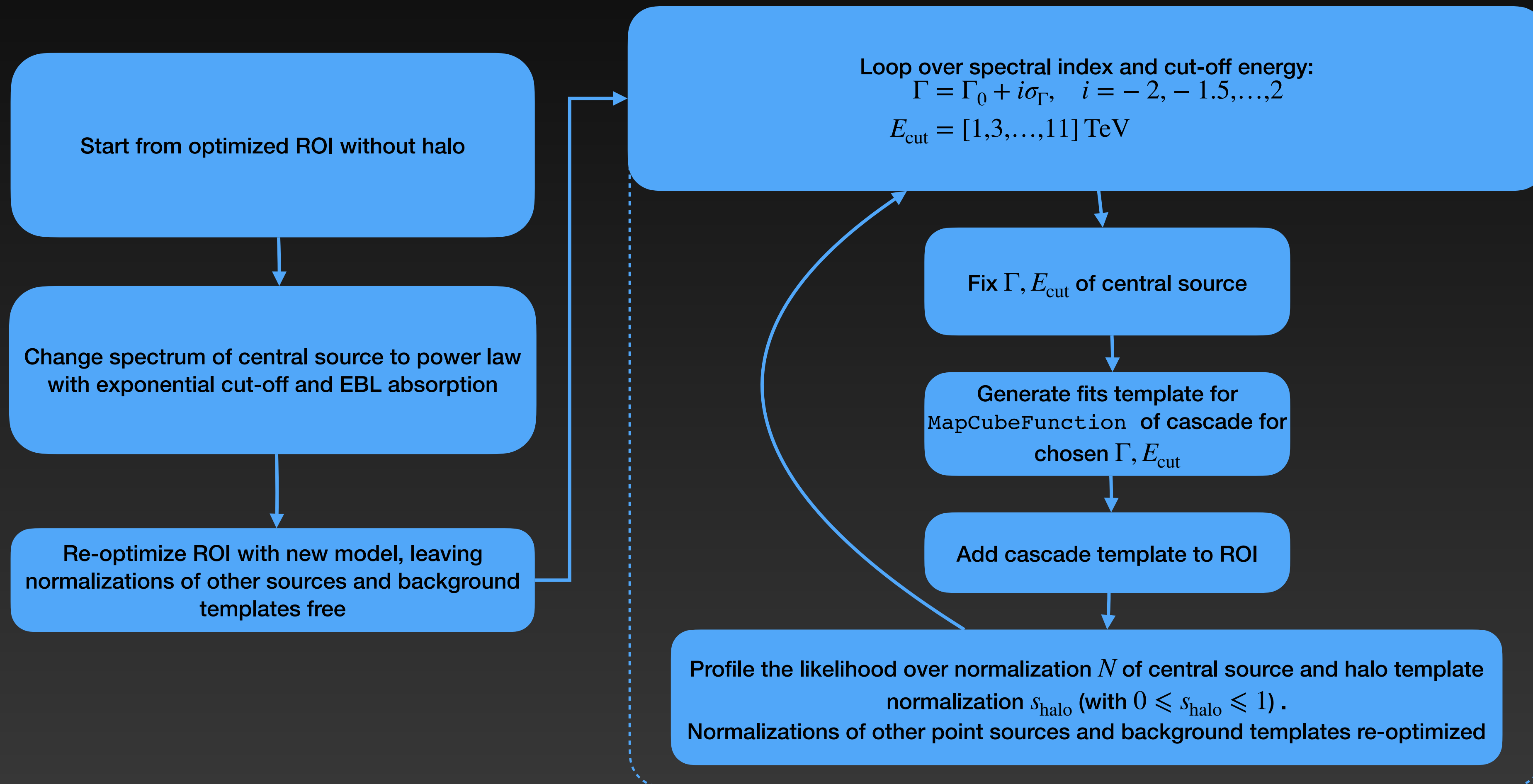
Fermi-LAT analysis with halo component



Fermi-LAT analysis with halo component



Fermi-LAT analysis with halo component



Building cascade templates

Building cascade templates

- From the simulated events we build the intensity as function of injected gamma-ray energy ϵ , observed energy E , solid Ω , and delay time τ :

Building cascade templates

- From the simulated events we build the intensity as function of injected gamma-ray energy ϵ , observed energy E , solid Ω , and delay time τ :

$$\frac{d\mathcal{N}}{d\epsilon dE d\tau d\Omega} = \frac{1}{N_{\text{inj}}(\Delta\epsilon)} \frac{\mathcal{N}}{\Delta E \Delta\epsilon \Delta\tau \Delta\Omega}$$

Building cascade templates

- From the simulated events we build the intensity as function of injected gamma-ray energy ϵ , observed energy E , solid Ω , and delay time τ :

$$\frac{d\mathcal{N}}{d\epsilon dE d\tau d\Omega} = \frac{1}{N_{\text{inj}}(\Delta\epsilon)} \frac{\mathcal{N}}{\Delta E \Delta\epsilon \Delta\tau \Delta\Omega}$$

- Simulation done for discrete injection energies ϵ_i

Building cascade templates

- From the simulated events we build the intensity as function of injected gamma-ray energy ϵ , observed energy E , solid Ω , and delay time τ :

$$\frac{d\mathcal{N}}{d\epsilon dE d\tau d\Omega} = \frac{1}{N_{\text{inj}}(\Delta\epsilon)} \frac{\mathcal{N}}{\Delta E \Delta\epsilon \Delta\tau \Delta\Omega}$$

- Simulation done for discrete injection energies ϵ_i
- From this, we can re-weight the cascade histogram for an arbitrary source spectra $dN/d\epsilon$ (e.g., a power law), by computing weights for bins of injected energy:

Building cascade templates

- From the simulated events we build the intensity as function of injected gamma-ray energy ϵ , observed energy E , solid Ω , and delay time τ :

$$\frac{d\mathcal{N}}{d\epsilon dE d\tau d\Omega} = \frac{1}{N_{\text{inj}}(\Delta\epsilon)} \frac{\mathcal{N}}{\Delta E \Delta\epsilon \Delta\tau \Delta\Omega}$$

- Simulation done for discrete injection energies ϵ_i
- From this, we can re-weight the cascade histogram for an arbitrary source spectra $dN/d\epsilon$ (e.g., a power law), by computing weights for bins of injected energy:

$$w_i = \int_{\Delta\epsilon_i} \frac{dN}{d\epsilon} d\epsilon$$

Building cascade templates

- From the simulated events we build the intensity as function of injected gamma-ray energy ϵ , observed energy E , solid Ω , and delay time τ :

$$\frac{d\mathcal{N}}{d\epsilon dE d\tau d\Omega} = \frac{1}{N_{\text{inj}}(\Delta\epsilon)} \frac{\mathcal{N}}{\Delta E \Delta\epsilon \Delta\tau \Delta\Omega}$$

- Simulation done for discrete injection energies ϵ_i
- From this, we can re-weight the cascade histogram for an arbitrary source spectra $dN/d\epsilon$ (e.g., a power law), by computing weights for bins of injected energy:

$$w_i = \int_{\Delta\epsilon_i} \frac{dN}{d\epsilon} d\epsilon$$

- With the spectral weights, we obtain the expected cascade flux that arrives within some maximum time delay (assuming constant emission with time)

Building cascade templates

- From the simulated events we build the intensity as function of injected gamma-ray energy ϵ , observed energy E , solid Ω , and delay time τ :

$$\frac{d\mathcal{N}}{d\epsilon dE d\tau d\Omega} = \frac{1}{N_{\text{inj}}(\Delta\epsilon)} \frac{\mathcal{N}}{\Delta E \Delta\epsilon \Delta\tau \Delta\Omega}$$

- Simulation done for discrete injection energies ϵ_i
- From this, we can re-weight the cascade histogram for an arbitrary source spectra $dN/d\epsilon$ (e.g., a power law), by computing weights for bins of injected energy:

$$w_i = \int_{\Delta\epsilon_i} \frac{dN}{d\epsilon} d\epsilon$$

- With the spectral weights, we obtain the expected cascade flux that arrives within some maximum time delay (assuming constant emission with time)

$$\frac{d\mathcal{N}}{dE d\Omega} = \int_0^\infty d\epsilon \int_0^\infty d\epsilon' \frac{dN}{d\epsilon'} \int_0^{\tau_{\text{max}}} d\tau \frac{d\mathcal{N}}{d\epsilon' dE d\tau d\Omega} \approx \sum_i \sum_j \Delta\epsilon_i \Delta\tau_j w_i \left(\frac{d\mathcal{N}}{d\epsilon dE d\tau d\Omega} \right)_{ij}$$

Building cascade templates

- From the simulated events we build the intensity as function of injected gamma-ray energy ϵ , observed energy E , solid Ω , and delay time τ :

$$\frac{d\mathcal{N}}{d\epsilon dE d\tau d\Omega} = \frac{1}{N_{\text{inj}}(\Delta\epsilon)} \frac{\mathcal{N}}{\Delta E \Delta\epsilon \Delta\tau \Delta\Omega}$$

- Simulation done for discrete injection energies ϵ_i
- From this, we can re-weight the cascade histogram for an arbitrary source spectra $dN/d\epsilon$ (e.g., a power law), by computing weights for bins of injected energy:

$$w_i = \int_{\Delta\epsilon_i} \frac{dN}{d\epsilon} d\epsilon$$

- With the spectral weights, we obtain the expected cascade flux that arrives within some maximum time delay (assuming constant emission with time)

$$\frac{d\mathcal{N}}{dE d\Omega} = \int_0^\infty d\epsilon \int_0^\infty d\epsilon' \frac{dN}{d\epsilon'} \int_0^{\tau_{\text{max}}} d\tau \frac{d\mathcal{N}}{d\epsilon' dE d\tau d\Omega} \approx \sum_i \sum_j \Delta\epsilon_i \Delta\tau_j w_i \left(\frac{d\mathcal{N}}{d\epsilon dE d\tau d\Omega} \right)_{ij}$$

- Cascade flux will depend on IGMF strength B and coherence length λ , injection spectrum, maximum activity time of the source t_{max} , as well as θ_{jet} , θ_{obs} and source redshift z

Cascade templates as function of IGMF strength: sky maps

Smoothed with ASMOOTH

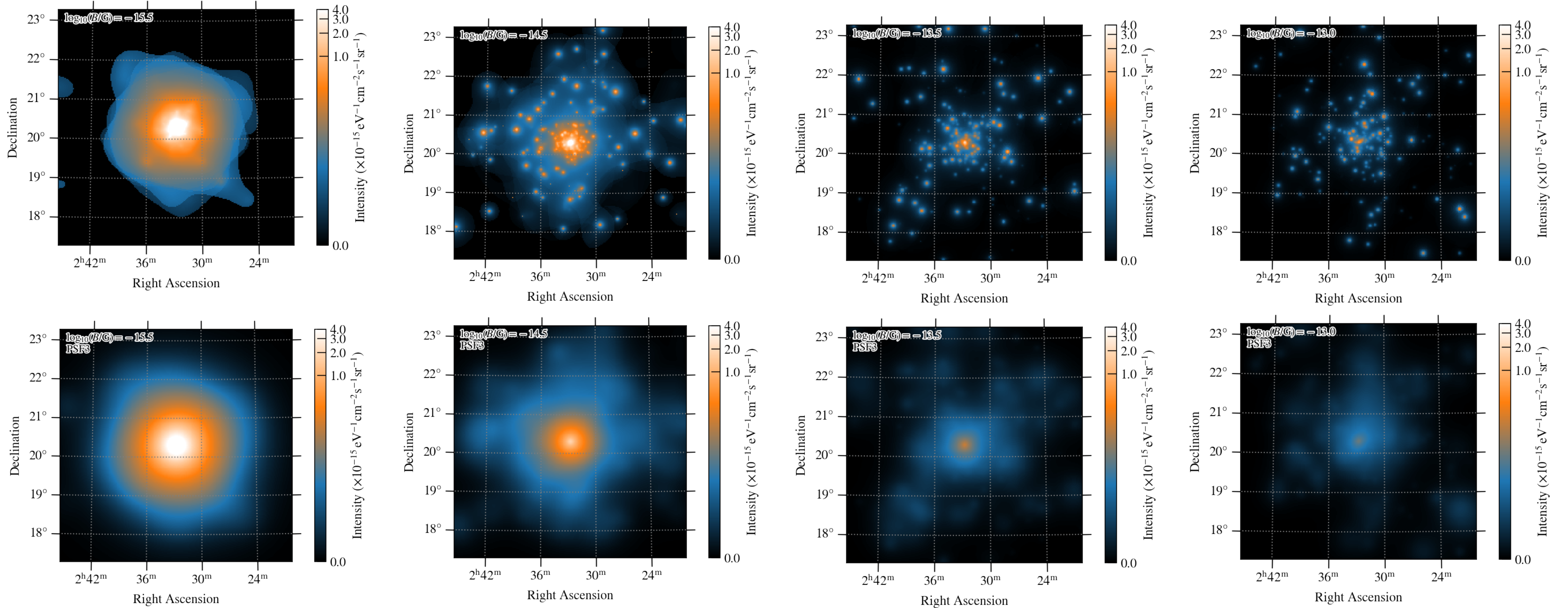
Convolved with Fermi PSF3

$$B = 3.16 \times 10^{-16} \text{ G}$$

$$B = 3.16 \times 10^{-15} \text{ G}$$

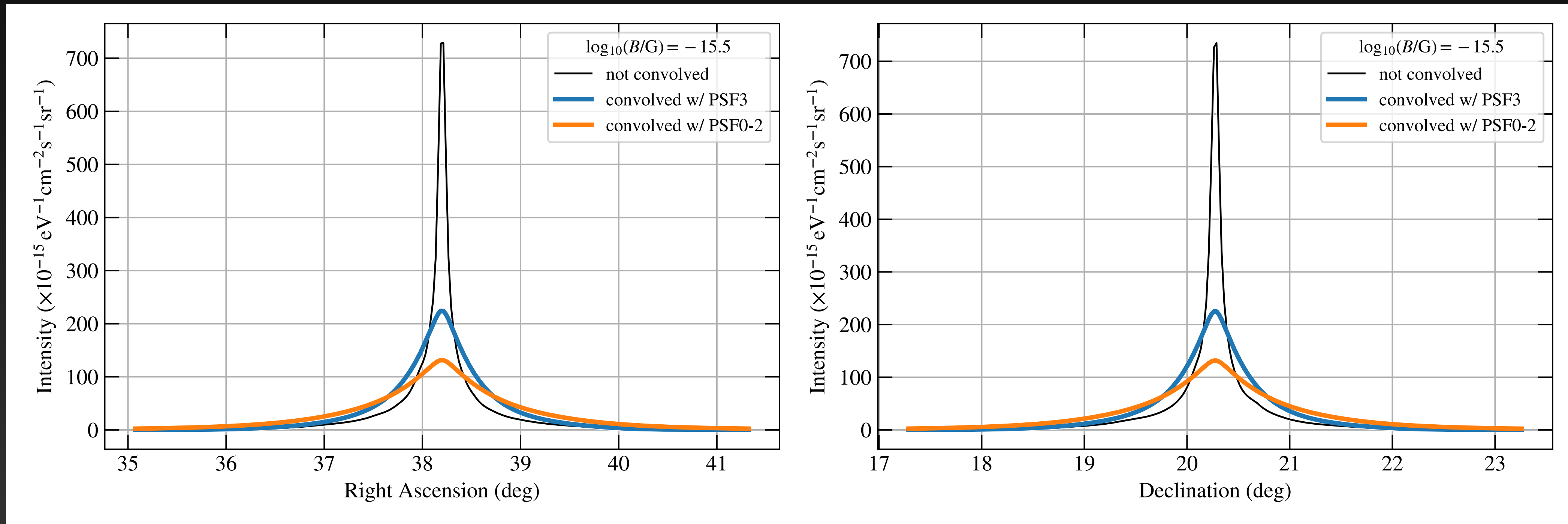
$$B = 3.16 \times 10^{-14} \text{ G}$$

$$B = 10^{-13} \text{ G}$$



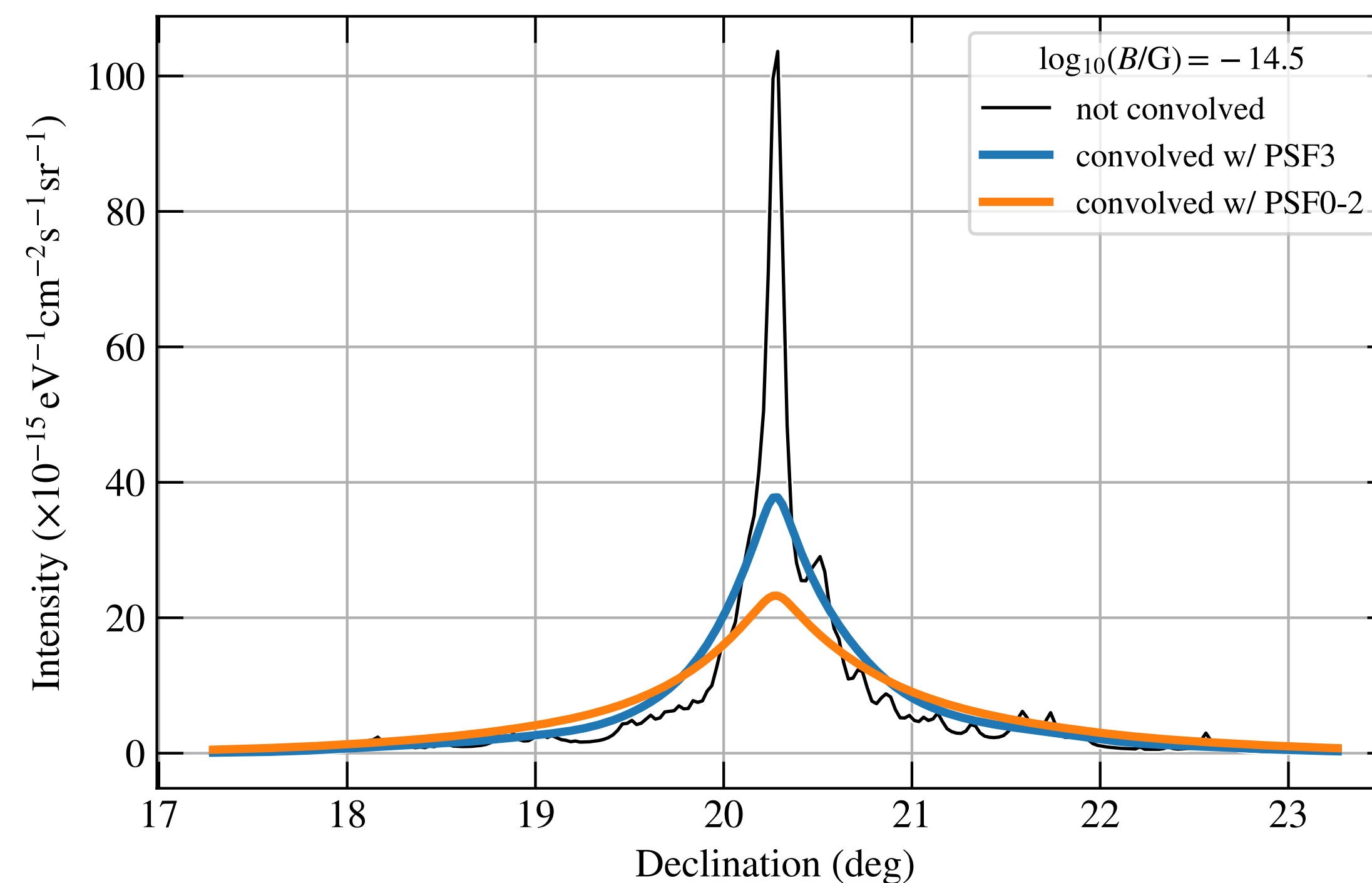
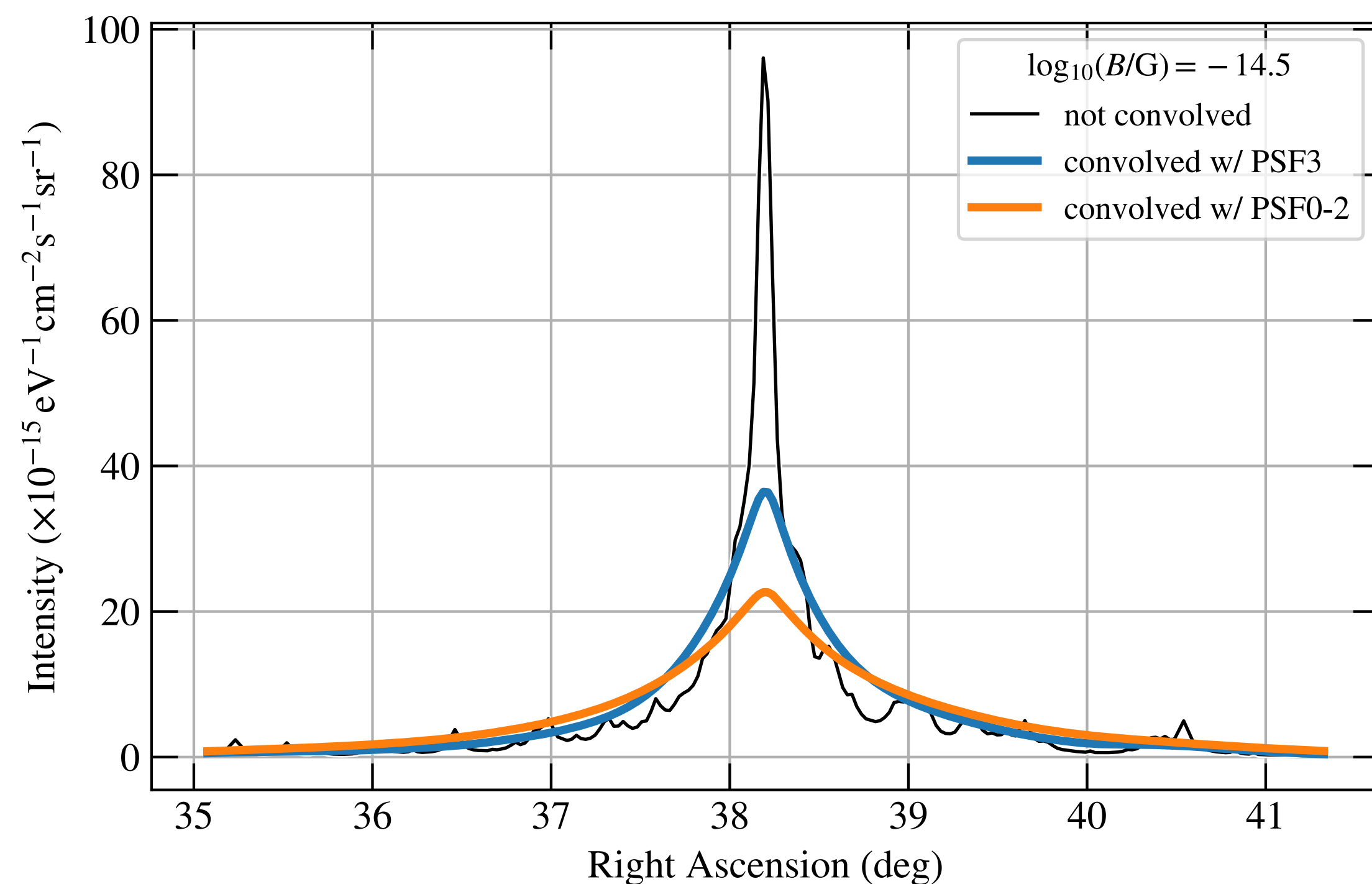
Cascade templates as function of IGMF strength: lon/lat profiles

$B = 3.16 \times 10^{-16}$ G, sky map summed over lon/lat and energy



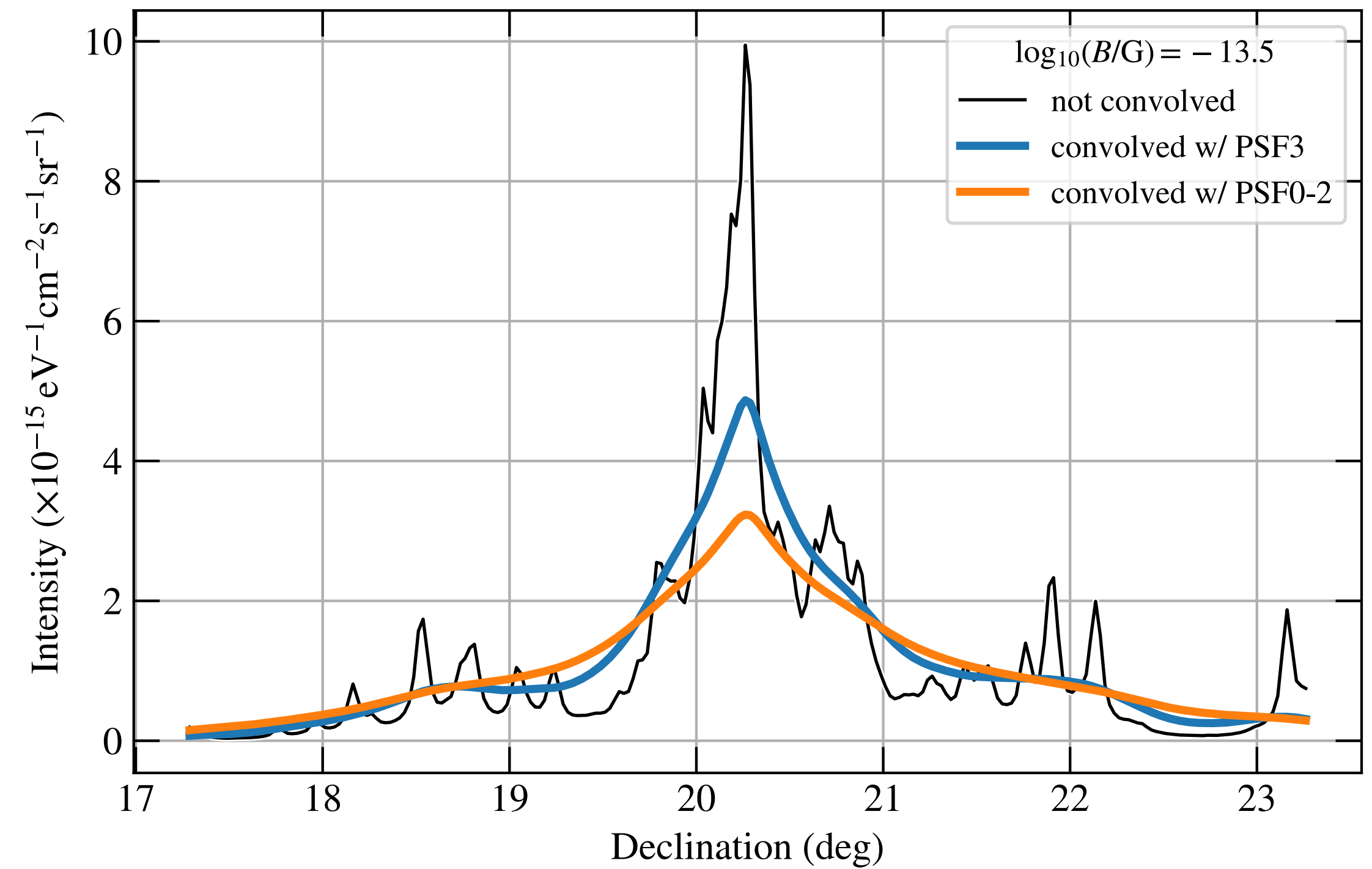
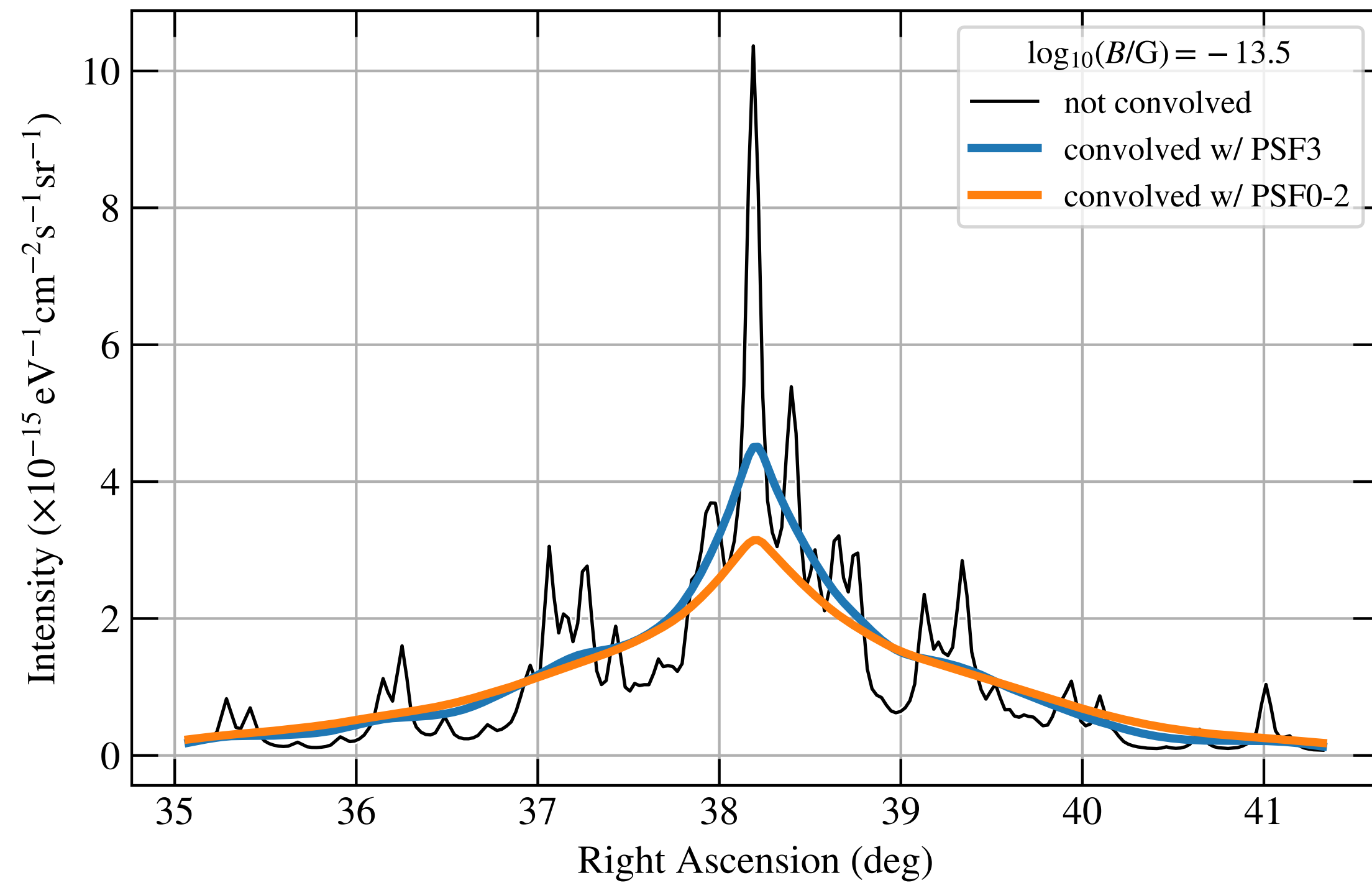
Cascade templates as function of IGMF strength: lon/lat profiles

$B = 3.16 \times 10^{-15}$ G, sky map summed over lon/lat and energy



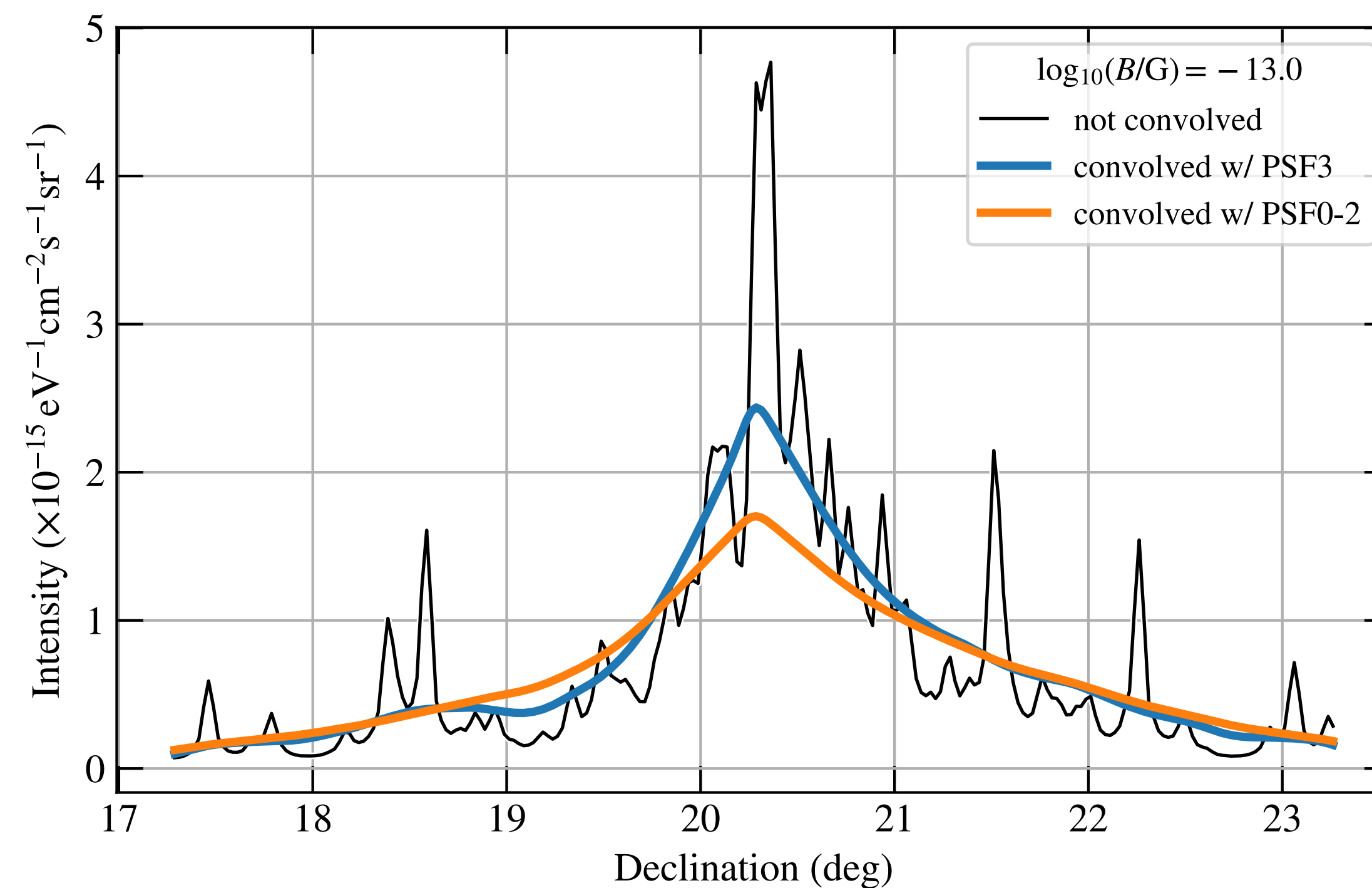
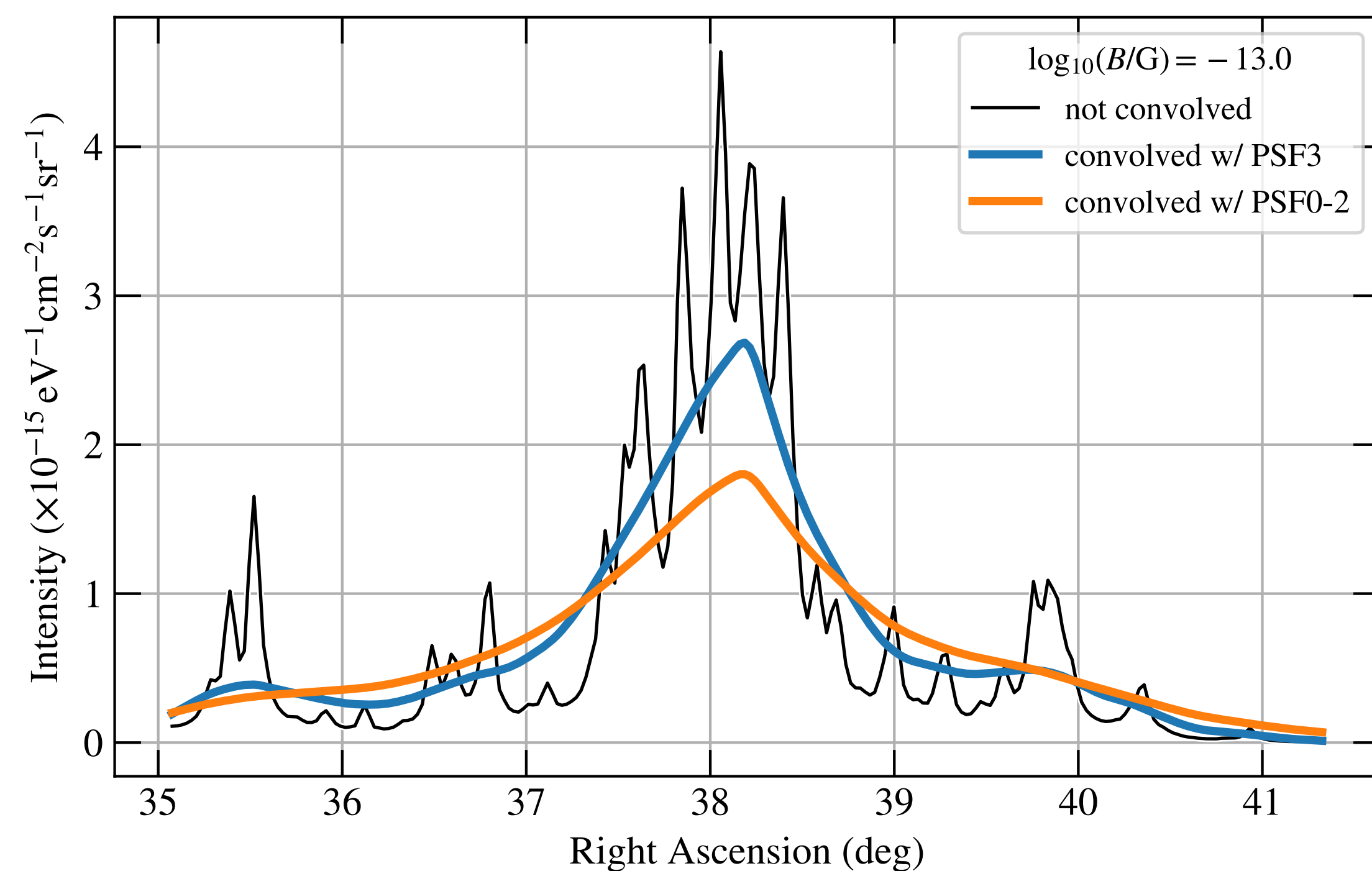
Cascade templates as function of IGMF strength: lon/lat profiles

$B = 3.16 \times 10^{-14}$ G, sky map summed over lon/lat and energy

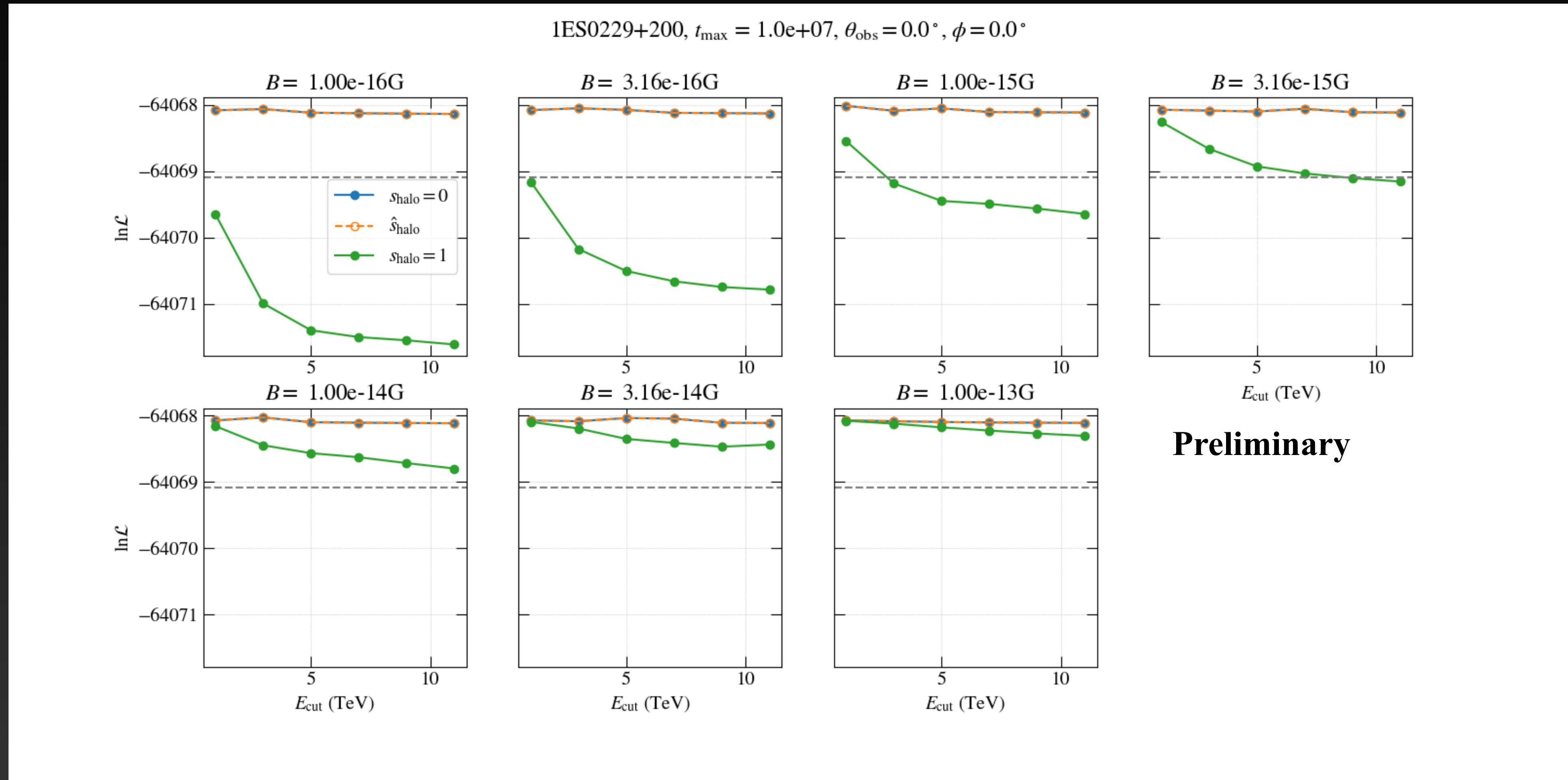


Cascade templates as function of IGMF strength: lon/lat profiles

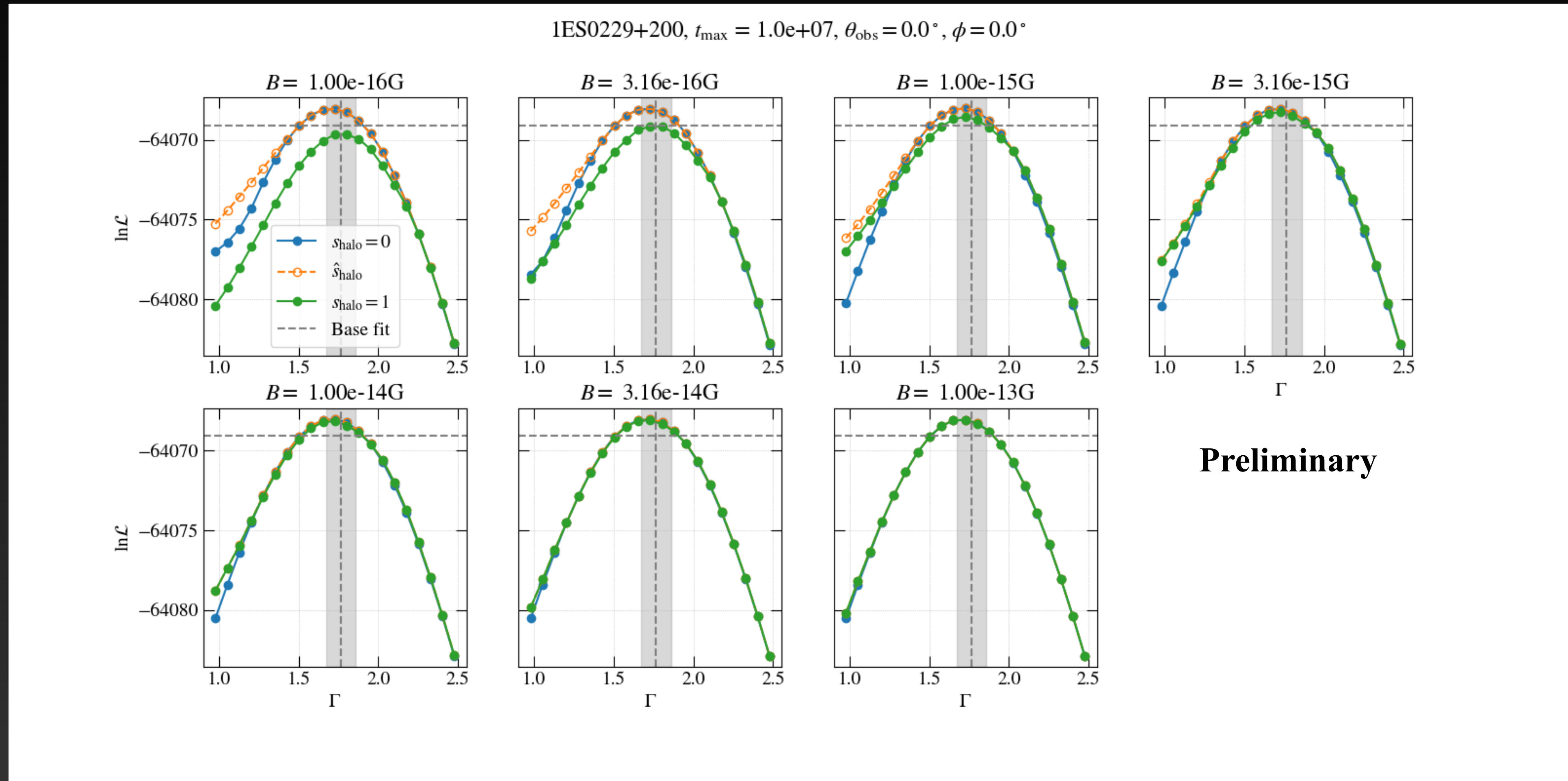
$B = 10^{-13}$ G, sky map summed over lon/lat and energy



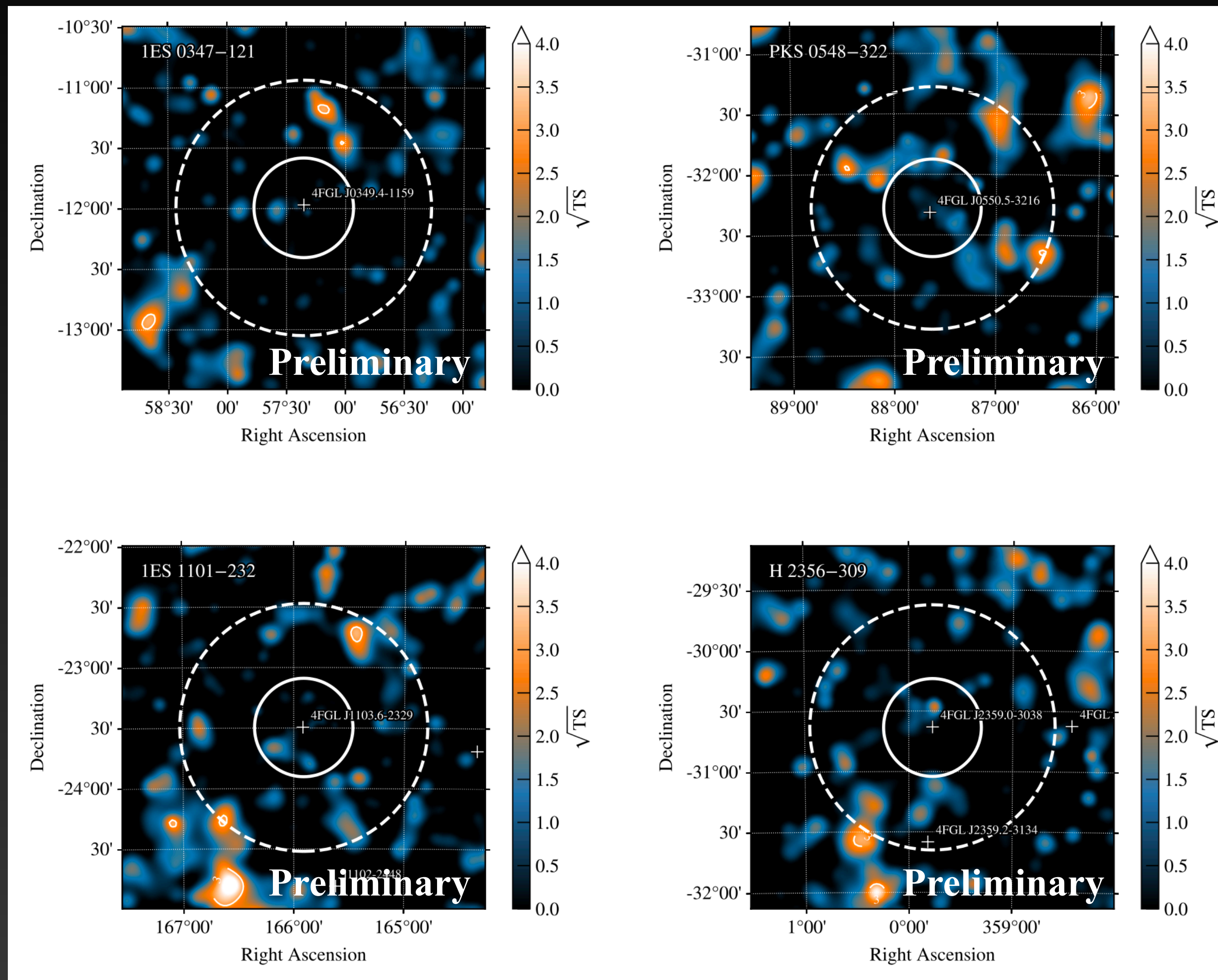
Fermi-LAT Analysis with halo component — Examples of likelihood profile with E_{cut}



Fermi-LAT Analysis with halo component — Examples of likelihood profile with Γ



TS maps for all sources



Source Spectra

1ES0229+200

1ES0347-121

PKS0548-322

1ES1101-232

H2356-309

$$B = 10^{-16} \text{ G}$$

$$B = 10^{-15} \text{ G}$$

$$B = 10^{-14} \text{ G}$$

